UNIVERSITY OF CAPE TOWN

IYUNIVESITHI YASEKAPA •UNIVERSITEIT VAN KAAPSTAD

DEPARTMENT OF CIVIL ENGINEERING

FACULTY OF ENGINEERING AND BUILT ENVIRONMENT

ASSESSING THE AGE AT CRACKING OF CONCRETE REPAIR MORTARS/OVERLAYS SUBJECTED TO RESTRAINED DRYING SHRINKAGE

Submitted in partial fulfillment of the requirements for the degree of

MASTER OF SCIENCE IN CIVIL ENGINEERING

by

MASUZYO CHILWESA

Supervisor: Dr.H.Beushausen

Co-supervisor: A/Prof.P.Moyo

July 2012

PLAGIARISM DECLARATION

I know the meaning of plagiarism and I declare that all of the work in this document, save for that which is properly acknowledged, is my own. I also affirm that this work has not been submitted in this, or any other university for examination, or for any other purposes.

Signature..... Date.....

DEDICATION

To the memory of my late mother, Berlina Katumba Chilwesa, to whom

I am forever indebted!

ACKNOWLEDGEMENTS

The author wishes to express sincere gratitude to his supervisor Dr H.D.Beushausen, for the invaluable guidance and mentorship throughout the study. The author is also grateful to A/Prof. P. Moyo and Prof. Alexander for challenging my ideas through constructive criticism, especially during the presentations. Warmest gratitude goes to all my good-natured COMSIRU colleagues for their friendship and help throughout the study. The author would also like to thank Elly, Noor and the laboratory staff for all their tremendous help. And the author is also profoundly grateful to his family for their encouragement, faith, support and above all, love. To Chito and GC, thanks for being such great mates. God bless you all.

The author would like to acknowledge COMSIRU and the Department of Civil Engineering, University of Cape Town, for the opportunity and financial assistance throughout the study.

ABSTRACT

The amount of concrete infrastructure needing repair and rehabilitation is increasing worldwide. The bonded overlay technique, which involves removal of a damaged concrete layer on an existing concrete base (substrate) and replacing it with a new layer is one of the most widely used techniques. Due to thermal and hygral differences in the two composites, differential shrinkage occurs. This leads to overlay shrinkage restraint by the relatively mature substrate.

Restrained shrinkage in bonded overlays can cause stress build up and may result in cracking. Cracking due to restrained deformation is a major problem as it may lead to durability concerns. Overlay resistance to crack initiation, development and propagation depends on a number of time-dependent properties of the concrete. To be able to predict the onset of cracking requires knowledge of the different material properties and how they interact with each other.

In this study, an investigation was carried out on whether the performance with respect to cracking of concrete overlays can be adequately predicted from tests such as ring test, free shrinkage strain, tensile strength test, tensile relaxation and elastic modulus. Five concrete mortar types i.e. three commercially available mortars and two laboratory mixed mortars with water-to-cement ratio (w/c) = 0.45 and w/c = 0.6 were used in the ring test and material property tests. The influence of curing on the crack resistance of overlays was also investigated.

An analytical model for predicting age at cracking in bonded overlays based upon time development of overlay material properties and the superposition principle was developed. Results from the model were compared with results from the ring test. Results indicate that crack resistance of repair mortars depends upon the combined influence of the different material properties. In particular tensile stress relaxation appears to have a large influence. Curing was observed to delay the onset of cracking. Results also indicate that although the ring test will give the correct order of cracking, it will not give the actual age at cracking when assessing materials for crack resistance.

TABLE OF CONTENTS

LIST OF FIGURES

LIST OF TABLES

CHAPTER ONE: INTRODUCTION

1.1 Background and Problem statement

The amount of concrete infrastructure needing repair and rehabilitation is increasing worldwide. For example, the American Society of Civil engineers (ASCE) report card for 2009 states that in the USA alone, the annual cost of concrete repair (including protection and strengthening) is estimated at $ 18 billion to $21 billion. The bonded overlay technique, which involves removal of a damaged concrete layer on an existing concrete member and replacing it with a new layer, is particularly suitable for both large area and small area structures and is one of the most widely used techniques. It is used for both structural and non-structural repairs in concrete members or elements such as slabs on grade, pavements, toppings and linings, etc. Not only is it used on existing structures but also on precast elements which receive an in-situ topping (Banthia *et al.*, 1996; Granju *et al.*, 2004; Beushausen & Alexander, 2006).

The performance of overlays is weakened by such effects as early age surface cracking, spalling or interface debonding. Early age surface cracking due to restrained deformation is a major problem arising in bonded overlays. Loss of moisture can lead to plastic shrinkage in newly cast concrete or drying shrinkage in aging concrete, while a temperature gradient will cause thermal shrinkage. Free shrinkage will cause lateral strains which, if concrete is restrained, may result in tensile stresses. In bonded overlays, the differential shrinkage between concrete substrate and repair material generates tensile stresses. These stresses may lead to cracking of concrete if the tensile strength of the concrete is exceeded, thus compromising both the durability and serviceability requirements (Banthia & Gupta, 2009; Kheder, 1997).

Overlay resistance to crack initiation, development and propagation depends on a number of time-dependent properties of the concrete. In addition to free shrinkage and tensile strength, several other factors can also influence the potential for cracking including tensile relaxation and elastic modulus, as well as degree of restraint and environmental conditions such as relative humidity. The advent of cracking will depend upon the interaction of these material properties.

Tensile relaxation has been recognized as one of the main stress relief mechanisms (Beushausen, 2005; Masuku, 2009). Researchers have reported that relaxation can relieve up to 60% of overlay tensile stress (Carlsward, 2006). This decrease in overlay stress is beneficial because it delays the onset of cracking. Creep, like relaxation, can lead to a decrease in overlay tensile stress (Altoubat & Lange, 2001; Tarek *et al.*, 2008). Elastic modulus also affects the development of tensile stress in the overlay. A lower elastic modulus implies a less stiff concrete, therefore the resulting tensile stresses from restrained shrinkage are less excessive. Environmental factors viz. temperature and relative humidity affect tensile stress development through their effect on overlay shrinkage and relaxation.

The above discussion shows that overlay performance (i.e. overlay crack resistance) depends upon a number of different factors. To be able to predict the onset of cracking requires not just knowledge of the different material properties, but also how they interact with each other. To this end, substantial research has focused on the development of test methods to assess stress development and the corresponding potential for cracking (see Kovler, 1994; Pigeon *et al.*, 2000; Altoubat & Lange, 2001; Radlinska *et al.*, 2007). While these test methods describe outstanding approaches for performing carefully controlled experiments, these tests can be expensive to perform due to the cost of the testing apparatus. Therefore, simple economical test methods for early age shrinkage cracking are preferred. A good example of such tests is the ring test. The ring test has been used by researchers to evaluate the relative shrinkage cracking tendency of different concrete mixes (Carlson & Reading, 1988; Grzybowski & Shah, 1990). The evaluation in such tests is based on characterization of the cracks and their quantification in terms of maximum width, average width, number of cracks, etc.

Due to its simplicity and low cost, the ring test has been used for many years (Bentur & Kovler, 2003). Among the advantages of the ring test is the uniform state of stress that exists as a result of elimination of the edges associated with the longitudinal and panel tests. However, evaluations using the ring test are of qualitative nature. While such evaluations are useful for the comparison of the sensitivity to cracking of different concrete mixes, they are not sufficient for a study of the mechanisms involved. Besides, effort has not been made to study how the ring test

can be used to predict service life performance, and how the different material properties can be integrated to model overlay performance.

This research seeks to model and predict age at cracking of overlays based on experimentally established material properties and the ring test. The main question that the research seeks to answer is whether overlay performance, with the focus in this dissertation on specifically age at cracking, can be adequately predicted from tests such as ring test, shrinkage strain, tensile strength test, elastic modulus test and tensile relaxation.

1.2 Significance of research

The investigation covered in this study serves as an important contribution towards efforts aimed at controlling early age shrinkage cracking of concrete repair mortars. It complements various efforts by researchers in developing new testing methods and materials to tackle early age shrinkage cracking of concrete repair mortars.

1.3 Aim of research

The thesis aims at investigating whether the performance with respect to cracking of concrete repair mortars/overlays can be adequately predicted from the ring test, free shrinkage strain, tensile strength test, elastic modulus and tensile relaxation, and if so, which of these tests or combination of tests would suffice for prediction of overlay performance.

1.4 Research hypothesis

This research proposes that the age at cracking of a concrete repair mortar depends upon the time development of the restrained shrinkage-tensile stress and material properties such as tensile

strength, tensile relaxation and elastic modulus, and that this can be modeled experimentally to predict the age at cracking of the mortar.

1.5 Objectives of research

In order to achieve the aims of the study, the following objectives have been set:

i. To identify key material properties of concrete repair mortars/overlays, and how these properties influence cracking behaviour.
ii. To investigate the influence of curing period on the cracking behaviour of concrete repair mortars.
iii. To determine the age at cracking and quantify the cracking behaviour of concrete repair mortars/overlays with the ring test.
iv. To model and predict age at cracking in bonded overlays, and to check how the model results compare with ring test results.

1.6 Scope

The research will focus on 5 concrete repair mortars viz. three commercial mortars and two laboratory made mixes (w/c = 0.60 and w/c = 0.45). These materials were chosen because they are representative of the repair materials used in the Western Cape Province. Though not comprehensive, this generally covers the range of mortars that may be used in overlay repairs.

1.7 Outline of thesis

The thesis document comprises six chapters namely; Chapter One, which presents an overall introduction to the study; in Chapter Two, a detailed survey of the relevant literature is presented; Chapter Three, discusses the materials and various testing methods employed; Chapter Four, discusses the results of the experimental techniques; Chapter Five, discusses the analytical modeling and in Chapter Six, summary and conclusions are given on the study.

CHAPTER TWO: LITERATURE REVIEW

2.1 Introduction

In Chapter One it was briefly noted that crack resistance of concrete repair mortars depends upon the interaction of many different material properties. In this chapter, a detailed literature review is conducted on the different factors affecting performance of concrete repair mortars/bonded overlays. The problems such as cracking, debonding, etc. that are associated with performance of bonded overlays are discussed. A discussion of the many methods of testing restrained-shrinkage cracking in concrete is provided. The chapter closes by listing measures that can be taken to minimize restrained shrinkage cracking in bonded overlays.

2.2 Performance of concrete repair mortars

Concrete repair mortars/ overlays have a wide range of applications. They are used for both structural and non-structural repairs in concrete members or elements such as slabs on grade, pavements, tunnel linings etc. (Banthia *et al.*, 1996). The use of repair mortars/overlays affords the following advantages:

- Restoring structural integrity i.e. strength, abrasion resistance, etc. of the repaired member.
- Restoring or improving appearance of the existing structure or member.
- Improving the serviceability of the member or structure.
- Restoring performance level of member or structure, hence improving its durability.

Despite the above advantages, the long term performance of overlay repairs is usually affected by such effects as early age surface cracking, spalling, edge lifting or interface debonding as shown in Figure 2.1. If debonding and cracking are severe, premature failure occurs. While debonding can be successfully tackled by proper surface preparation techniques such as water-jetting, sand-blasting, shotblasting and the use of bonding agents, surface cracking, especially

early age cracking, has proven a more difficult problem to control. Cracking is undesirable because it compromises the durability of the structure or member by allowing deleterious substances such as chlorides into the member that might harm the reinforcement. The main cause of cracking is restrained shrinkage (Masuku, 2009). Figure 2.2 below shows some examples of shrinkage cracking and spalling.

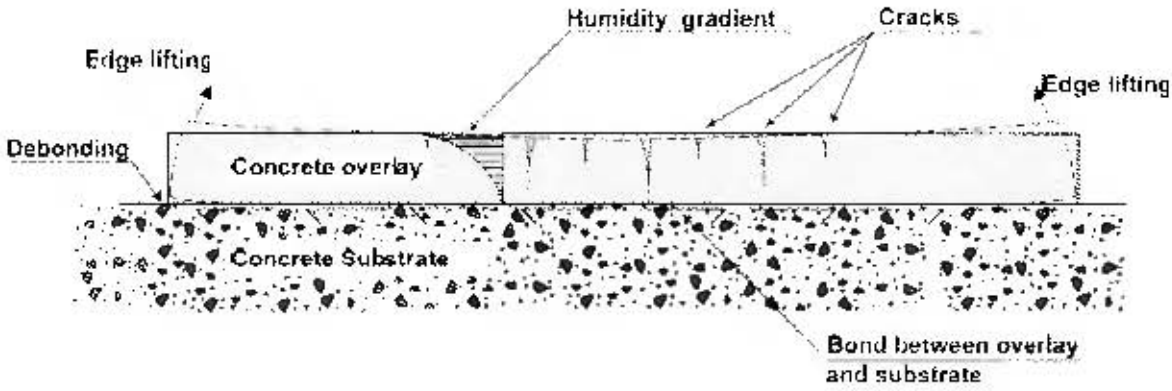

Figure 2.1 Cracking, debonding and edge lifting in concrete overlays as presented in Carlsward (2006).

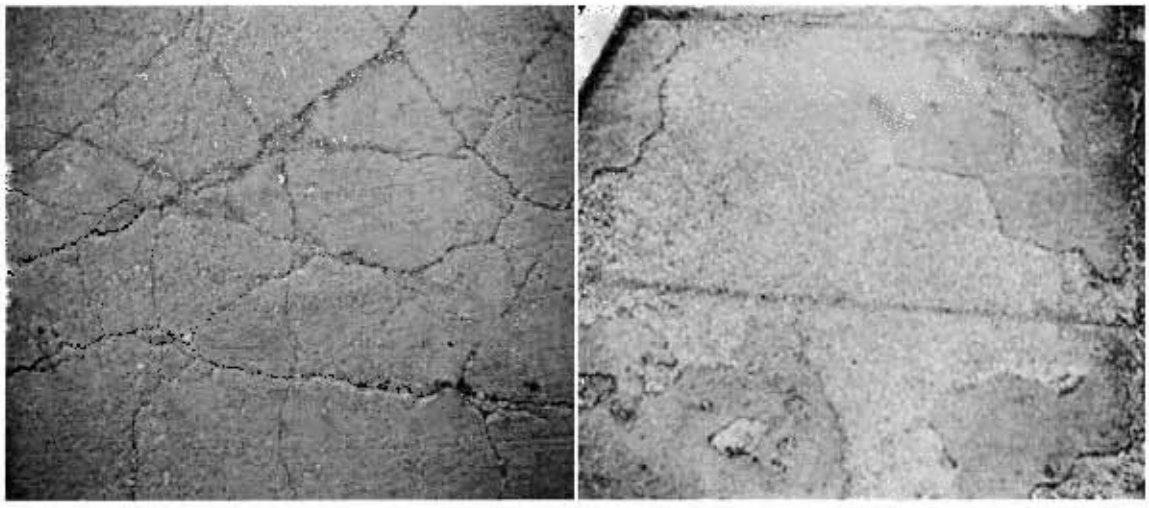

Figure 2.2 Cracking and spalling in overlays.
(www.concretenetwork.com)

Restrained shrinkage arising due to moisture loss may lead to early age (within 72 hrs after casting) cracking. Loss of moisture can lead to plastic shrinkage in newly cast concrete or drying shrinkage in aging concrete, while a reduction in overall concrete temperature will cause thermal shrinkage (see Section 2.3.5). Free shrinkage will cause lateral strains which, if concrete is restrained, may result in tensile stresses. In bonded overlays, the differential shrinkage between concrete substrate and repair material generates tensile stresses. These stresses may lead to cracking of concrete if the tensile strength of the concrete is exceeded, thus compromising both the durability and serviceability requirements (Banthia & Gupta, 2009; Kheder, 1997).

The performance of overlays with respect to cracking is governed by the interaction of the residual stresses arising from restrained shrinkage with the different material properties e.g. tensile strength, elastic modulus, tensile relaxation, etc. Crack initiation and development will depend upon the time development of the concrete material properties and how these affect the residual stresses. As shown in Figure 2.3, if the tensile strength of the material is greater than the tensile stresses, the material will not crack. However, if the arising tensile stresses from restrained shrinkage are greater than tensile strength, the material may crack. Whether the material cracks or not, also depends upon the degree or amount of relaxation due to creep that the concrete undergoes. As can be seen from the graph, relaxation helps alleviate some of the tensile stresses. Tensile relaxation delays crack initiation through stress relief. Also important is the time development of elastic modulus. A very stiff mix results in very high tensile stresses that may lead to cracking.

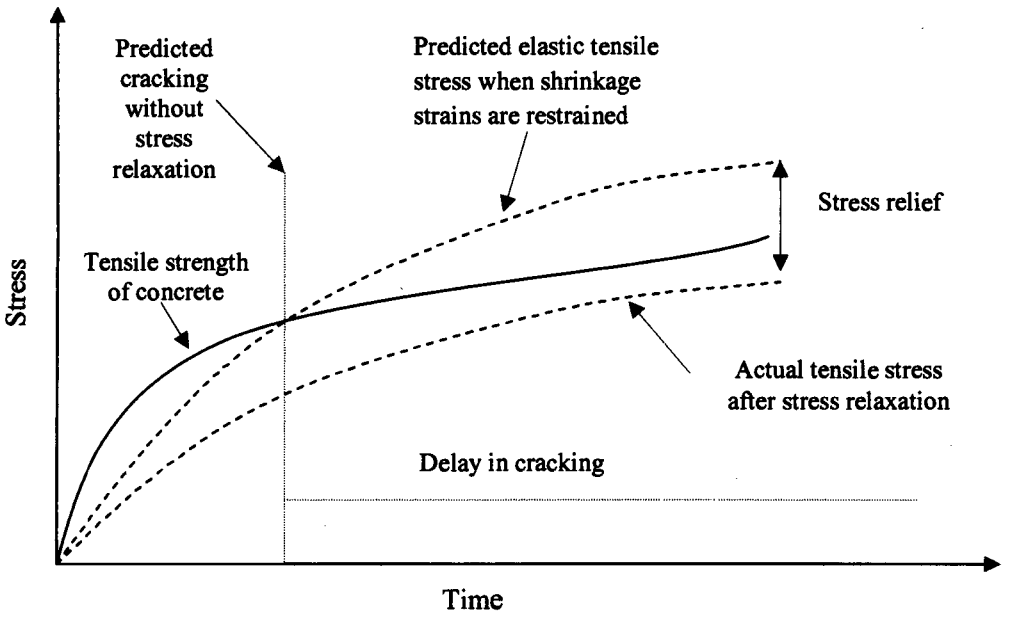

Figure 2.3 Influence of shrinkage and creep on concrete cracking adopted from Troxell *et al.* (1968).

As discussed above, the interaction of restrained shrinkage and the different material properties determines whether the material will crack. It is therefore, important to understand shrinkage and the different factors that affect it.

2.3 Shrinkage

Shrinkage is the time-dependent decrease in volume in both fresh and hardened concrete. A decrease in volume can be as a result of moisture movement within and out of the concrete due to hydration processes and surrounding environment, respectively (Alexander & Beushausen, 2009). Typically, the major contribution of total shrinkage is a result of drying shrinkage due to moisture diffusion and autogenous shrinkage due to the hydration process between water and cement.

Shrinkage is affected by both intrinsic and extrinsic factors. Intrinsic factors include structure and volume of the cement paste, aggregate type and content, cement type etc. while extrinsic factors include temperature, relative humidity, member geometry etc. At high relative humidity

the rate of shrinkage drops as the degree of moisture loss decreases, while the converse is true for concrete exposed to low relative humidity. If concrete is allowed to shrink freely a curve similar to that shown in Figure 2.4, is observed. However if concrete is stored in water after being allowed to shrink, the curve would drop as shown. Shrinkage therefore consists of reversible and irreversible components, and Figure 2.4 shows its basic characteristics.

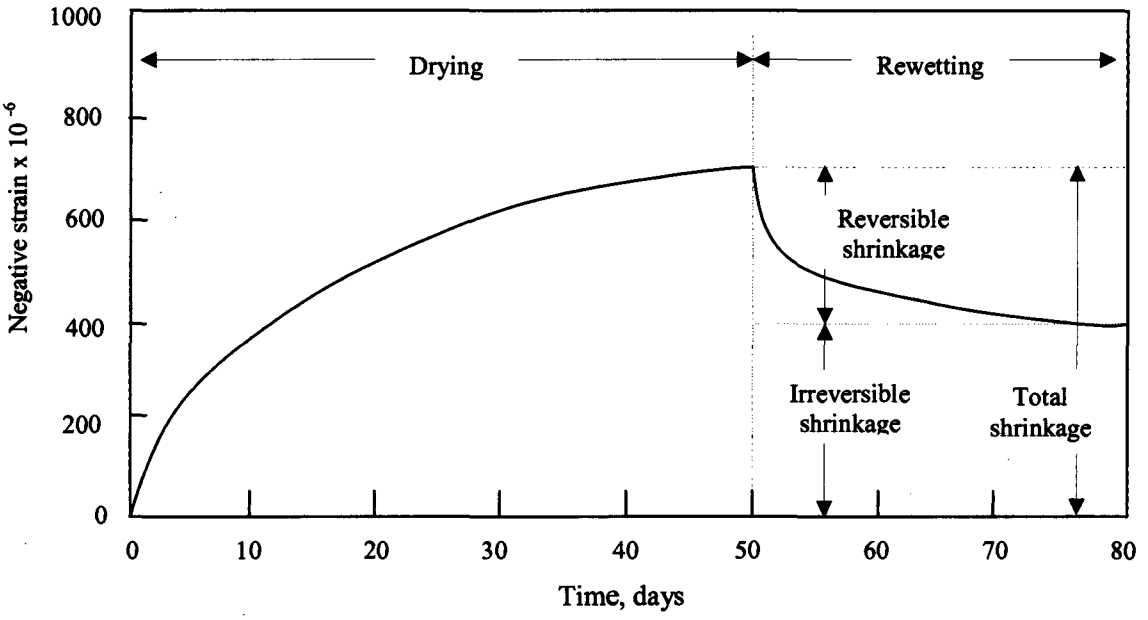

Figure 2.4 Basic characteristics of shrinkage as presented in Mehta & Monteiro (2006a).

Shrinkage can be classified into four broad categories, namely: plastic shrinkage, autogenous shrinkage, carbonation shrinkage, and drying shrinkage.

2.3.1 Plastic shrinkage

Plastic shrinkage is the volume reduction of concrete due to rapid removal of water from the concrete surface during early ages. It occurs within the first few hours after casting or placement. Plastic shrinkage occurs when the rate of moisture loss to the surrounding exceeds the rate of bleeding of the concrete. If excessive surface moisture loss occurs, a drop in the capillary pressure may lead to development of compressive strains. If concrete is restrained, these compressive strains may result in tensile stresses far in excess of those needed to cause cracking

in young concrete with poorly developed strength (Banthia & Gupta, 2009). Fresh concrete is susceptible to plastic shrinkage cracking especially during hot, windy, and dry weather conditions, in addition to high concrete temperature (Grzybowski & Shah, 1990). Concrete elements with high surface area to volume ratio e.g. thin bonded overlays, patch repairs, etc. are typically susceptible to early age cracks. These cracks are roughly straight but discontinuous and closely spaced depending on dimensions of the specimen. In overlays with large surface area, crack patterns due to plastic shrinkage are random.

Ravina & Shalon (1968) showed that rapid evaporation has a predominant effect on plastic shrinkage of concrete. Surface evaporation results in a hygral gradient in the concrete, which may lead to cracking at the surface. Therefore, complete elimination or reduction of evaporation immediately on casting reduces plastic shrinkage. When there is a high speed wind, concrete casting should be avoided, or wind breaks or fogging should be used to prevent water loss. Proper curing has been recognized as key in controlling plastic shrinkage cracking (see Lerch, 1957; Uno, 1998; NRMCA, 1998; ACI Committee 224, 2007).

2.3.2 Autogenous shrinkage

Autogenous shrinkage or basic shrinkage is the reduction in volume due to internal water consumption by hydration reactions. The autogenous shrinkage develops very early (immediately after setting) due to internal consumption of water in hydration reactions, and then the rate drops rapidly (Alexander & Beushausen, 2009). During the hydration process, hydration products have volumes less than their reactants resulting in volume reduction. Autogenous shrinkage is considered basic component of shrinkage as volume reduction occurs without loss of water from the surface of concrete. It is relatively low in normal concretes with w/c ratios above 0.4 compared to concretes having w/c lower than 0.4. In High Performance concrete (HPC) and Ultra High Performance concrete (UHPC), autogenous shrinkage is of the same order as drying shrinkage because of the higher rates of hydration in both HPC and UHPC concretes.

Carlsward (2006) argued that even though autogenous shrinkage may be lower in normal concrete, its presence could be substantial. Chen *et al.* (2010) used a novel experimental technique viz. Cure Reference Method (CRM) to study surface shrinkage characteristics in

cementatious materials, in particular, to explore the relative contribution of autogenous shrinkage to overall shrinkage in cementitious materials. They investigated the effect of w/c ratio on overall shrinkage in sealed specimens, and found that the surface shrinkage of specimens with w/c of 0.4 was greater than that of specimens with w/c of 0.6. They attributed this phenomenon to the difference in hydration rate of cementitious specimens with different w/c, where lower w/c specimens hydrate and experience shrinkage at a faster rate.

To prevent autogenous shrinkage, low water-cement ratios are not preferred. When it is necessary to use a low water-cement ratio, other methods should be used to compesate for the lack of water due to the low water-cement ratio in the mix design. Traditional curing methods are ineffective in reducing autogenous shrinkage because of its internal and chemically initiated nature. Zhutovsky *et al.* (2004) used pre-soaked lightweight aggregates in their concrete mix in order to reduce autogenous shrinkage. Such aggregate acts as an internal water reservoir preventing reduction of relative humidity in the concrete. They concluded that through control of size and porosity of lightweight aggregates, autogenous shrinkage was reduced.

2.3.3 Carbonation shrinkage

Carbonation shrinkage is the reduction in volume resulting from the reaction of the constituents of the hardened cement paste with atmospheric carbon dioxide (Alexander & Beushausen, 2009). The chemical reaction of carbonation leads to a reorganization of the microstructure, a decrease in porosity, and also a decrease in total volume involving a differential shrinkage between the surface and the bulk of the concrete. Carbonation shrinkage occurs over a long period, and may in some cases exceed the drying shrinkage in magnitude.

According to Verbeck (1958), humidity during exposure to carbon dioxide is the major factor influencing the shrinkage directly produced by carbonation. Figure 2.5 shows that carbonation shrinkage is a function of relative humidity and is greatest at intermediate humidities. Carbonation is reduced at either higher or lower humidities, in the former case since carbon dioxide cannot penetrate the water-filled pore spaces easily, and in the latter case due to the

absence of water fumes (water is needed in the chemical reaction). As can be seen from the figure, carbonation shrinkage is greatest when carbonation occurs subsequent to drying.

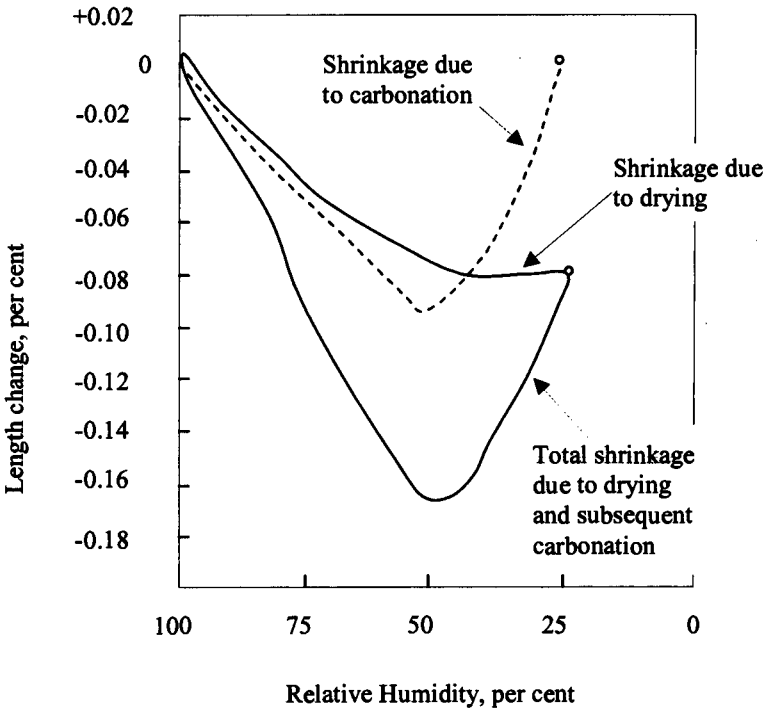

Figure 2.5: The effect of relative humidity on carbonation and drying shrinkage as reported by Verbeck (1958).

2.3.4 Drying shrinkage

Drying shrinkage is the time-dependent reduction in volume of concrete caused by loss of moisture from concrete to the environment. Evaporation of free water from capillary pores results in a decrease in the volume of concrete. The rate at which moisture is lost is fairly slow and the strain response is time dependent. In normal strength concrete (w/c > 0.4) which experiences little autogenous shrinkage, the total measured shrinkage is usually taken to be the drying shrinkage (Alexander & Beushausen, 2009).

The principal source of drying shrinkage in concrete is the cement paste. According to Asad *et al.* (1997), drying shrinkage of cementitious materials is caused principally by contraction of

calcium silicate hydrate (C-S-H) gel in hardened cement paste. It is within the cement paste that water is lost and volume changes occur. The three mechanisms by which the loss of water causes volume changes are capillary stress, disjoining pressure and surface tension. Capillary stress occurs at relative humidities between 45 and 95% when a meniscus forms on the adsorbed water between cement surfaces. The meniscus is under hydrostatic tension and places the cement in hydrostatic compression. This compressive stress reduces the size of the capillary pores, and thus causes a reduction in the overall volume of the cement paste. Capillary stress is a function of the capillary pore size, surface tension of the water, and the relative humidity. Disjoining pressure is the pressure caused by adsorbed water confined within the small spaces of the capillary pores. In this narrow space, the water exerts pressure on the adjacent cement surfaces. When the adsorbed water is lost, the disjoining pressure is reduced and the cement particles are drawn closer together, which results in shrinkage. Changes in surface tension are the causes of shrinkage at relative humidies below 45%. The last molecular layers of water surrounding cement particles are the most strongly adsorbed. This water has a high surface tension and exerts a compressive force on the cement gel, causing a net reduction in volume (Mindess *et al.*, 2003).

Many factors can directly affect the drying shrinkage of concrete e.g. paste volume, water-cement ratio, aggregate volume etc. Since the principle source of shrinkage is the cement paste, drying shrinkage will be greatly reduced if the paste volume is reduced.

2.3.5 Thermal shrinkage

In massive structures and under extreme climatic condition, the combination of heat produced by cement hydration and relatively poor heat dissipation conditions results in large rise in concrete temperature within a few days after placement (Mehta & Monteiro, 2006a). In fact, work by Ballim and colleagues (Ballim & Graham, 2003; Ballim, 2004; Ballim & Graham, 2004; Ballim & Graham, 2009; Beushausen *et al.*, 2012) has shown that this temperature rise is considerable within a few hours after placement. The restrained thermal shrinkage that occurs during the cooling phase can introduce cracking. For the more normal applications of concrete, the factors affecting its thermal movement are moisture content, type of aggregate, and volume concentration of aggregate (Alexander & Beushausen, 2009). Efforts to control temperature rise in massive structures is made through proper selection of materials, mix proportions, curing

conditions and construction practices. The use of slag can significantly reduce the heat of hydration, thereby reducing the possibility of thermal cracking (Mizobuchi *et al.*, 2000).

2.4 Creep and tensile relaxation

While cracking of bonded overlays is as a result of restrained shrinkage, creep effects have been shown to reduce the resulting tensile stress through relaxation. Creep and relaxation are both manifestations of the viscoelasticity of concrete and as such, researchers have tended to use one or the other. Most studies on tensile relaxation have generally used creep properties for determination of relaxation in composite systems (see Gutsch & Rostasy, 1995; Gutsch, 2002; Yuan *et al.*, 2003; Carlsward, 2006; Ghali *et al.*, 2006). This may be due to lack of sufficient data accumulated on tensile stress relaxation (Morimoto & Koyanagi, 1995; Alexander & Beushausen, 2009). Tensile relaxation is defined as the time dependent decrease in the stress of the body under a sustained strain (Alexander & Beushausen, 2009), Figure 2.6. Creep, on the other hand, is the time dependent increase in the strain of the body under a sustained stress.

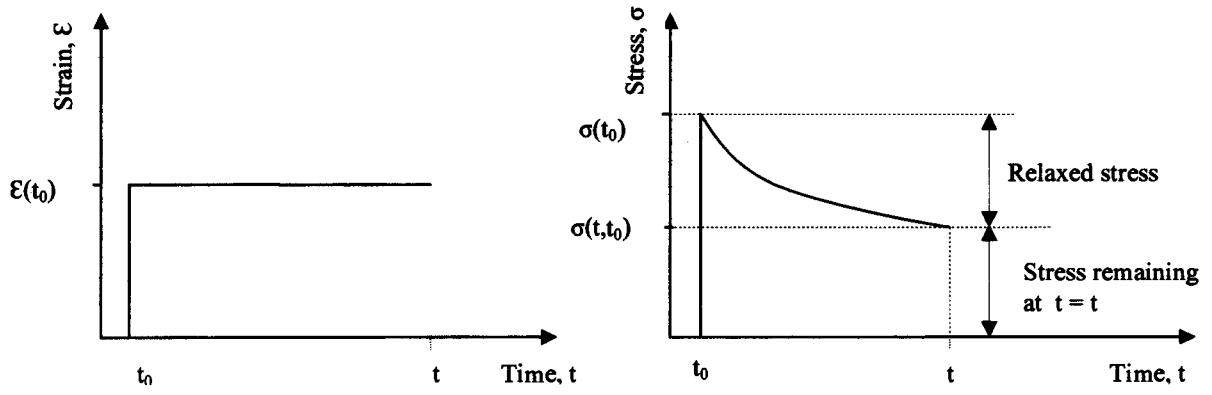

Figure 2.6: Stress relaxation in concrete exposed to sustained strain.

As stated above, creep and relaxation are both a result of the visco-elastic behaviour of concrete and their source is in the cement paste. Various authors attribute creep and relaxation to different processes. Powers (1968) explains that when concrete is subjected to sustained loading, load bearing water within cement paste moves through diffusion mechanisms. On the other hand Feldman & Sereda (1968) proposed that creep is caused by movement of interlayer water

between gel layers. Furthermore, movement of water causes gel layers to slide over each other causing micro-structural changes. With cement paste consisting of numerous such layers sliding over each other, global deformation is imminent. Pigeon & Bissonnette (1999) use the viscous shear theory to explain mechanisms occurring in concrete under tensile loading. From their study they concluded that the dominant mechanism in relaxation was viscous shear and also the presence of microcracking.

Creep in concrete occurs at all stress levels, and it imparts a degree of ductility to the concrete which is desirable for stress relief. The study by Altoubat and Lange (2001) found that tensile creep relaxes the shrinkage stress by as much as 50% and doubles the failure strain capacity. Tensile relaxation values as high as 60% have been reported by researchers (Yokoyama, *et al.*, 1994; Gutsch & Rostasy, 1995; Beushausen & Alexander, 2006; Masuku, 2009). According to Pigeon & Bissonnette (1999), tensile creep is the main mechanism of stress relief in very thin bonded concrete overlays. It is generally acknowledged that a high level of relaxation will help reduce the tensile stress resulting from restrained shrinkage. Loser & Leemann (2009) note that efforts to reduce risk of cracking in concrete overlays have to be based on a control of the relation between stress development and relaxation.

Masuku (2009) studied the effect of mix design (w/c) and age at loading on tensile stress relaxation in bonded overlays. In this study, dog bone specimens of three mortar types with w/c = 0.6, w/c = 0.45 and a commercial mortar were investigated. To investigate the influence of age at loading, the specimens were tested either at 2 days or 7 days. A higher stress-strength ratio of 80% was used so as to simulate tensile relaxation under extreme conditions. Results indicated that tensile relaxation is w/c sensitive: 0.6 w/c specimens generally showed 10% higher relaxation after 72 hours compared to their 0.45 w/c counterparts. He attributed this to the pore structure which may determine the strength and stiffness of the mix. Generally in low w/c mixes, strength and elastic modulus are higher than in higher w/c mixes. Therefore there is a tendency to resist mechanisms which promote relaxation. It was also found that irrespective of w/c, concrete age had a higher influence on tensile relaxation. Specimens tested at 2 days had 15% more relaxation than those tested at 7 days. Relaxation was found to reduce with increasing age. This was attributed to the dependence of relaxation on the degree of hydration (Neville, 1996).

The degree of hydration is initially rapid but reduces gradually with time. Results in this study also indicated that stress relaxation progressed more rapidly in specimens tested at 2 days compared to those tested at 7 days. Generally tensile relaxation was found to be in the order of 20% to 45% in the mixes tested.

2.5 Factors affecting restrained shrinkage cracking

2.5.1 Paste content and water-cement ratio

The hydrated cement paste plays an important role in the shrinkage cracking of concrete. This is due to the fact that the source of both shrinkage and relaxation due to creep effects is in the cement paste. It is within the cement paste that water is lost and volume changes occur. The most important factor influencing drying shrinkage is the amount and composition of cement paste. The paste is affected by the w/c ratio and the cement content. For concrete with w/c ratios between 0.35 and 0.5 it was shown that the extent of shrinkage is directly proportional to the amount of cement paste (Carlsward, 2006). For a given cement content, with increasing water-cement ratio, both the drying shrinkage and creep are known to increase. The data in Figure 2.7 show that, for a given water-cement ratio, both the drying shrinkage and the creep increased with increasing cement content. This is expected due to an increase in the volume of the cement paste (Mehta & Monteiro, 2006a).

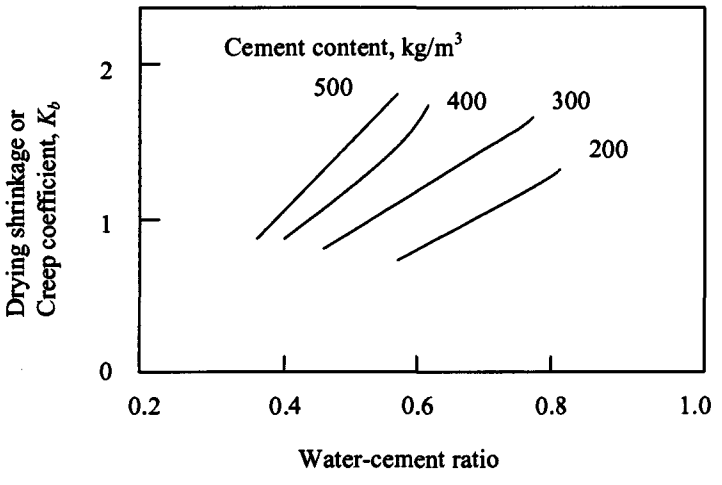

Figure 2.7: The effect of water-cement ratio on shrinkage or creep as presented in Mehta & Monteiro (2006a).

Loser & Leemann (2009) studied the effects of volume of paste and water content on the shrinkage of self-compacting concrete (SCC) compared to conventionally vibrated concrete (CVC) and concluded that, shrinkage is mainly dependent on the volume of paste. Since SCC has generally a higher volume of paste compared to CVC, its shrinkage is higher than that of CVC. They found that the difference in shrinkage between the two concretes at the same age ranged between 10% and 40%.

The w/c ratio affects the strength, elastic modulus and permeability of the cement paste, and therefore indirectly affects the creep of the paste. Ruetz (1965) showed that a decrease in w/c ratio caused a decrease in creep. This is because stronger pastes (pastes with low w/c) are also stiffer, hence they creep less. A decrease in water-cement ratio also implies an increase in the tensile strength of the material. High tensile strength is beneficial because of its desirable effect on the material's cracking potential.

In practice, the cement content and the water-cement ratio are limited to reduce the risk of shrinkage cracking. Literature indicates that a minimum cement content should be used to reduce cracking (Brown *et al.*, 2003). The investigations by Xi *et al.* (2003) on early age cracking of newly constructed concrete bridge decks in Colorado, USA, showed that a concrete mix with a cement content of about 279 kg/m^3 and water-cement ratio of about 0.4 could provide an optimum mix for Colorado conditions. The importance of paste volume on shrinkage implies that, shrinkage can be mitigated by reducing the water content or cement content, and increasing the content of aggregates.

2.5.2 Fineness and composition of cement

Physical characteristics of cement such as particle size also play an important role in shrinkage cracking. Drying shrinkage is affected by the fineness of the cement. Finer cement particles generate greater heat of hydration and require a greater amount of water during the hydration process, which may lead to the increased risk of cracking in the concrete. Larger cement particles that do not undergo full hydration can provide a restraining effect similar to that of aggregates. According to Tritsch *et al.* (2005), replacing a fine-ground cement (Type I Portland cement) with a coarse-ground cement (Type II Portland cement) lowers the free shrinkage and shrinkage rate,

and adding a shrinkage-reducing admixture significantly reduces these values. However, Mehta & Monteiro (2006a) point out that, normal changes in cement fineness or composition which tend to influence the drying shrinkage behaviour of small specimens of cement paste or mortar, have negligible effect on concrete.

2.5.3 Aggregate type and content

The type and content of aggregate has an effect on the restrained shrinkage cracking of concrete. According to Alexander (2001) aggregates have two effects on paste shrinkage viz. dilution and restraint. Dilution refers to the fact that shrinkage of the concrete will decrease with increasing aggregate concentration, while restraint refers to the fact that concrete shrinkage will decrease with increase in aggregate stiffness. Aggregates provide restraint because they do not undergo volume changes due to changing moisture conditions. The amount, size,grading, texture and stiffness of an aggregate determine how much restraint it provides (Mindess *et al.*, 2003). Well-graded aggregates with a large maximum size have a low void space and, consequently, require a relatively small amount of paste. Larger maximum sizes of aggregates are effective in reducing shrinkage. Emmons & Vaysburd (1995) report that concrete of the same cement content and slump containing 10 mm maximum size aggregate usually develop from 10% to 20% greater drying shrinkage than concrete containing 19 mm maximum size aggregate, and from 20% to 35% greater drying shrinkage than concrete containing 38 mm maximum size aggregate.

Troxell *et al.* (1958) state that the most important aggregate characteristic influencing shrinkage cracking is the aggregate stiffness. In their study, they found that both the drying shrinkage and creep of concrete increased 2.5 times when a high elastic modulus aggregate was sustituted with a low elastic modulus aggregate. Granite, limestone, and quartzite do not shrink (Neville, 1996). Lightweight aggregates with low moduli of elasticity exhibit higher shrinkage (Mindess *et al.*, 2003). For normal concretes, aggregates do not exhibit creep at the stress levels to which they are subjected. According to Alexander (2001), aggregates reduce the creep of concrete by diluting the paste and restraining its movement. Concrete creep is therefore affected by aggegate volume concentration and aggregate stiffness. The higher the elastic modulus of the aggregate, the greater will be the restraint offered by the aggregate to the creep of the paste.

Banthia & Gupta (2009) investigated the effect of sand-cement (s/c) ratio and aggregate-cement ratio (a/c) on shrinkage of concrete. They noted that while s/c ratio appears to affect the evaporation rate, time to first crack and crack width of the concrete, a definite trend of its influence could not be established. They however noted that an increase in the a/c ratio on the other hand was highly effective in reducing shrinkage cracking. This was in agreement with the earlier finding by Pickett (1956), who found that the shrinkage of concrete was reduced by 20% for mixes with the same water-cement ratio in which the aggregate content was increased from 71% to 74%. Figure 2.8 shows the influence of aggregate content on the shrinkage and creep of concrete.

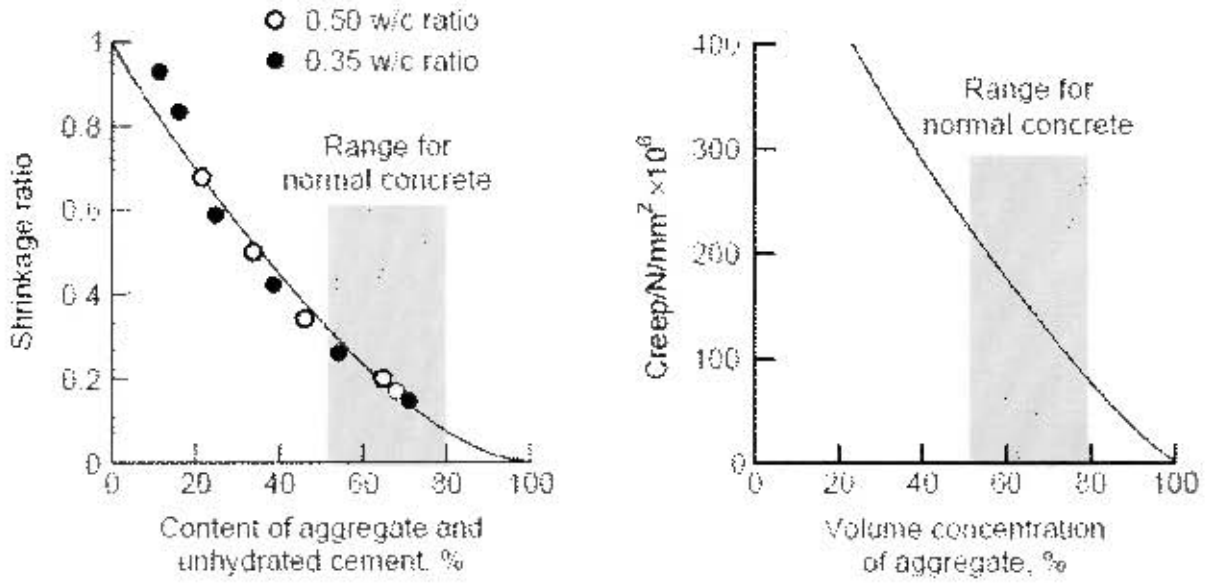

Figure 2.8: Influence of aggregate content on the shrinkage and creep of concrete as reported by Mehta & Monteiro (2006a).

2.5.4 Cement extenders

Many researchers have noted that the use of cement extenders has a significant influence on creep and shrinkage of concrete. Many authors (Mindess *et al.*, 2003; Krauss & Rogalla,1996; Neville, 1996) have indicated that concrete shrinkage is little influenced by condensed silica fume (CSF) contents, at least up to 10% by mass of cement. CSF has the effect of densifying the microstructure of concrete, thus reducing the rate of moisture loss from concrete. Shrinkage thus

takes place at a slower rate in CSF concretes, although the final shrinkage will be similar to other comparable concretes.

Pane & Hansen (2002) studied the effect of fly ash (FA), ground granulated blastfurnace slag (GGBS) and CSF on early age tensile creep of concrete. Figure 2.9 shows the result of their study. In their study, creep was represented as a compliance function i.e. the sum of the instantaneous and creep strains at time t produced by a sustained unit stress applied at t'. The graphs show that creep compliance of concrete is reduced by the presence of additives except for the CSF concrete. This seems to agree with findings from South Africa, except for CSF which has been indicated to reduce creep also (Grieve, 1991; Alexander, 1994). However, in a study by Tarek & Sanjayan (2008) on early age cracking of slag concretes, it was found that no significant change in tensile creep occurred with slag replacement levels of 0, 35, 50% and 65%.

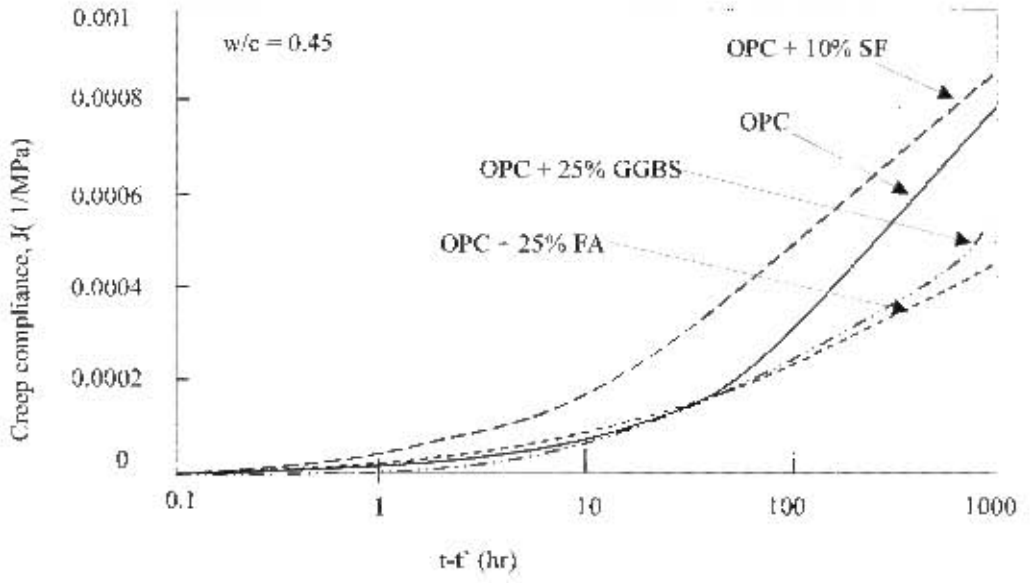

Figure 2.9: Typical tensile creep compliances of concrete containing blended cements at age = 3 days, as presented in Pane & Hansen (2002).

In the study by Tarek & Sanjayan (2008) mentioned above, it was found that, at lower slag levels (0, 35 and 50%) the tensile strength decreased with increasing slag replacement. However, this is more than compesated by decreasing elastic modulus of the slag concrete compared to the

ordinary concrete. This has significance in reducing the stress development in slag concretes, and thereby reducing the cracking potential.

2.5.5 Shrinkage Reducing Admixtures

Many researchers (Shah *et al.*, 1998; Weiss & Shah, 2002; See *et al.*, 2003) have observed improved shrinkage and cracking resistance in concrete by using shrinkage reducing admixtures (SRA). SRAs work by reducing the surface tension of the mix water, which in turn reduces the stresses in the capillary pores (Shah *et al.*, 1998). Pease *et al.* (2005) showed that there is a linear relationship between the surface tension of the SRA-pore water solution of concrete and the shrinkage coefficient as shown in Figure 2.10. According to Radlinska *et al.* (2007), SRAs have two effects on concrete shrinkage; firstly, SRAs reduce the overall magnitude of shrinkage, and secondly SRAs reduce the rate of shrinkage.

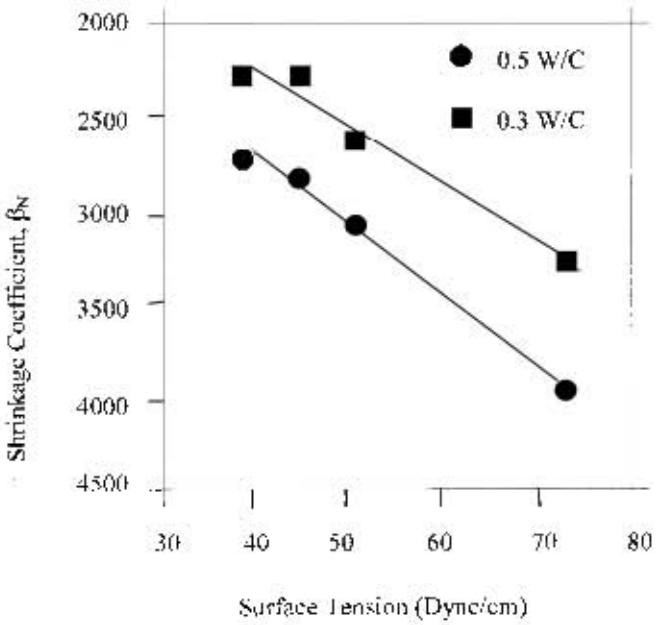

Figure 2.10: A plot of surface tension of SRA-pore water solution of concrete against shrinkage coefficient, from Pease *et al.*(2005).

2.5.6 Curing and fibers

Banthia & Gupta (2006) have recommended that the degree of early age shrinkage can be reduced by good curing practice. Deshpande *et. al* (2007) noted a reduction in overall shrinkage strain with an increase in curing period in ordinary concrete specimens. According to Krauss & Rogalla (1996), increasing the curing period decreases the shrinkage rate and also the extent of shrinkage. However, the ACI Committee 364 (2006) notes that curing only delays moisture evaporation and its associated drying shrinkage but does not reduce the overall shrinkage strain. Curing provides sufficient moisture to prevent the surface from drying out. Consequently this reduces the effects of surface cracking.

Bissonette & Pigeon (1995), Banthia & Gupta (2006) and Carlsward (2006) showed that the use of fibers reduces occurrence of early age shrinkage cracks. Banthia *et. al* (1996) investigated the effect of steel fibers on restrained shrinkage cracking of thin bonded overlays cast directly on substrate beams and exposed to a drying environment to induce shrinkage. Lengths and widths of the resulting cracks in the overlays were expressed as a function of time. Addition of fibers was found to delay the onset of cracking and also reduce the widths of the cracks. According to Shah & Weiss (2006), the age at which cracking becomes visible is slightly delayed by the inclusion of steel fibers presumably due to the fibers' ability to arrest cracking before the crack propagates across the specimen unstably. Fibers reduce crack widths by bridging the cracks formed and preventing them from widening.

2.5.7 Member size and shape

Drying shrinkage is also affected by the size and shape of the concrete member. Since drying shrinkage of concrete takes place from exposed surfaces, it generates moisture-content and thermal differentials, with associated restrained strains and internal strain gradients. Thus, actual observed shrinkage will depend upon member geometry and dimensions despite the fact that potential drying shrinkage is conceptually an intrinsic property of concrete (Alexander & Beushausen, 2009). Amba *et al.*, (2010), investigated the effect of property gradients (hydric and hydration) on the sensitivity to cracking of bonded overlays. Property gradients were measured using the "slice test" (Care & Nicolle, 2005) and strain gauges were used to measure strain

gradients. It was observed that moisture gradient, porosity and strain gradients were both dependent on the extent of the drying surface, and also the depth from it.

2.5.8 Temperature, relative humidity and time

Relative humidity (RH), temperature and time also affect shrinkage cracking of concrete. Figure 2.11 shows the effect of RH and time on the shrinkage of concrete. The rate of shrinkage decreases with time even though it is still measurable after 20 years (Troxell *et al.*, 1958). In a study done by Baroghel-Bouny & Godin (2001) a linear relationship between shrinkage strains and relative humidity was found for a large range of concrete mixes.

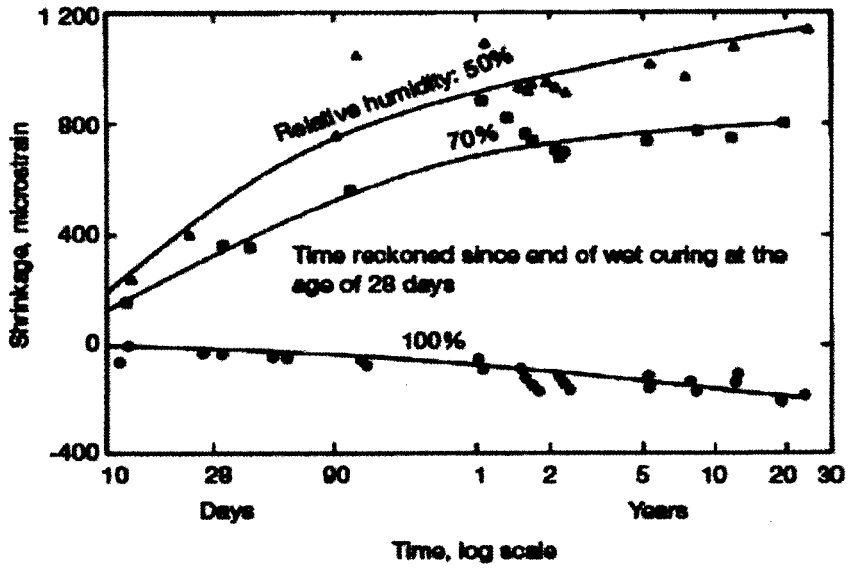

Figure 2.11: Relationship between shrinkage and time for concretes stored in different RH, as given in Troxell *et al,* (1958).

Appropriate curing and slow drying have a positive influence on drying shrinkage. Garas *et al.,* (2009), investigated the influence of thermal treatment on shrinkage of UHPC, and observed that steam curing reduced both drying shrinkage and swelling of UHPC. This was attributed to the improvement in the cementitious matrix achieved via thermal treatment, as the reaction of CSF and other phases may be activated, reducing the average pore size. This was in agreement with what was observed by Collepardi *et al.* (1997).

Environmental conditions such as relative humidity (RH) and temperature also affect the creep of concrete. The total creep comprising basic and drying creep will increase with a decrease in ambient RH or an increase in temperature. Lower RH considerably increase the creep of concrete that is allowed to dry for the first time under load. The enhanced creep seems to be due to higher creep rates during the earlier stages of drying. The RH effect is much smaller if concrete has previously reached hygral equilibrium with the environment before application of the load.

2.6 Methods of testing restrained shrinkage cracking

Various methods of testing restrained shrinkage and cracking of concrete have been developed by different researchers. Adequate performance with respect to cracking cannot be properly assessed on the basis of free shrinkage tests alone. In addition to shrinkage strains, testing methods need to account for arising stresses and stress relaxation. According to Bentur & Kovler (2003), the restrained shrinkage tests can be classified into four categories: ring tests with a restraining core, longitudinal tests where the restraint is at the edge of the specimen, panel tests in which the restraint is along the circumference of the panel, and tests in which restraint is offered by the substrate, simulating performance required in repair and retrofit.

2.6.1 Plate tests

Plate tests (also referred to as panel tests) are tests in which restraint is generated on the perimeter of the plate, and are generally used to evaluate plastic shrinkage cracking. Different researchers have used different test specimen sizes and test details. Usually very flat and thin concrete specimens are used, and the maximum aggregate sizes are small or no course aggregates are used. To simulate adverse drying conditions, some researchers use fans to blow hot air across the plate surface.

Kraai (1985) used a cracking test in which flat concrete specimens were exposed to severe drying conditions achieved by hot air blown by a fan, Figure 2.12. 19 mm thick plate specimens were cast in 610 x 910 mm wood forms with the bottom lined with plastic to prohibit absorption and reduce restraint. Edge restraint was provided by 13 x 25 mm mesh hardware cloth bent in an L-shape and attached to the base of the mold. Fresh concrete was then cast into the molds,

compacted and troweled, and then the specimens were immediately placed in front of fans producing air speeds of 4.5 - 5.4 m/s. The use of fans, in addition to low thickness and large surface area specimens, accelerated both evaporation and shrinkage rates. After 24 hours of drying, the specimens' cracking characteristics such as crack lengths and widths were measured. Two concrete specimens, one control and one with a single property altered were simultaneously cast and relative cracking potential was determined by comparing the two panels. The mixes tested contained 418 kg/m^3 of cement and a high water-cement ratio, 0.7. For this test, the suggested proportion of cement to aggregate was 1:4 by weight and no coarse aggregate was used due to the 19 mm thickness of the specimens. Kraai found that cracking began around one hour after drying was initiated and most of the cracking occurred within 4 hour.

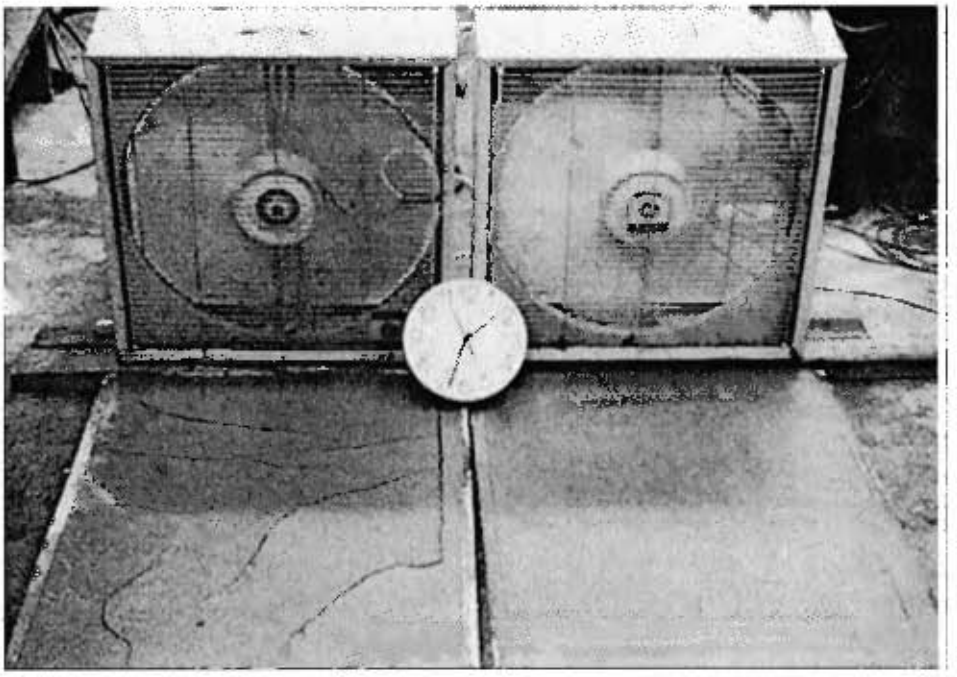

Figure 2.12: Plate test used in the study by Kraai (1985).

The above test by Kraai (1985) was also adopted by Shacles & Hover (1988) to assess how mix proportions and construction practices affect plastic shrinkage in concrete. In this test, the authors used plexiglass forms to make the specimens, and also expanded metal lath affixed to the inside perimeter of the form as edge restraint. The use of plexiglass forms prevented additional

moisture loss from the concrete to the forms, and also enhanced the durability of the test. In addition, the expanded metal laths improved the edge restraint of the test.

Figure 2.13 shows a schematic diagram of the plate test used by Yokoyama *et al.* (1994) to investigate the performance of low volume content polymer fibers, to reduce plastic shrinkage cracking. In this test, 600 x 600 mm slab moulds were used to cast concrete specimens, with restraint achieved by short steel bars at the edges of the plate. The surface was then subjected to drying by exposing it to hot air blown by a fan, simulating windy conditions. Performance of the concrete was then quantified in a variety of ways to estimate the extent of cracking: maximum crack width, total crack length and crack area.

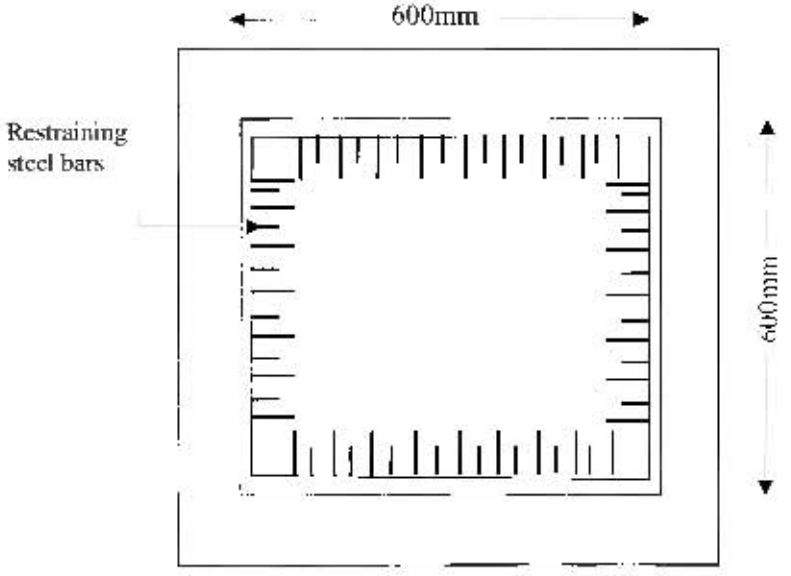

Figure 2.13: Plate test used in the study by Yokoyama *et al.* (1994).

2.6.2 Longitudinal test

Longitudinal tests are tests in which a linear specimen is restrained at one end and the other end is used to monitor the deformation or the force causing the deformation. Longitudinal tests can further be divided into longitudinal-qualitative, longitudinal-active and longitudinal-passive, as discussed in the following sections.

2.6.2.1 Longitudinal-qualitative

In the longitudinal-qualitative setup, the longitudinal geometry is used as a restraint to measure cracking only. There is no instrumentation used to estimate deformations or resulting stresses, except for a microscope that may be used when recording the width and number of cracks. The tests developed by Banthia. *et al.* (1993) and Berke & Dallaire (1994) are good examples.

In the test developed by Banthia *et al.* (1993), Figure 2.14, a 40 x 40 x 500 mm specimen was cast into a mould with triple bar anchors at its ends. The anchors were rigidly fixed to a 50 mm base plate through vertical posts. The mould itself was mounted on two frictionless rollers that were free to slide in the longitudinal direction. Concrete specimens were mounted on this assembly after demoulding, and the whole assembly was placed in an environment chamber at 50°C / 50% RH. Cracking was observed by means of a microscope travelling above the specimen, and the number of cracks, together with their widths, was recorded. This study investigated the effect of seven types of fibers (divided into two groups viz. macro-fibers and micro-fibers) on restrained shrinkage cracking of cement pastes and mortars. The results indicated different cracking patterns for the two different fiber groups, and this was attributed, in part, to their different reinforcing mechanisms.

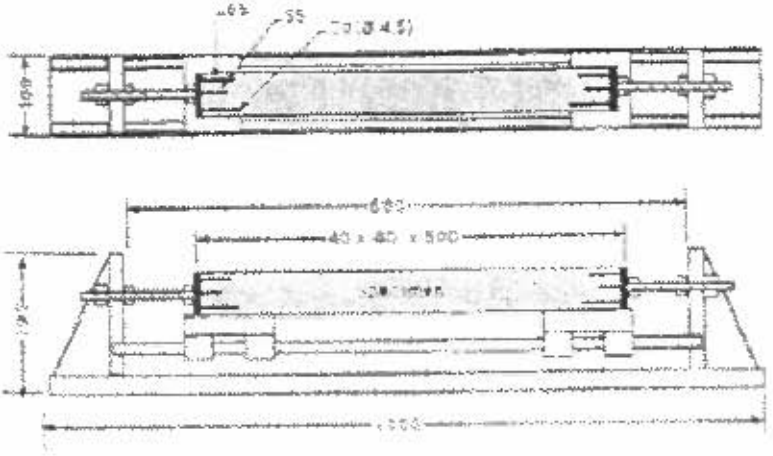

Figure 2.14: Longitudinal tests used in the study by Banthia *et al.* (1993).

2.6.2.2 Longitudinal-passive

In this test setup, the rig is partially instrumented to determine also the restraining forces and stresses. The test is passive in nature, since the restraint is achieved by longitudinal bars on which strain gauges are mounted. A good example of this setup is the RILEM cracking frame Standard test TC 119 (1997) used for crack evaluation (RILEM). Figure 2.15 shows a schematic of the test apparatus. The test is made up of a concrete beam and two surrounding steel bars in the longitudinal direction. The grip is of a tapered geometry, to eliminate stress concentrations that may result in premature cracking. This arrangement does not eliminate the deformations entirely, and the small deformations that occur are measured by the strain gauges on the steel bars. Restraining stress is calculated from the strain data and the steel and the concrete cross-section areas.

The cracking frame can be used to estimate both the compressive restraining stresses, which occur as the temperature increases immediately after casting, as well as restraining tensile stresses that occur on cooling later on. The bars are made of steel with a low coefficient of thermal expansion, so that the strain in it will not be affected by the temperature build up which occurs in the near concrete.

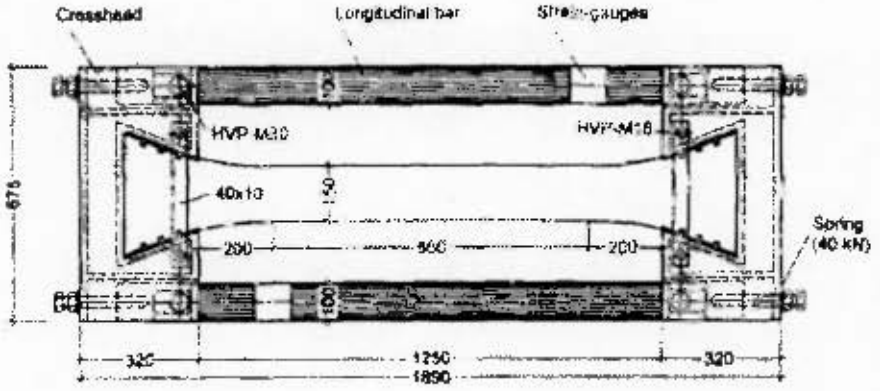

Figure 2.15: The RILEM cracking frame test (RILEM TC 119, 1997).

In the thermal tests, the parameters obtained are the stress development curves, the zero stress temperature (the temperature at which the compressive stress induced early on during heating is reduced back to zero) and the cracking temperature (the temperature in the cooling range at

which cracking occurs). If the cracking frame is cooled to the surrounding temperature and the specimen does not crack in four days, its temperature is decreased at a fixed rate until cracking occurs. The temperature at which cracking occurs is recorded as an indication of the cracking resistance property of the concrete mix in actual service conditions. The lower this temperature can be, the better the cracking resistance.

2.6.2.3 Longitudinal-active

In this setup, the rig is instrumented so that the grip position is adjusted to keep the specimen at zero deformation or close to it, while measuring the load in the grip. This test is viewed as an active one since there is a continuous need for external intervention to keep the specimen at zero strain. This category also includes fully instrumented tests in which a closed loop computer controlled system is used to control the grip position and fix it to zero strain while recording the load and deformation in the specimen.

A good example is the test by Paillere *et al.* (1989), in which autogenous shrinkage of silica fume concrete with steel fibers was studied. In this test, a concrete specimen was cast in a mould on a horizontal bench. The specimen was placed in a vertical position after the concrete had set to prevent any bending effects. The specimen had a cross-section of 8.5 x 12 cm and a total length of 1.50 m. One end of the specimen was fixed, while the other end was mobile to allow for shrinkage. A monitoring system at the mobile end of the specimen controlled a dynamometer that applied and recorded the force required to keep the specimen at constant length. The restrained shrinkage stress was calculated from this force and the cross-sectional area. Figure 2.16 shows this test setup. A companion specimen with the same geometry was also cast in a mould that allowed it to shrink freely without restraint at one end. Six concrete mixes with water-cement ratios between 0.26 and 0.44 and a constant cement content of 425 kg/m^3 were tested. The maximum size of coarse aggregate was 20 mm. Five mixes contained varying amounts of superplasticizer, and four of those mixes included 63.75 kg/m^3 of silica fume. Two different sizes of steel fibers were used, one size at a time, in three of the mixes. The authors found that addition of steel fibers to concrete increased the time to cracking and also restricted crack width development in silica fume concretes.

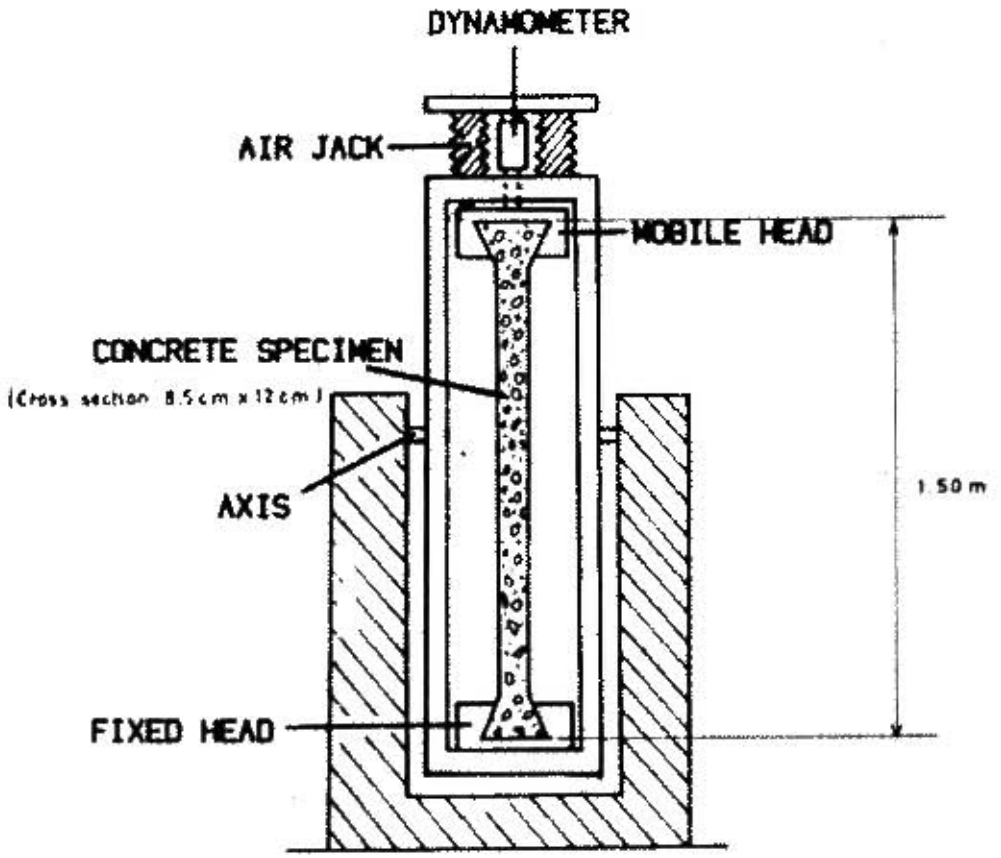

Figure 2.16: Longitudinal test used by Paillere *et al.* (1989).

2.6.3 Substrate restrained tests

Substrate restrained tests are test methods in which restraint is induced by the substrate. According to Bentur & Kovler (2003) these types of tests simulate better the conditions which occur in practice, especially in repair and resurfacing applications. They classified these tests into two categories, depending on the variable being assessed by the test: either cracking or curling. The cracking tests include the test described by Banthia *et al.* (1996) and the German angle test (German Federal Ministry of Transport, Highway Construction Department, 1990).

In the test by Banthia *et al.* (1996), Figure 2.17, a mold measuring 1010 mm long and 100 mm wide with a restraining substrate at the bottom was used to assess the cracking potential of fiber

reinforced concrete. The restraining substrate was a 40 mm concrete whose surface was roughened by manually placing 20 mm aggregates on the fresh concrete, followed by curing in hot water at 50°C for 3 days. After curing, the mold, together with the substrate, was thoroughly cleaned and dried. This ensured that the substrate surface was free of any loose material. Thereafter, an overlay of 100 mm deep concrete was cast on this substrate and placed in an environmental chamber in which hot air was blown over the specimen. The environment in the chamber was 38°C / 5% RH. The drying test started 2.5 hours after casting the overlay. Crack monitoring was carried out with a hand held microscope equipped with a vernier, and parameters such as time to first crack, crack width and crack length were recorded and used in the results analysis.

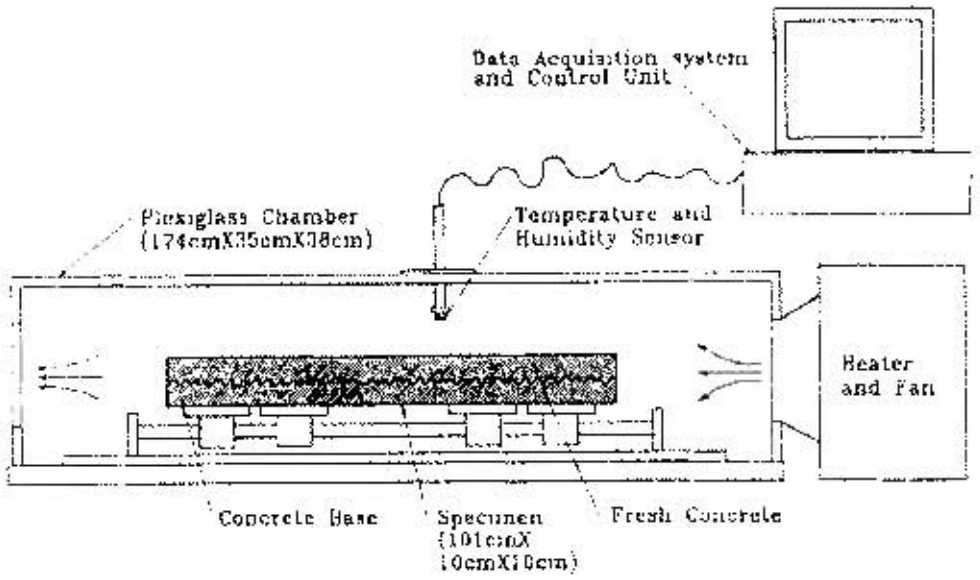

Figure 2.17: Substrate type test used by Banthia *et al.* (1996).

The German angle test is a linear restrained shrinkage test developed in German and adopted by the Highway Construction Department of the Federal Ministry for Transport. In this test, concrete is poured into a V-shaped channel (70 mm cross-section and 1000 mm long), which is kept uncovered in standard atmosphere (Figure 2.18). This method is intended for evaluation of plastic additives for overlays. Crack monitoring is continuously carried out at sensitivity better than 0.02 mm. After 90 days, any cracks having occurred are measured for crack width to within 0.02 mm, the number of cracks, the time of cracking, and also large areas of detachment from the

steel are also noted. Materials tested by this method with cracks wider than 0.1 mm are not accepted. Also, no bonding failure in large areas is allowed in this test.

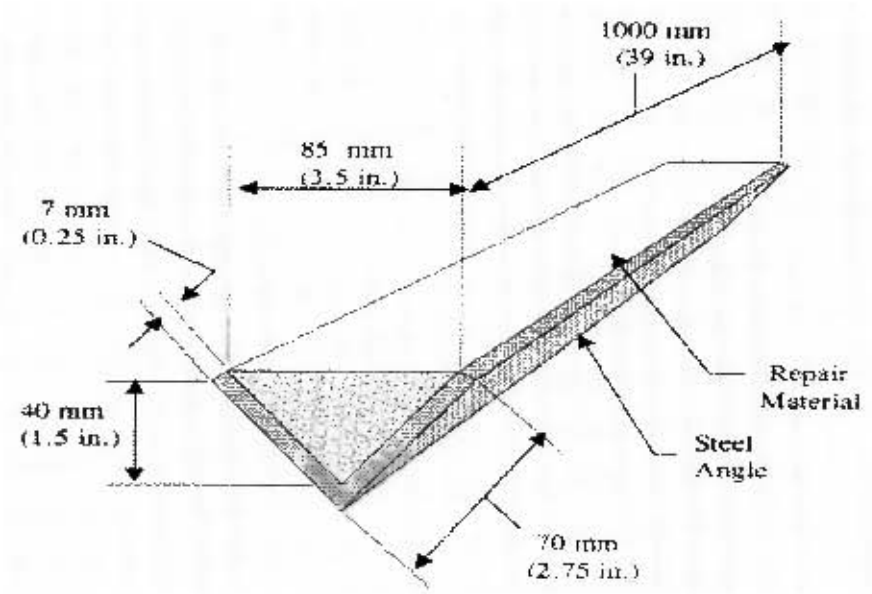

Figure 2.18: German angle test (Federal Ministry for Transport, German, 1990).

Banthia & Gupta (2009) developed a bonded overlay method to investigate the influence of mixture proportions on plastic shrinkage cracking in cementitious repairs and overlays. This test was based on the test by Banthia *et al.* (1996), although the size of the specimen was reduced to 325 x 95 x 40 mm and a base with protuberances was used. In this method, the cementitious material to be investigated was cast on a substrate base with protuberances and the entire assembly was subjected to drying in an environmental chamber, Figure 2.19. The use of a base with protuberances enabled a high degree of restraint, which resulted in cracking developing faster. Overlay cracking was then characterised with the help of a magnification device and image analysis software.

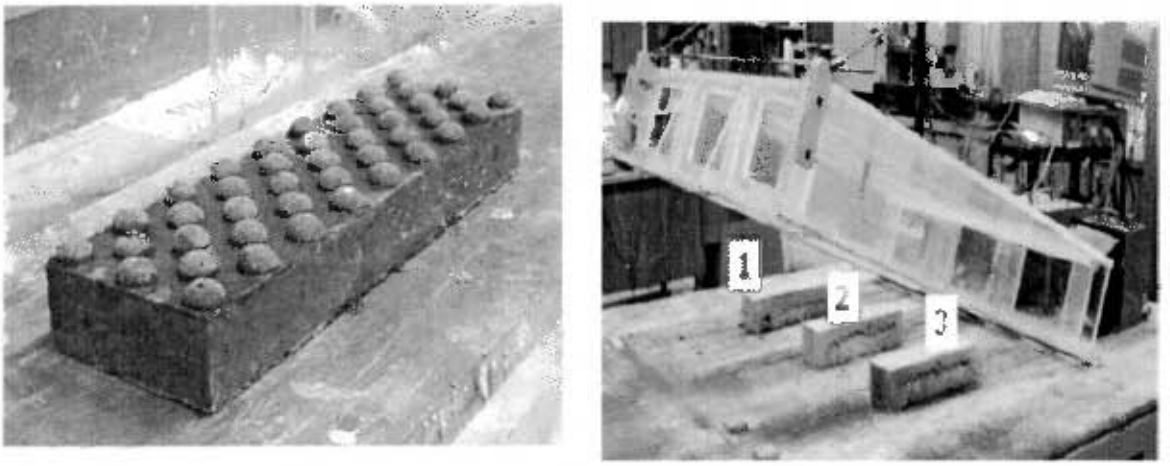

Figure 2.19: A substrate base with protuberances and a drying chamber used by Banthia & Gupta (2009).

2.6.4 Ring test

According to Bentur & Kovler (2003), the Ring test is the most common test used for estimating the cracking potential of repair mortars. It is applied to evaluate both the plastic shrinkage cracking of fresh concrete, as well as the shrinkage cracking of hardened concrete. In the ring test, a concrete annulus is cast around a restraining core (usually made of steel) and is allowed to shrink against it. Tensile tangential stresses are developed in the concrete ring, and if large enough (if they exceed the tensile strength of the material under test) they may lead to cracking.

The ring test has been used to evaluate cracking potential of cement-based materials for many years. Carlson and Reading (1988) discussed the first ring tests which were performed between 1939 and 1942. These tests were used to investigate the resistance of concrete to shrinkage cracking in concrete walls. The authors cast a ring of concrete (25 mm thick) around a polished ring of steel (25 mm thick and 175 mm diameter) and dried the concrete at 25, 50 and 75 % relative humidity, after a preliminary moist curing period. The height of the specimen was 38 mm, and only circumferential drying was allowed (the top and bottom surfaces were sealed). Time of cracking was determined by periodical visual inspection. Companion free shrinkage bars with the same cross section area as the ring were used to establish the strain at the time of cracking. So as to simulate shrinkage at the circumferential surface of the concrete ring, the free

shrinkage specimens were sealed to allow drying from one side only. Carlson and Reading used the strain from the free shrinkage bars to estimate the strain and stress in the ring at the time of cracking.

Two American standards for the ring test exist: the American Association of State Highways and Transportation Officials (AASHTO) standard and the American Society for Testing and Materials (ASTM) standard. These two tests are used to compare restrained shrinkage cracking potential of different concrete mixes. Factors such as cement paste content and water-cement ratio, cement type, aggregate type and content, and admixtures as related to the time and cracking potential of concrete are evaluated.

2.6.4.1 AASHTO Ring test

In the AASHTO Ring test (AASHTO PP34, 1998), the standard inside steel ring has a wall thickness of 12.7 ± 0.4 mm, an outside diameter of 305 mm, and a height of 152 mm. The outer ring can be made of 6.4 mm thick cardboard form tube with an inside diameter of 457 mm. Four strain gauges are mounted on the inner surface of the steel at equidistant points at mid height. Data acquisition equipment is used to record automatically the readings on the strain gauges. Forms can be made of 0.6 x 0.6 x 0.016 mm thick plywood sheet or PVC. Curing can be applied by using pre-wetted burlap covered with plastic. The outer forms are removed at an age of 24 ± 1 hr, and then the specimens are moved to the condition room with a constant air temperature of 23 ± 2.0° C and 50 ± 4 % relative humidity. The time and strain from the strain gauges are recorded every 30 minutes, and review of the strain and visual inspection of cracking is conducted every 2 or 3 days. A sudden strain decrease of more than 30 micro strains usually indicates cracking. After the concrete ring cracks, the time to cracking, cracking width and length on the exterior radial face is recorded (Zhuang, 2009).

2.6.4.2 ASTM Ring test

The ASTM Ring test (ASTM C 1581, 2004) differs from the AASHTO test in dimensional sizes. The standard inside steel ring has a wall thickness 13 ± 0.12 mm, an outer diameter of 330 ± 3.3 mm and a height of 152 ± 6 mm. At least two electrical resistance strain gauges are wired in a quarter bridge configuration. The base can be made of epoxy coated ply wood or other non-

absorptive and non-reactive surface. The outer ring can be made of PVC pipe with 406 ± 3 mm inside diameter and 152 ± 6 mm height. The testing environment has the conditions of 23 ± 2.0° C and 50 ± 4 % relative humidity. The dates and strain from the strain gauges must be recorded at least every 30 minutes. A sudden decrease of more than 30 micro-strains in compressive strain in one or both strain gauges indicates cracking. After the concrete ring cracks, the time and cracking length and width on the radial face are recorded. The specimen is then monitored for two additional weeks after cracking. The figure below shows the ring set up.

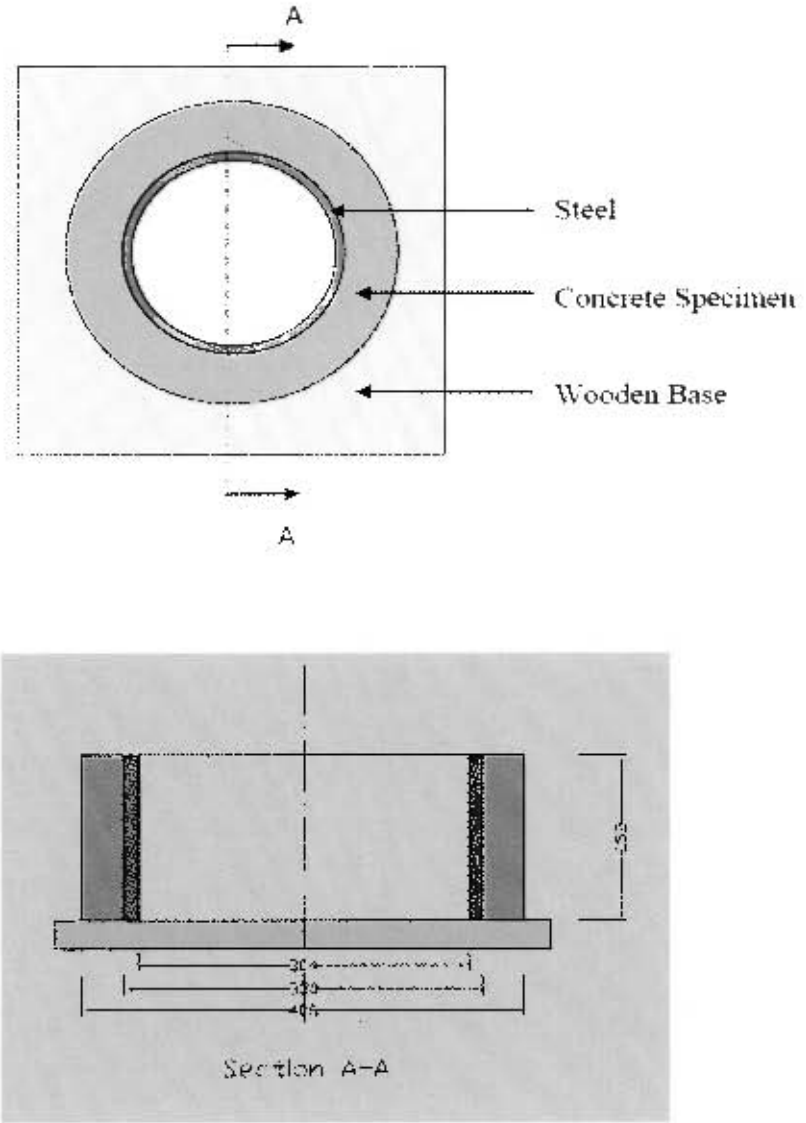

Figure 2.20: Ring test as described by ASTM (2004).

2.6.5 Summary of test methods

The above section (Section 2.6) has provided a brief review of the various test methods that have been developed for measuring restrained-shrinkage cracking tendency of concrete repair mortars/overlays. Among these methods, the ring test is the most common method used. The usefulness of the ring test stems from the fact that it is simple, the test apparatus is relatively inexpensive to construct, and it can be used to compare most of the factors that affect the cracking tendency of concrete at the same time. The ring test also produces easily visible cracks. However, it should be noted that the ring test method only reflects the relative tendency of concrete with different mixes and different conditions, and it cannot represent the concrete in actual service life.

A ring test method similar to the one described in ASTM C 1581-04 standard (2004) was adopted in this study.

2.7 Tensile strain and stress in bonded concrete overlays

Overlays may exhibit performance problems which manifest as cracking and/or debonding, which result from differential volume changes between substrate and overlay. The overlay is subjected to shrinkage and thermal movements, while the substrate deformations are negligible. The restraint of overlay shrinkage by substrate causes tensile stresses in the overlay.

2.7.1 Strain due to restrained shrinkage

Figure 2.21 shows the strain 'ε' acting through the composite section; where the section is taken to be very thin so that the strain gradient may be considered to be negligible. Since perfect bond is assumed between substrate and overlay i.e. there are no irregularities at the interface causing poor bonding, both substrate and overlay undergo the same linear contraction. Therefore, this imposed linear strain leads to an induced linear stress in each section. Effects of curvature, interface slip and strain gradients across both overlay and substrate are ignored in this simplification.

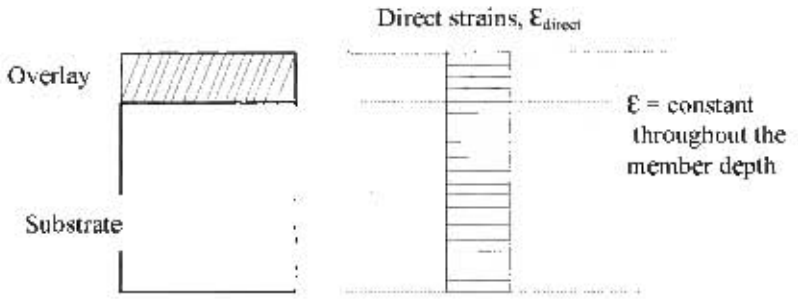

Figure 2.21: Distribution of strain in a very thin composite section, as reported by Beushausen & Alexander (2007).

Effects of curvature can only be ignored for common concrete repairs i.e. thin overlays on very stiff substrates. In this case, effects of bending moments resulting from differential shrinkage can usually be neglected. However, in members with relatively low substrate stiffness e.g. structural overlays on concrete slabs, bending moments due to differential shrinkage might cause considerable curvature, resulting in compressive strain in the overlay and hence in partial relief of tensile overlay stress (Beushausen, 2005).

Beushausen & Alexander (2007) carried out experiments on overlays of different thicknesses. In their study, they assumed the substrate to be fully fixed at the bottom. Figure 2.22 presents the strain profiles obtained from their experiments. Since members denoted B1, B2 and B3 were not allowed to curve, their strain values are due to differential shrinkage disregarding effects of curvature. It is interesting to note that maximum strain observed was due to shrinkage of the thinnest overlay i.e. 20 mm thick, and that the strain profile observed is non-linear. This is in direct contrast to the assumptions made in Figure 2.21.

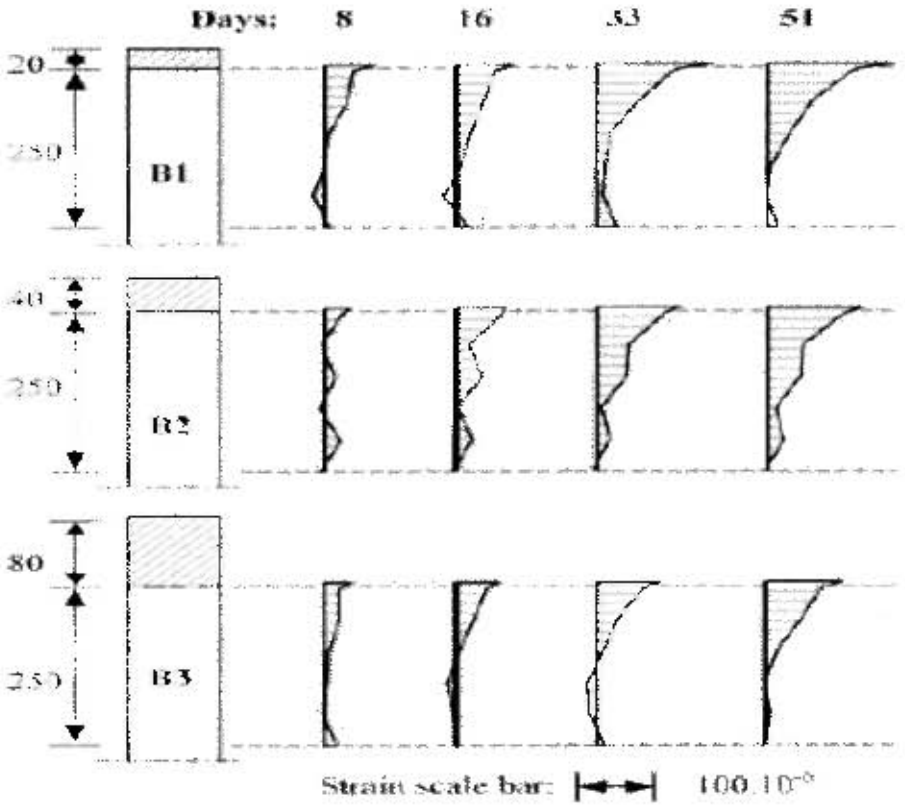

Figure 2.22: Distribution of strain across the substrate depth, from Beushausen & Alexander (2007).

It was further observed that the overlay depth has little appreciable influence on the interface strain development. Results of the simulation showed that substrate strain is constant throughout the length of the interface, an indication that overlay shrinkage restraint remains constant over the whole overlay surface area. The above measured strain represents the sum of different components namely; direct elastic strain, strain reduction due to overlay stress relaxation, and substrate creep strains (Beushausen & Alexander, 2007).

2.7.2 Stress due to restrained shrinkage

It is not easy to predict stresses resulting from shrinkage restraint in bonded concrete overlays. It is not possible to calculate these stresses from the product of the free shrinkage strain and the elastic modulus because of the effects of creep and relaxation. Therefore, the influence of factors such as increase in rate of overlay shrinkage coupled with shrinkage restraint, increase in elastic

modulus, creep etc. complicate matters. It is simpler to look at the effects of direct stresses alone before considering influences of other stress mechanisms. In this case for a fully bonded overlay with consistent restraint along the interface, it can be shown that instantaneous elastic strain of the overlay [2.1] and substrate strain [2.2] at the interface is as follows (Beushausen, 2005)

$$\varepsilon_{restr.O,I} = \left(\varepsilon_{FSS} - \frac{\varepsilon_{FSS}}{1+\frac{E_S}{E_O} \cdot C_\varepsilon} \right) \quad [2.1]$$

$$\varepsilon_{S,I} = \left(\frac{\varepsilon_{FSS}}{1+\frac{E_S}{E_O} \cdot C_\varepsilon} \right) \quad [2.2]$$

Where $\varepsilon_{restr.O,I}$ = restrained overlay strain at the interface

ε_{FSS} = overlay free shrinkage strain

E_S = modulus of elasticity of substrate

E_O = modulus of elasticity of overlay

C_ε = constant accounting for combined influences of relative member dimensions and strain profile characteristics

$\varepsilon_{S,I}$ = substrate strain at the interface. $\varepsilon_{S,I} = \varepsilon_{O,I} = \varepsilon_I$

($\varepsilon_{O,I}$ = Overlay interface strain, ε_I = interface strain)

In the linear-elastic range the stress profile is determined by the strain. In bonded concrete overlays the top surface of the overlay has more freedom to shrink compared to the interface, and for the substrate the higher strains are at the interface since it is bonded to the shrinking overlay. Figure 2.23 shows the strain profile.

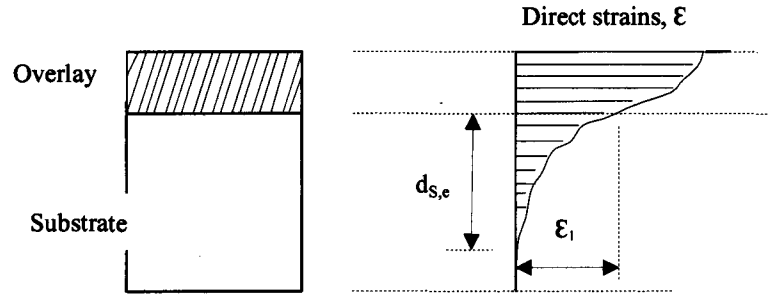

Figure 2.23: Distribution of strain across the substrate depth, as reported by Beushausen & Alexander (2007).

Another influence is that of elastic strain. This complies with linear elastic theory i.e. restrained shrinkage at any given time is proportional to overlay stress. Hence direct elastic stresses due to overlay and substrate strain are represented by [2.3] and [2.4] respectively (Beushausen H. , 2005).

$$\sigma_{O,I} = \left(\varepsilon_{FSS} - \frac{\varepsilon_{FSS}}{1+\frac{E_S}{E_O}\cdot C_\varepsilon}\right)\cdot E_O \qquad \text{(tension)} \qquad [2.3]$$

$$\sigma_{S,I} = \left(\frac{\varepsilon_{FSS}}{1+\frac{E_S}{E_O}\cdot C_\varepsilon}\right)\cdot E_S \qquad \text{(compression)} \qquad [2.4]$$

Where $\sigma_{O,I}$ = direct elastic stress in overlay

$\sigma_{S,I}$ = direct elastic stress in substrate

The rest of the parameters have been defined above

The stresses in equations [2.3] and [2.4] exclude the effects of overlay relaxation. In bonded concrete overlays, direct elastic stresses do not remain constant. They are subject to overlay relaxation and substrate creep. Substrate creep contributes to stress relaxation by increasing the overlay strain. This leads to a reduction in restrained shrinkage. Therefore resultant overlay stress is due to stress relaxed by substrate creep plus stress relaxed due to tensile relaxation.

These mechanisms are interdependent, and thus cannot be separately dealt with. Other stress release mechanisms in concrete overlays can be attributed to curvature and interface slip. However, these apply to situations where overlays are bonded to relatively flexible substrate or the overlay-substrate interface is poorly bonded.

Therefore including the contribution of creep and relaxation, overlay and substrate stresses can be represented as shown in equations [2.5] and [2.6]. It is worth noting that variables in equations [2.5] and [2.6] are time dependent (Beushausen, 2005).

$$\sigma_{S,I}(t) = \varepsilon_I(t) \cdot E_S = \frac{\psi_O(t,t_o) \cdot \varepsilon_{FSS}(t)}{1+\frac{E_S}{E_O(t)} \cdot C_\varepsilon} \cdot E_S \qquad [2.5]$$

$$\sigma_{O,I}(t) = (\psi_O(t,t_o) \cdot \varepsilon_{FSS}(t) - \varepsilon_I(t)) \cdot E_O(t)$$

$$= \left(\psi_O(t,t_o) \cdot \varepsilon_{FSS}(t) - \frac{\psi_O(t,t_o) \cdot \varepsilon_{FSS}(t)}{1+\frac{E_S}{E_O(t)} \cdot C_\varepsilon}\right) \cdot E_O(t) \qquad [2.6]$$

$$= \psi_O(t,t_o) \cdot \left(\varepsilon_{FSS}(t) - \frac{\varepsilon_{FSS}(t)}{1+\frac{E_S}{E_O(t)} \cdot C_\varepsilon}\right) \cdot E_O(t) \qquad \text{(tension)}$$

Where $\sigma_{S,I}(t)$ = direct stress in substrate at age t

$\sigma_{O,I}(t)$ = direct stress in overlay at age t

t = age at the time of testing

t_O = age at the time of loading

$\psi_O(t,t_o)$ = relaxation function within the period $(t - t_O)$

$\varepsilon_{FSS}(t)$ = free shrinkage strain of overlay at age t

$E_O(t)$ = modulus of elasticity of overlay at age t

the rest of the parameters have been described earlier.

Stress caused by restrained shrinkage, if in excess of the tensile strength of the overlay after tensile relaxation, will result in cracking and debonding of the overlay. Stress can also partly be reduced by curvature and substrate creep (the rest is dealt with in equation [2.6]).

2.7.3 Restraint is proportional to free shrinkage

Beushausen (2005) cast overlays of realistic dimensions (1600 x 155 x 40 mm) on substrate beams (1600 x 155 x 200 mm) and attached strain targets, Figure 2.24. Based on strain measurements along the interface at both the overlay and the substrate , the composite behaviour could be identified through the strain response. Through strain measurements, it was observed that in the case of bonded overlays , strain measured was proportional to 60% of free shrinkage strain.

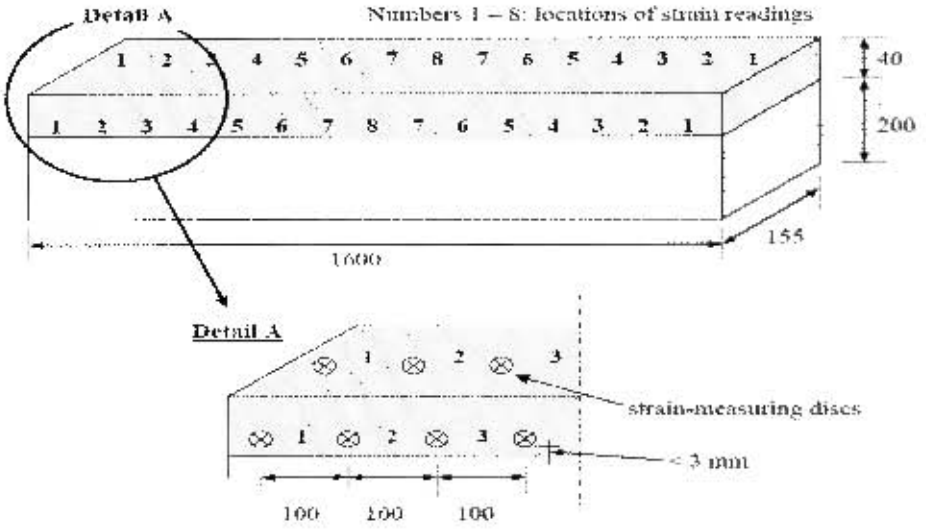

Figure 2.24: Member dimensions and measuring setup in Beushausen (2005).

2.8 Measures employed to minimize shrinkage cracking

To minimize and/or eliminate shrinkage cracking, a number of strategies may be used and they include:

- Proper curing techniques to prevent excessive loss of water due to evaporation e.g. use of wind breaks is encouraged when casting in windy and hot conditions.
- Internal curing techniques (Delatte *et al.*, 2007) – (a) Utilizing high absorption aggregate i.e. absorption level greater than 1%, (b) replacing fine aggregate with light weight aggregate (LWA) of higher water absorption, etc.
- Improved mix designs that minimize the paste content, and also using larger size aggregates with optimized gradation to reduce the need of water and cementitious materials in the concrete.
- Improved construction practices that reduce the degree of restraint of the concrete.
- Addition of single or hybrid fibers (specific fiber types and mix combinations need to be matched to achieve desired characteristics) to increase the bonding strength of concrete to resist restrained shrinkage cracking.
- Incorporation of shrinkage reducing admixtures (SRA).
- Inclusion and use of cement extenders.

The above measures are some of the strategies that can be employed to minimize restrained shrinkage cracking in concrete. The importance of proper construction practices such as proper curing cannot be over emphasized.

2.9 Conclusion

In this chapter the various factors that affect performance of concrete repair mortars/overlays were identified, as well as the different tests used for evaluating performance. It was found that performance of bonded overlays depends upon the interaction of many factors, and to be able to predict overlay performance would require understanding of these factors. In the next chapter, the methods used to evaluate the different factors affecting overlay performance are discussed.

CHAPTER THREE: EXPERIMENTAL TECHNIQUES

3.1 Introduction

In Chapter Two the various factors that affect the performance of concrete repair mortars/overlays were identified, as well as the different innovative tests used for evaluating performance. It was established that whether an overlay cracks or not depends upon the interaction between the tensile stress from restrained shrinkage and the other material properties such as tensile strength, tensile relaxation and elastic modulus. Therefore, it is important to understand how the different material properties affect overlay performance. To this end, material property tests were carried out in order to find out how these properties affect cracking behaviour of repair mortars/overlays. This was in line with research objective (i) given in chapter one. Material property tests involved determination of parameters such as free shrinkage strain, tensile strength, elastic modulus and tensile relaxation. Effects of varying water-to-cement ratio (i.e. mix type) and curing period on the different material properties were investigated.

In order to determine the age at cracking and extent of cracking (crack area), ring tests and bonded overlays were also carried out. The ring test was chosen as the restrained shrinkage test because of its simplicity as pointed out in Section 2.6.4. Analysis of the ring test results together with results from the material parameters allowed conclusions to be drawn on the influence of the different material properties on restrained shrinkage cracking. This was also checked with results from the bonded overlays. A comparison of results from the bonded overlays and ring test enabled an assessment of how close the ring test would predict restrained shrinkage cracking in overlays.

Material parameters results were further used in the analytical modeling of age at cracking in Chapter Five. Bonded overlays results were compared with the results from the analytical modeling and this allowed an assessment to be made on how close the analytical model predicts age at cracking in bonded overlays used in this research. A detailed flow chart of the experimental process is given in Figure 3.1.

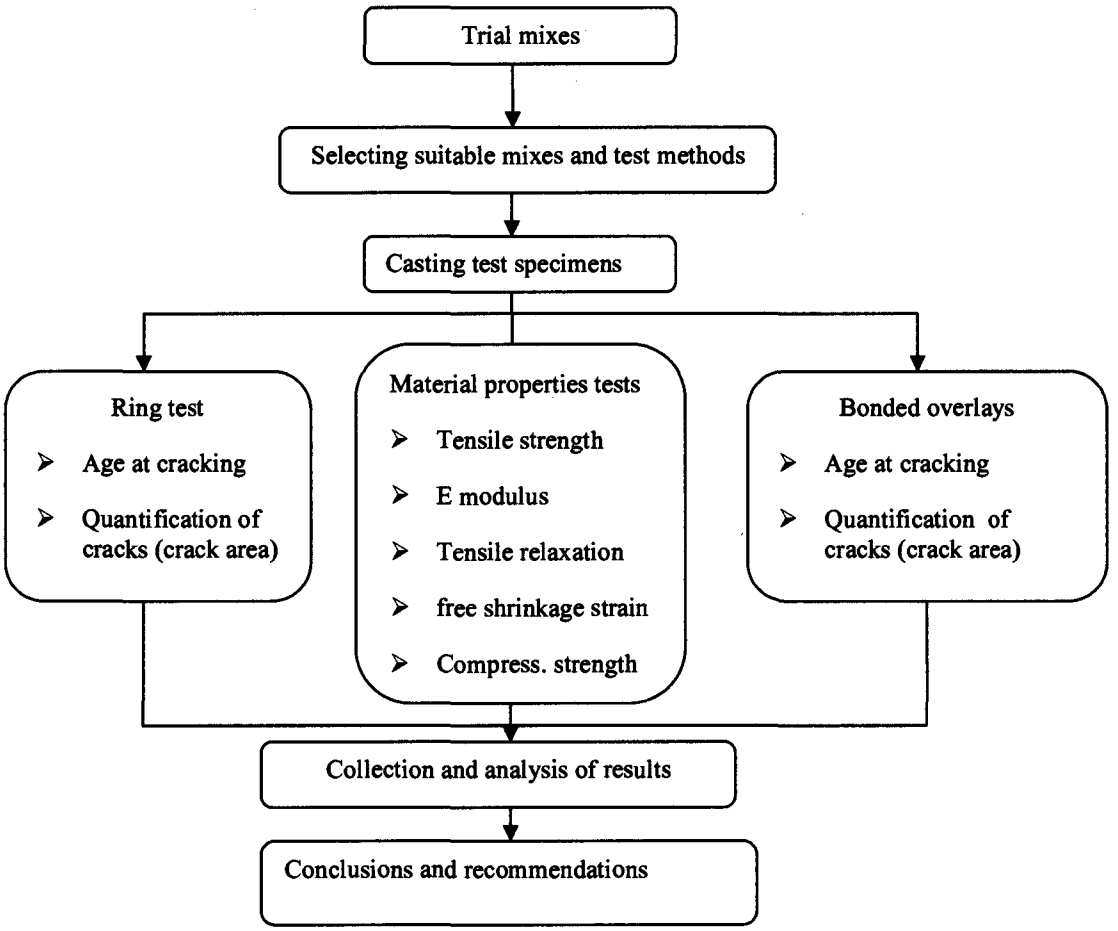

Figure 3.1: Structure of experimental research.

The experimental procedure started with trial mixes. This enabled and facilitated the selection of suitable mixes and test methods. After the mix selection, dog bone specimens were cast. These were used for free shrinkage, tensile strength test and tensile relaxation tests. Furthermore, compressive strength test cubes were also cast to monitor the strength gain at the ages of 2, 7, 10, 14, 21 and 28 days. These tests were carried out for material characterization purposes only. Elastic modulus test cylinders were also cast to monitor the development of elastic modulus with time. These were also evaluated at ages 2, 7, 10, 14, 21 and 28 days. Due to the difficulty associated in carrying out elastic modulus tests in tension, it was decided to do the tests in compression. According to Mehta & Monteiro, (2006a), the elastic modulus of concrete in tension is the same as that in compression. Free shrinkage specimens were monitored for a period of 12 weeks, while tensile relaxation tests were carried out for 72 h. According to Masuku

(2009), bonded overlays often crack in practice as they experience stress close to their tensile strength. Therefore, it was decided to carry out tensile relaxation tests at a stress level equivalent to 80% of the tensile strength.

Due to the large amount of work involved and limited manpower, it was advantageous to divide the testing program into three stages namely: stage 1 (this included all tests for material properties such as free shrinkage, elastic modulus, tensile strength etc), stage 2 (which included casting and testing bonded overlays for cracking potential) and stage 3 (this was comprised of the ring test for restrained shrinkage cracking). Stage 1 tests were carried out for a period of four months, stage 2 tests for a period of one month, and stage 3 tests for a period of one month. The testing program took a period of six months in all.

The following sections describe the materials used and also the methods of testing employed in order to meet the objectives of the study set out in chapter one.

3.2 Test materials and conditions

In order to test materials that are representative of repair materials used in the Cape Province, five materials representing three commercial mortars and two laboratory made mortars were selected for investigation. The three commercial mortars comprised a non-sag multipurpose mortar (Sika Rep LW), an overhead, horizontal and vertical repairs mortar (Sika MonoTop-615 HB) and a synthetic fiber modified mortar (Sika MonoTop-612). Laboratory made mixes comprised two mixes with water-to-cement ratio (w/c) of 0.6 and 0.45. Though the above list is not comprehensive, it generally represents the materials that are available for overlay repairs.

3.2.1 Commercial repair mortars

The three commercially available repair mortars selected for investigation were (a) Sika MonoTop-612, (b) Sika MonoTop-615 HB and (c) Sika Rep LW. These were selected for investigation because they best represented the range of products (based on application) that are available on the market for overlay repairs. Sika MonoTop-612 is a synthetic fiber reinforced mortar used for horizontal, vertical and overhead repairs. According to the manufacturer (Sika

Product Manual, 2011), it is a low shrinkage, easy to mix mortar with good mechanical properties. Sika MonoTop-615 HB is cement based mortar for horizontal, vertical and overhead applications. It is made up of cement and silica fume. Sika Rep LW is also a non-sag cement based repair mortar. The manufacturer of the repair mortars does not provide information on the constituents of the mortars; therefore, their contents are unknown. The commercial mortars were mixed according to the manufacturer's instructions on the data sheet. A slump of 0 mm was obtained.

3.2.2 Laboratory made mixes

In addition to commercial repair mortars, two laboratory made mixes with w/c = 0.6 and w/c = 0.45 were investigated. These were chosen based on literature survey. According to Masuku (2009), this generally falls within the range of normal concrete mortars that may be used in overlay repairs.

The mortars were made of CEM I-42.5 (OPC) cement and Klipheuwel sand. Klipheuwel sand was used as it is more well graded compared to Phillipi dune sand. Klipheuwel sand has good workability hence lower water demand. The water content was kept constant for both mixes and all mixes did not contain coarse aggregates. This is because coarse aggregates may contribute to dilution and restraint effects (Alexander, 2001). Superplasticiser was used for the low w/c = 0.45 to improve workability. The table below shows the mix design.

Table 3.1 Mix design for repair mortars

Constituent	*Normal concrete mortars*	
w/c ratio	0.45	0.6
Cement (kg/m^3)	556	417
Water (kg/m^3)	250	250
Klipheuwel sand (kg/m^3)	1490	1605
Superplasticizer (ml/m^3)	66	-
Slump (mm)	85±5	

3.2.3 Materials for substrate beams

The beam substrates for bonded overlays were cast from locally available materials so as to best imitate the concrete used locally in repairs. The conventional C&CI method was used to design the 40 MPa concrete used in the substrate beams. The aggregate was 13 mm nominal size Greywacke, typically used for construction in the Western Cape Province. Klipheuwel sand was chosen over Philippi dune sand for reasons given in Section 3.2.2. The table below gives the mix design and material properties.

Table 3.2 Mix design and properties for substrate beams

Constituent	Kg/m^3
w/c ratio	0.5
Cement CEM I 42.5	350
Water	175
Klipheuwel sand	875
Greywacke (13 mm)	1025
Slump (mm)	80 ± 15
Density (kg/m^3)	2415
Average comp. strength (28 day)	49.7 MPa

3.2.4 Curing and laboratory conditions

The period of curing was varied between 2 days and 7 days. This was done in order to capture the influence of curing on overlay performance at early age up to late age. This was in line with research objective (ii) as given in chapter one. There is a gradual increase in strength and stiffness of concrete with increasing duration of concrete. The curing procedure was such that after samples were demoulded, they were covered in wet hessian and plastic sheets for a prescribed curing period i.e. either 2 days or 7 days.

It is important that laboratory conditions remain consistent throughout the testing period. This is because temperature and relative humidity have considerable effect on material properties of overlays. In particular, temperature and relative humidity affects the hydration of cement. There is an increase in flexural, tensile and compressive strength of concrete with an increase in concrete maturity (Newbolds & Olek, 2002; Neville, 1996). Also higher temperatures result in a higher degree of relaxation (Letsch, 1991). Relative humidity has a marked influence on the degree of shrinkage attained by concrete. Particularly drying shrinkage increases with a decrease in relative humidity whilst carbonation shrinkage may exhibit a more complex response (Alexander, 2001). Hence for consistency, all test specimens (except tensile relaxation specimens) were kept and tested under standard conditions of temperature and relative humidity (23.0 ± 2.0° C and 50 ± 4 %). Tensile relaxation specimens were tested under prevailing laboratory conditions. To prevent moisture loss, tensile relaxation specimens were coated with wax as detailed in Section 3.3.3.

3.3 Parameters and test methods

Consistent and reliable test methods are essential in investigating the different parameters that affect cracking potential of repair mortars. The following sections give details on the individual tests employed in order to assess crack resistance in bonded overlays.

3.3.1 The Ring test

The Ring test is the most common test method for restrained shrinkage cracking of concrete repair mortars. In this study, a ring test similar to the one described in ASTM C 1581-04 standard (2004) was adopted.

Figure 3.2 shows the ring setup used in the experiment. The steel ring has a wall thickness of 13 ± 0.12 mm, an outer diameter of 326 mm, and a height of 155 mm just as given in ASTM standard. The base is made of plywood coated with a non-absorptive substance to prevent moisture loss from the mortar into the base. The outer ring is made from a PVC pipe, with 380 mm inside diameter and 155 mm height.

Figure 3.2 Ring specimens used in the test.

The testing procedure involved doing the following:

- Prior to mixing, the outer surface of the steel ring and inner surface of the outer ring (PVC ring) were coated with a release agent (oil) to ensure easy removal of the outer ring after casting.
- The material to be tested was then mixed according to the manufacturer's recommendation.
- After the slump test was taken to gauge consistency of the mix, the mix was then cast in between the steel ring and the outer ring to form an annulus. The mould was filled in two approximately equal layers, with each layer compacted by placing the ring set-up on a vibrating compactor.
- The specimens were then transferred to the conditioning room (with constant temperature of 23.0 ± 2.0° C and 50 ± 4 % relative humidity) within 10 minutes after completion of casting.
- The outer mould was then removed after 24 hours, and the specimens subjected to moist curing for either 2 days or 7 days depending on the curing period.
- After curing, the top surface of the test specimens were coated with paraffin wax to prevent moisture loss, thus ensuring that only circumferential drying took place when the specimens were allowed to dry under standard conditions.

- The test specimens were then monitored for the appearance of cracks twice daily (i.e. once in the morning and once in the evening) until cracking occurred.
- After the mortar cracked, the time and the average crack width and length were recorded.
- The specimens were then monitored for an additional two (2) weeks after cracking.

The time to first crack and crack characteristics such as average crack width, length etc. were used in the results analysis.

3.3.2 Tensile strength

Tensile strength tests were carried out on dog bone specimens shown in Figure 3.3. Three specimens were used per test and the Zwick Roell Z020 Testing Machine, Figure 3.4, was used for tensile strength tests.

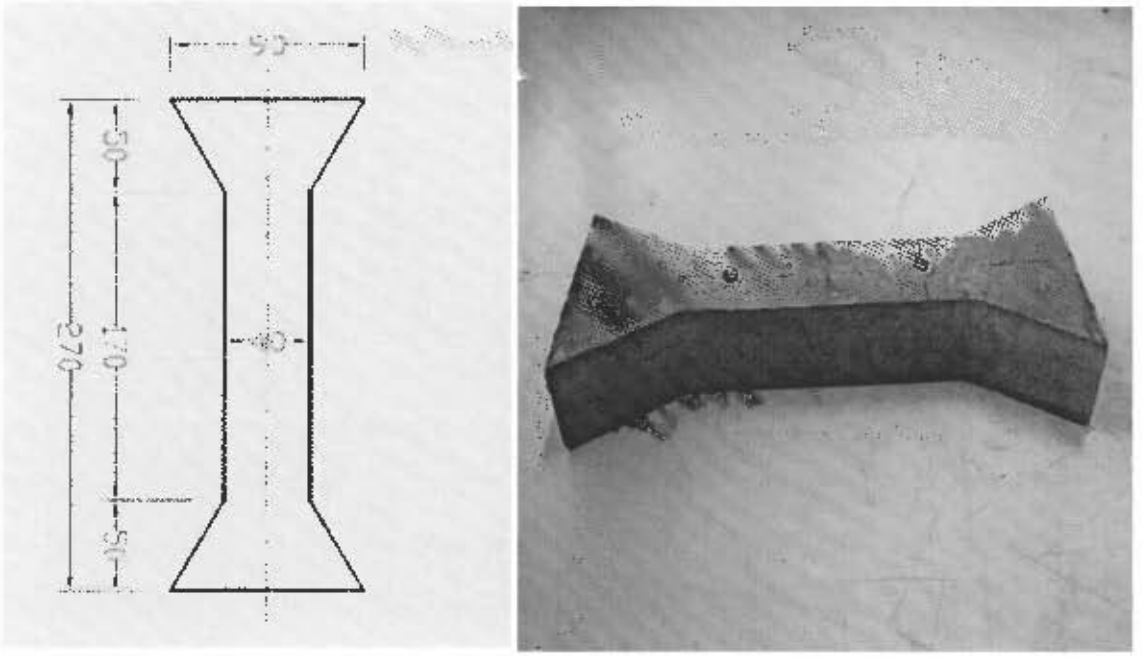

Figure 3.3: A schematic drawing and a picture showing the dog bone geometry used in the test.

The testing procedure for tensile strength was as follows:

- After the specimen was removed from the curing environment, it was wiped thoroughly with a dry cloth so as to ensure that there were no loose materials on the specimen. Loose materials would prevent the specimen from fitting perfectly into the gripping jaws. This would introduce unnecessary eccentricity in the test specimen.
- The specimen was then placed in the loading apparatus, making sure the specimen was firmly fixed between the gripping jaws.
- The load was then applied by the upper crosshead set to a travel rate of about 0.2 mm per minute until failure.
- The load at failure was then read off from the PC connected to the Zwick Z020, and recorded as the uniaxial tensile strength of the specimen.

The average of three specimens was taken as the tensile strength of the material at the specified age. The raw results and standard deviations are given in Appendix C.

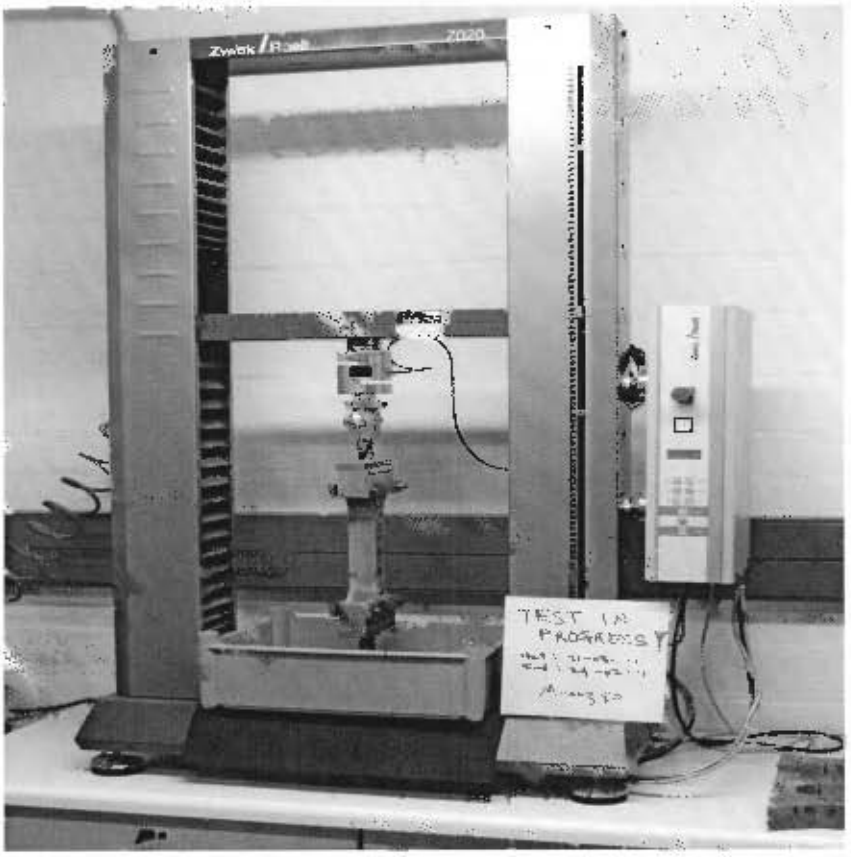

Figure 3.4: The Zwick Roell Z020 used in the tensile relaxation and tensile strength tests.

3.3.3 Tensile relaxation

Tensile relaxation tests were carried out on specimens of the same geometry as tensile strength test specimens, Figure 3.3. Each relaxation test was carried out for a period of 72 hours, with the relaxation value at the end of 72 hours taken as ultimate relaxation. Thereafter, all other values were expressed as a percentage of the ultimate value. Two specimens were tested for each relaxation test and the Zwick Roell Z020 Testing Machine (UTM) was used for the tensile relaxation tests (Figure 3.4).

The procedure for tensile relaxation was as follows:

- After the specimen was removed from the curing environment, it was coated with paraffin wax to ensure no moisture loss occurred during testing.
- The specimen was then cleaned thoroughly with a dry cloth before being placed in the Zwick Roell testing machine. This ensured that there were no loose materials on the specimen, which would otherwise prevent the specimen from fitting perfectly into the gripping jaws.
- The test specimen was then loaded to a stress level equivalent to 80% of its ultimate tensile strength.
- The resulting tensile strain was then kept constant and the stress decay in the specimen was recorded automatically by a PC.
- After 72 hours, the test was automatically stopped and the stress value at 72 hours was noted.

The relaxation values at 72 hours (ultimate relaxation value) were then used in the analysis of results. This involved comparing of relaxation values across the different mixes (effect of mix type) and also for the different curing regimes (effect of curing) in chapter four. Relaxation values were also used as input data in the analytical modeling of age at cracking in chapter five.

3.3.4 Free shrinkage strain

Free shrinkage tests were carried out on dog bone specimens so as to measure the free shrinkage strain. The specimens used for free shrinkage were cast from the same batch as the specimens for tensile relaxation, tensile strength, elastic modulus and compressive strength. They were of the same dimensions as the relaxation specimens i.e. 270 x 40 x 40 mm as shown in Figure 3.5.

The procedure for measuring free shrinkage strain was as follows:

- After demoulding the specimens, demec points were attached along the prismatic section of the dog bone specimens at 100 mm gauge length.
- After the specimens had been given the appropriate curing, specimens were taken to the conditioned room.
- The specimens were unsealed on all surfaces and placed on a smooth surface so that shrinkage was not inhibited.
- An extensometer with gauge length 100 mm was then used to measure strain everyday for 3 months.

The free shrinkage strain data was then used in the analysis of results in Chapter Four and Chapter Five.

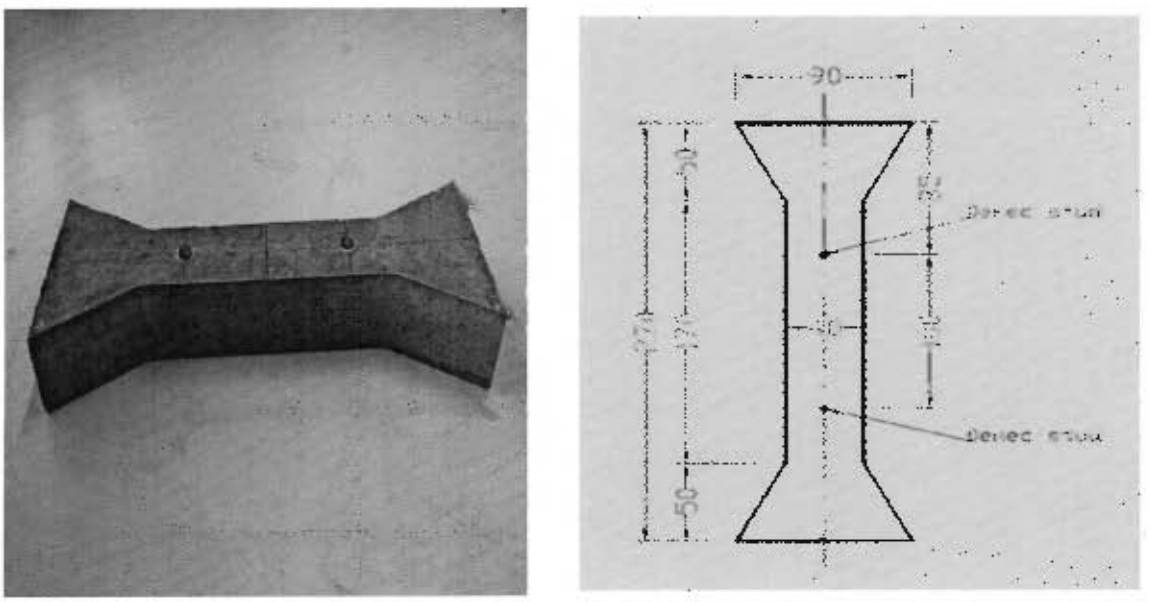

Figure 3.5: A picture and schematic drawing of dog bone specimens with demec studs used in the free shrinkage tests.

3.3.5 Compressive strength

Compressive strength tests were carried out on 100 x 100 x 100 mm concrete mortar cubes. These tests were performed to characterize the material and also to monitor strength development of the material. The test procedure was in accordance with SANS 5863:2006. An Amsler Compression Machine was used for compressive strength tests and four (4) specimens were tested per each test. Results from the compressive strength tests are given in Appendix C.

3.3.6 Elastic modulus

Tests for elastic modulus were carried out on cylindrical specimens, with Ø 100 mm and a height of 200 mm. Elastic modulus was determined in compression and was calculated from plotted stress–strain curves of the material. The modulus of elasticity values were calculated as the gradient of the curve in the linear portion i.e. between 0 and 40% of ultimate strength. The Amsler Compression Machine (used for applying stress) and an extensometer with 100 mm gauge length (used for measuring resulting strain) were used in this test.

The following procedure was followed when determining elastic modulus:

- After the specimen was removed from the curing environment, it was cleaned thoroughly prior to attaching strain targets.
- The specimen was then placed in the loading apparatus, making sure the specimen was firmly fixed and centered between the platens.
- The load was then applied in small increments so as to obtain enough data points for plotting stress-strain curves. The stress was increased up to a maximum corresponding to 40% of the tensile strength of the material. For each increment in the applied load, a corresponding strain was measured using the extensometer.
- Values of strain together with their corresponding values of stress were then tabulated, and stress-strain curves were plotted to obtain the gradient.

The average of three specimens was taken as the elastic modulus of the material. The raw results and standard deviations are given in Appendix C.

3.3.7 Bonded overlays on substrate beams

Bonded overlays were cast on substrate beams in order to simulate the behavior of concrete repair mortars in a real life situation. This was made further important by the fact that it would help to evaluate the performance of the ring test in predicting cracking potential. This was vital because the ring test has limitations such as: it does not take into consideration the actual restraint type and construction method used in a particular repair operation.

This study was carried out by casting 1000 x 150 x 30 mm (chosen based on literature survey) bonded overlays on 1000 x 150 x 200 mm beam elements. The beam elements were cast 2-3 months prior to testing to make sure that almost all the drying shrinkage took place before the testing of overlays began. The substrate concrete was designed as given in Table 3.2 with target strength of 40 MPa. A strong concrete (40 MPa) was chosen so as to make sure that the substrate would withstand the surface treatment employed. To facilitate bonding between the repair material and the beam substrates, the substrate surface was scrubbed with a wire brush until a consistent rough surface was obtained. The scrubbing removed loose materials and also ensured a rough surface. Figure 3.6 shows the substrate beams, on the left, and a bonded overlay cast on a beam, on the right.

Figure 3.6: Substrate beams in the moulds (in readiness for casting overlays), on the left, and cast bonded overlays, on the right.

The following procedure was followed:

- 15 substrate beams, measuring 1000 x 150 x 200 mm, were cast 2-3 months prior to casting bonded overlays.
- The substrate beams were then exposed to a suitable drying environment, so as to ensure that all the free shrinkage took place prior to casting overlays. In order to hasten drying, the beams were put into an oven and exposed to a temperature of 50° C for a week. This was done two weeks before the casting of overlays.
- Before casting overlays on the substrate beams, the surface of the substrate beams were thoroughly cleaned to ensure a strong bond between substrate and overlay. This was important because any loose materials would weaken the bond and eventually lead to debonding.

- The material to be tested was then mixed according to the recommendation of the manufacturer.
- After the slump test was taken to gauge consistency of the mix, the mix was then cast onto the substrate to a layer thickness of 30 mm. Prior to casting, the substrate surface had to be moistened. This prevented moisture loss by the overlay to the substrate and also ensured that a good bond formed between the two.
- The surface was then finished using a steel trowel to ensure a smooth surface finish.
- After being subjected to a specific curing duration, the composite member was then moved to the conditioned room and allowed to dry.
- The specimens were then monitored every day for cracking. A hand held magnifying glass was used to aid with the monitoring of cracks.
- After the material cracked, the age at cracking was noted together with the crack width and length, which were then used in the results analysis.

The results from this study are given in Chapter Four. Chapter Five gives a comparison of results from the ring test, analytical modeling and bonded overlays.

3.4 Conclusion

The sections above have given information on the materials used, test methods employed, as well as the details of curing and the testing environment. Chapter Four gives the results and discussions for the different tests carried out. Analytical modeling of age at cracking is given in Chapter Five.

CHAPTER FOUR: EXPERIMENTAL RESULTS AND DISCUSSIONS

4.1 Introduction

In order to assess the crack resistance of repair mortars, a number of material property tests together with the ring test and bonded overlays were carried out using the materials and methods documented in Chapter Three. This chapter presents and discusses results obtained from the above tests.

4.2 Material property tests

4.2.1 Free shrinkage strain

Drying shrinkage is one of the main causes of cracking in bonded overlays. According to Pigeon & Bissonnette (1999), drying shrinkage is the major cause of premature deterioration of thin bonded concrete repairs. Therefore, it was important to investigate the influence of shrinkage on cracking behaviour of concrete repair mortars. Free shrinkage strain tests were conducted on dog bone specimens as detailed in Section 3.3.4. To investigate the influence of curing on overlay cracking, specimens were subjected to two curing regimes viz. 2 days curing and 7 days curing. Specimens were then exposed to drying in a conditioned room with temperature 23.0 ± 2.0° C and relative humidity 50 ± 4 %. Measurements were taken using a demountable mechanical (Demec) strain gauge with a gauge length of 100 mm and accuracy of 10 micrometers. Results for free shrinkage strain are given in the following sections.

4.2.1.1 Effect of mix type

Free shrinkage strain results for specimens cured for 2 days are shown in Figure 4.1. Sika 612 specimens recorded the highest shrinkage values at all ages followed by Sika LW specimens. Sika 615 specimens had the lowest shrinkage values at 7 days and 28 days. Comparing laboratory mixes only, it is observed that w/c = 0.45 specimens recorded higher shrinkage values than w/c = 0.6 specimens. This is contrary to what would be expected. Results in literature e.g. Deshpande *et al.* (2007) suggest that in normal concretes there is an increase in free shrinkage strain with increase in water-to-binder ratio (w/c), due to increased porosity in higher w/c mixes.

The higher shrinkage values in w/c = 0.45 specimens may be due to approximately 25% higher volume of cement and about 10% less sand content for w/c = 0.45 specimens than for w/c = 0.6 specimens. Therefore, higher shrinkage in w/c = 0.45 specimens may have been due to higher cement and paste content (shrinkage takes place in the paste). These results agree with the findings by Masuku (2009) who found that free shrinkage strain was higher in w/c = 0.45 specimens than in w/c = 0.6 specimens. Water content was equal in both mixes.

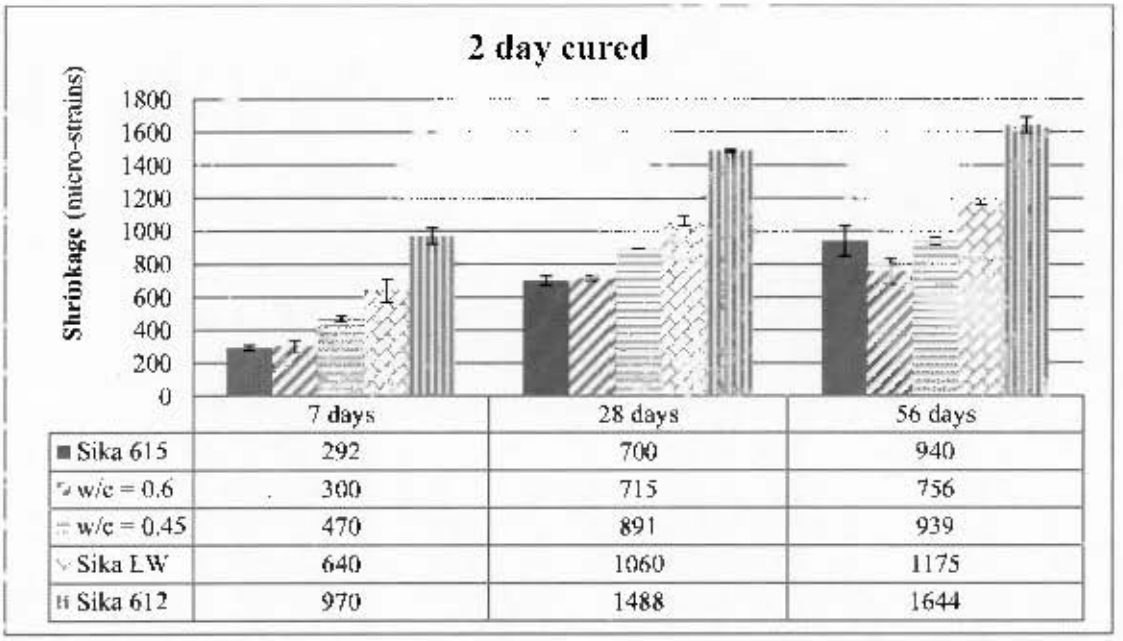

	7 days	28 days	56 days
Sika 615	292	700	940
w/c = 0.6	300	715	756
w/c = 0.45	470	891	939
Sika LW	640	1060	1175
Sika 612	970	1488	1644

Figure 4.1: Free shrinkage strain results for mortar specimens cured for a period of 2 days.

The results for 7 day cured specimens are shown in Figure 4.2. Again Sika 612 recorded the highest values of free shrinkage strain at all ages, followed by Sika LW. Sika 615 had the lowest values of shrinkage at both 14 and 28 days. As observed with the 2 day cured specimens, w/c = 0.6 specimens recorded lower shrinkage values compared to w/c = 0.45 specimens. Figure 4.2 also shows that early shrinkage rate is higher in Sika 612 specimens than in any other specimens. The shrinkage strain in Sika 612 specimens at 7 days is greater than even the 56 days shrinkage strain recorded in the other mixes. In bonded overlays, high early shrinkage rate may result in substantially high tensile stresses which may increase the risk of cracking.

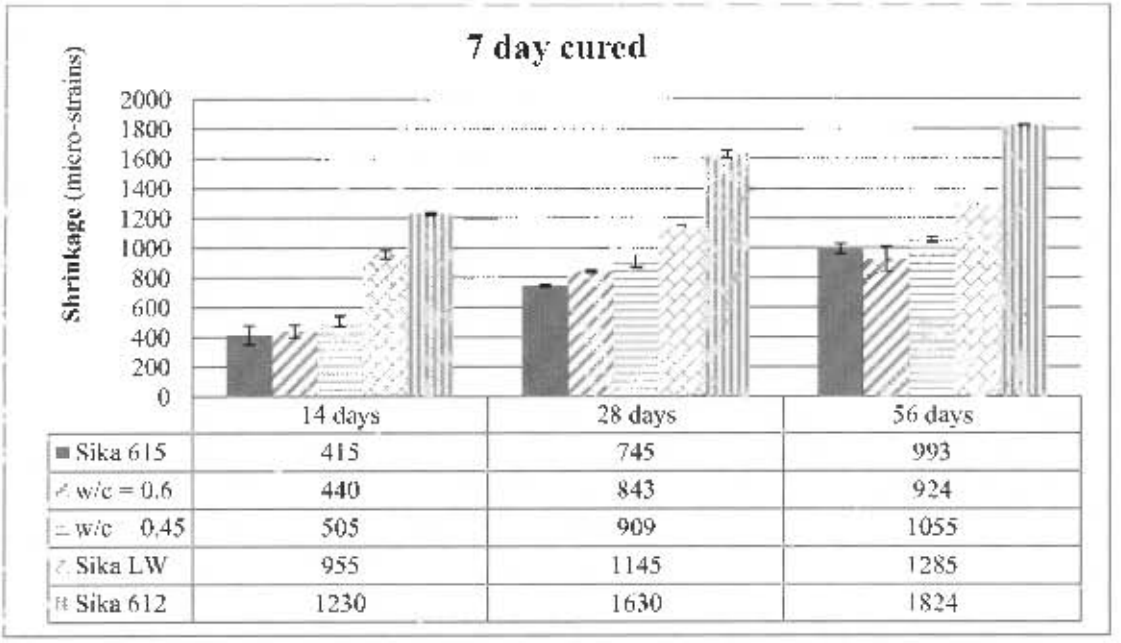

	14 days	28 days	56 days
Sika 615	415	745	993
w/c = 0.6	440	843	924
w/c 0.45	505	909	1055
Sika LW	955	1145	1285
Sika 612	1230	1630	1824

Figure 4.2: Free shrinkage strain results for mortar specimens cured for a period of 7 days.

4.2.1.2 Effect of curing

Figures 4.3(a) to 4.3(e) present the results of the influence of curing on free shrinkage strain of mortar specimens. It is observed that increase in curing period, from 2 days to 7 days, delays the early shrinkage strain by 5 days. Further, it is observed that 7 day cured specimens recorded higher values of later shrinkage strain than 2 day cured specimens. This is unusual. It is generally accepted that curing reduces the shrinkage strain of concrete, see West *et al.* (2010), Deshpande *et al.* (2007) and Nantung (2011). No explanation could be found for the observed increase in shrinkage strain with increase in curing period. The ACI Committee 364 (2006) notes that curing delays moisture evaporation and its associated drying shrinkage but does not reduce the overall shrinkage strain. In bonded overlays, both a delay in shrinkage and reduction of overall shrinkage strain would be beneficial for overlay crack resistance.

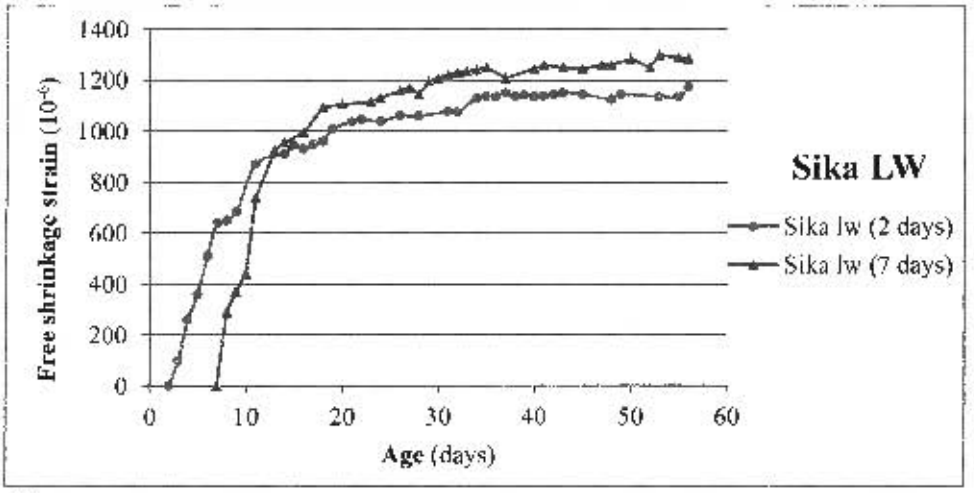
Free shrinkage strain (10^{-6})
1400
1200
1000
800
600
400
200
0
0
10
20
30
40
50
60
Age (days)
Sika LW
Sika lw (2 days)
Sika lw (7 days)

(a)

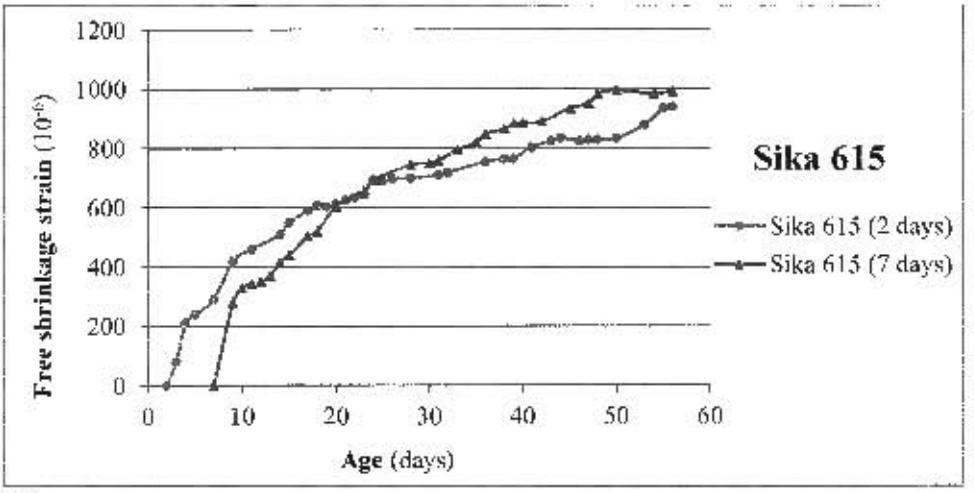
Free shrinkage strain (10^{-6})
1200
1000
800
600
400
200
0
0
10
20
30
40
50
60
Age (days)
Sika 615
Sika 615 (2 days)
Sika 615 (7 days)

(b)

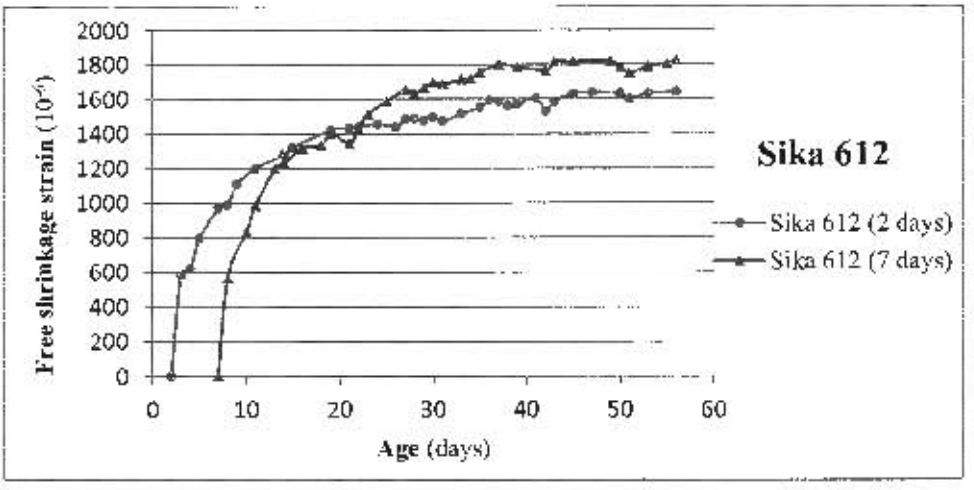
Free shrinkage strain (10^{-6})
2000
1800
1600
1400
1200
1000
800
600
400
200
0
0
10
20
30
40
50
60
Age (days)
Sika 612
Sika 612 (2 days)
Sika 612 (7 days)

(c)

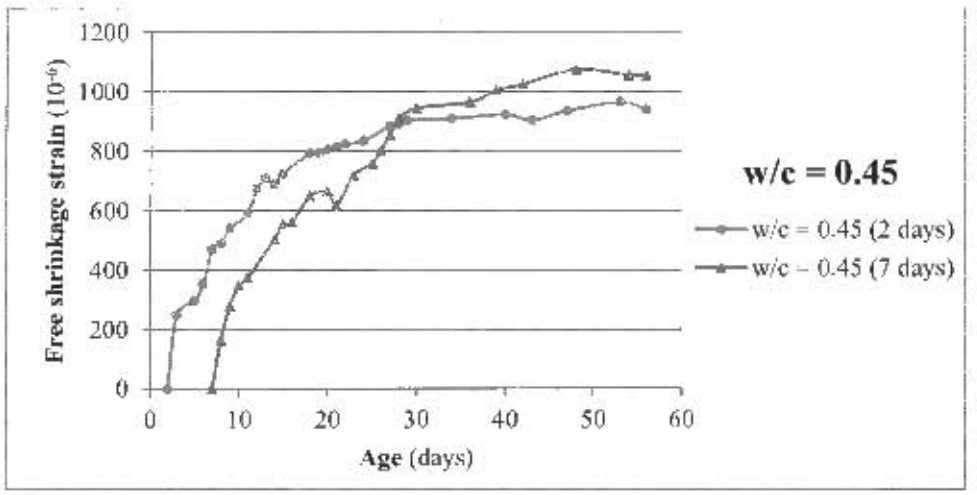

(d)

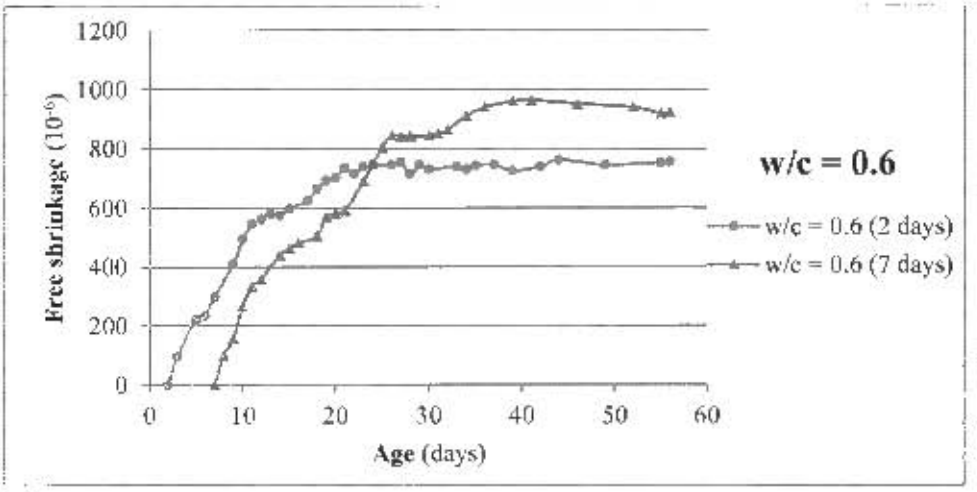

(c)

Figure 4.3: Effect of curing on free shrinkage strain of mortar specimens.

4.2.2 Tensile strength

Direct uniaxial tensile strength tests were carried out by subjecting dog bone specimens to increasing tensile stress until failure. The Zwick Roell Z020 Testing Machine was used for carrying out these tests as detailed in Section 3.3.2. These tests were conducted at ages 2, 7, 14, 21 and 28 days of concrete. Due to the holding mechanism for the specimens in the testing machine, not all specimens cracked in the prismatic section. Approximately, three quarters of the total number of specimens cracked in the prismatic section. The rest failed due to cracking below

the tapered or within the gripping jaws. This was as a result of high stress concentrations at those points within the holding mechanism. This also illustrates the difficulty associated with carrying out direct tension tests, as pointed out by Neville (1996) and Mehta & Monteiro (2006c). The direct tension test was preferred in this study because indirect tension strength tests such as the splitting tension test tend to overestimate the tension strength of concrete. Figure 4.4 shows typical dog bone specimens cracked at prismatic and non-prismatic sections. Three (3) specimens were tested per each tensile strength test, and results are given in Appendix C.

Figure 4.4: Specimens showing the mode of failure in the direct tension tests. In front, is a specimen cracked at the prismatic section, and at the back is a specimen cracked at a non-prismatic section.

4.2.2.1 Effect of mix type

Figure 4.5 shows the tensile strength across the different mixes for specimens subjected to 2 days curing. From the figure, w/c = 0.45 mix and Sika 615 had the highest 28 day tensile strength of 4.3 MPa and 4.2 MPa, respectively. This was followed by w/c = 0.6 mix with a tensile strength of 3.5 MPa. Sika 612 had a tensile strength of 2.7 MPa, while Sika LW recorded the lowest tensile strength of 2.5 MPa. Sika 612, a fiber reinforced mortar containing silica fume, recorded the lowest tensile strength both at ages 2 and 7 days. Nevertheless, its tensile strength met the

manufacturer's specified strength at 28 days of 2.5 MPa as given in Sika MonoTop 612 Data Sheet (2008). The other tensile strengths for Sika 615 HB and Sika LW could not be verified because they were not given in their respective data sheets. Comparing only the laboratory mixes i.e. w/c = 0.45 and w/c = 0.6 mixes, w/c = 0.45 mix recorded a higher tensile strength as can be expected due to its lower water-cement ratio. It is also observed that of the repair mortars, only Sika 615 HB had a higher tensile strength than the laboratory made mixes at any particular age.

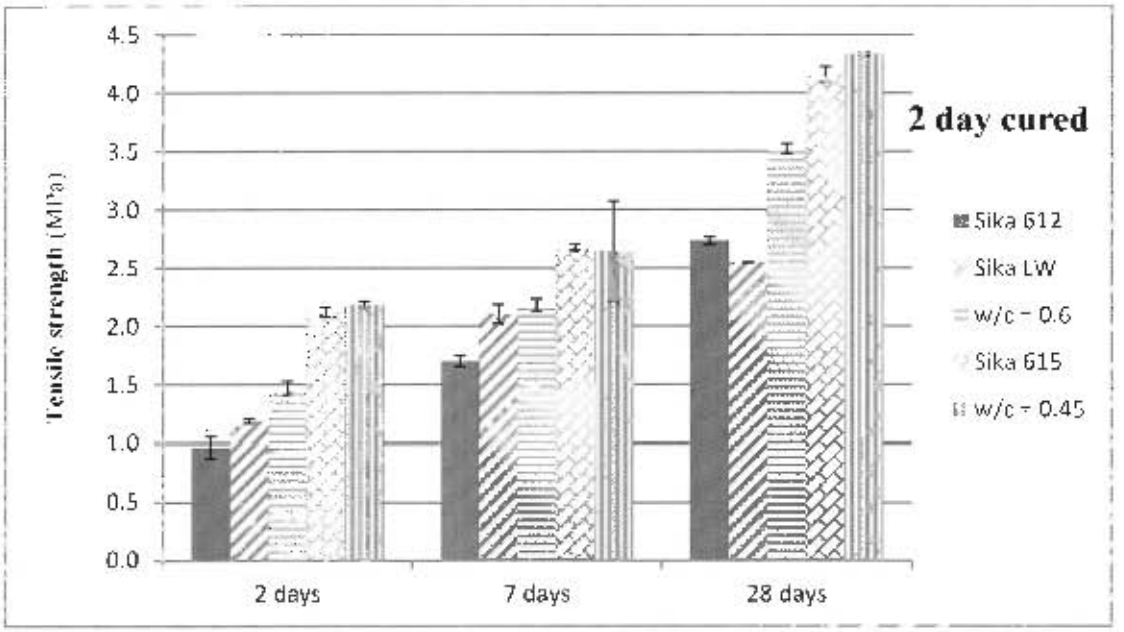

Figure 4.5: Tensile strength tests of 2 day cured specimens.

Results for the 7 day cured specimens shown in Figure 4.6 indicate a similar order to the one observed for the 2 day cured specimens. Once more w/c = 0.45 mix recorded the highest 28 day tensile strength, followed by w/c = 0.6 mix and Sika 615. Though in this case, the difference between the top two was quite substantial with w/c = 0.45 mix having 30% more strength than w/c = 0.6 mix. Sika 612 had the lowest tensile strength at all ages.

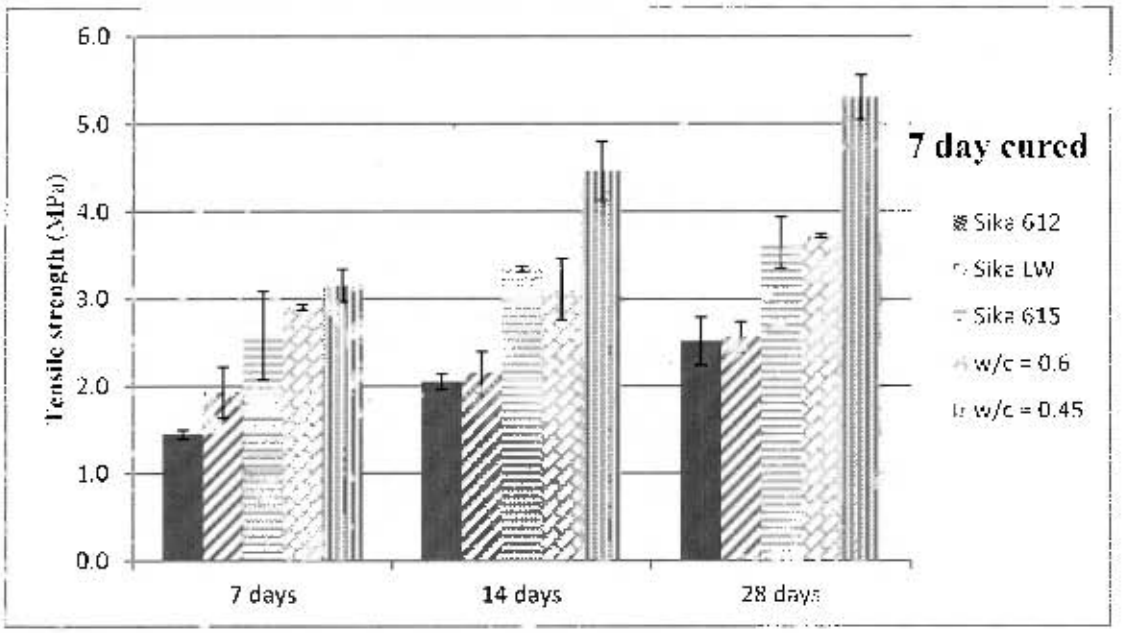

Figure 4.6: Tensile strength tests of 7 day cured specimens.

4.2.2.2 Effect of Curing

The effect of curing on the 28 day tensile strength of the repair mortars is shown in Figure 4.7. As expected, an increase in strength with increased curing period was observed in the laboratory made mixes. The mix with the lower water-to-cement ratio i.e. w/c = 0.45 had the larger increase in tensile strength of about 23% compared to w/c = 0.6 with an increase of about 10%. A strange behavior was observed in the commercial mortars. The tensile strength either stayed the same or decreased with an increase in the curing period. This seems to suggest that curing has no effect on the tensile strength of the commercial mortars tested. However, this could also be as a result of the large scatter observed in the results of the 7 day cured specimens (see Figure 4.7).

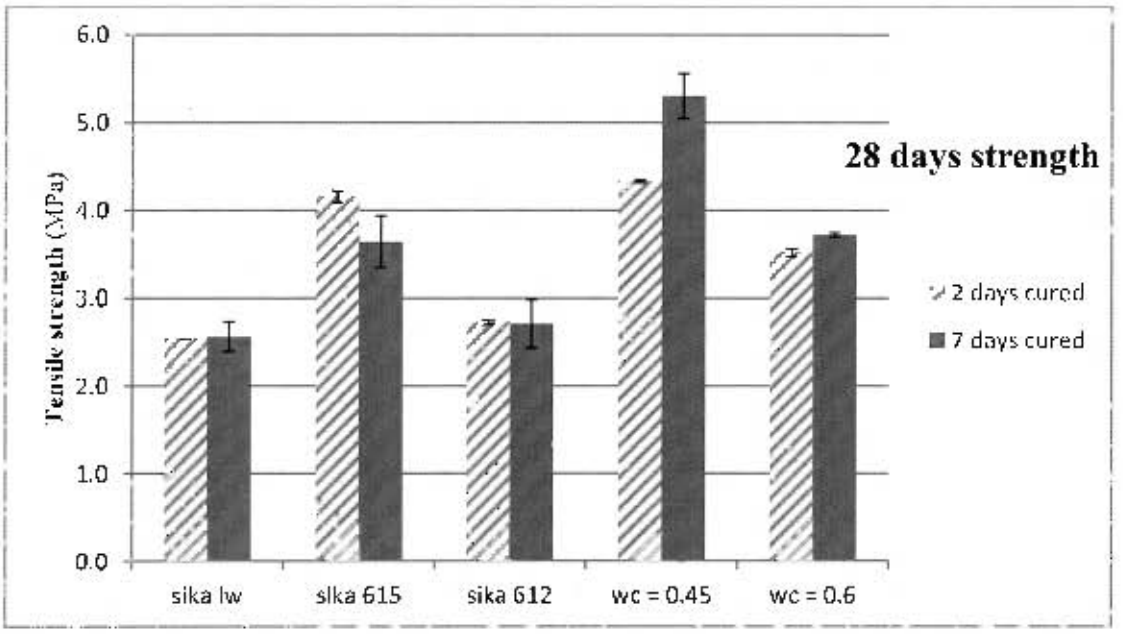

Figure 4.7: Effect of curing on 28 days tensile strength of repair mortars.

4.2.3 Elastic modulus

The elastic modulus is defined as the slope of the stress-strain curve within the proportional limit of a material. Elastic modulus values were calculated from the gradient of the tangent modulus of the stress-strain curves. The tangent modulus was calculated from stress-strain curves obtained from compressive strength tests. Compressive strength tests were used instead of tensile strength tests in obtaining the tangent modulus because of the difficulty involved in handling and attaching strain targets on tender dog bone specimens. For normal concrete, the modulus of elasticity is generally taken to be equal for both in tension and compression (Neville, 1996; Mehta & Monteiro, 2006a; Alexander & Beushausen, 2009). Elastic modulus was determined for each mix at ages 2, 7, 14, 21 and 28 for the 2 day cured specimens, and at 7, 10, 14, 21 and 28 days for the 7 day cured specimens. Three (3) specimens were used per each elastic modulus test, and results are given in Appendix C.

4.2.3.1 Effect of mix type

Figure 4.8 shows the results of elastic modulus tests for 2 day cured specimens across different ages for the different mixes. The values obtained for elastic modulus generally lie in the expected

range of elastic moduli for concrete mortars i.e. in the range 5 GPa to 30 GPa. Sika 615 had the highest 28 day elastic modulus (29.6 GPa), followed by w/c = 0.45 mix with 26.5 GPa and Sika LW with 25 GPa. Sika 612 recorded the lowest elastic modulus test across all ages. The 28 days elastic modulus of Sika 612 (11 GPa) was way below the stated elastic modulus on the manufacturer's data sheet (Sika MonoTop 612, 2008). It is also observed from Figure 4.8 that the elastic modulus of Sika 615 develops much faster than that of the other mortars. Sika 615 has an elastic modulus of about 50% of its 28 days modulus at age 2 days, while the other mortars at age 2 days have elastic moduli less than 25% of their 28 days moduli. An early increase in elastic modulus may result in high tensile stress which may result in cracking if it exceeds the tensile strength of the material.

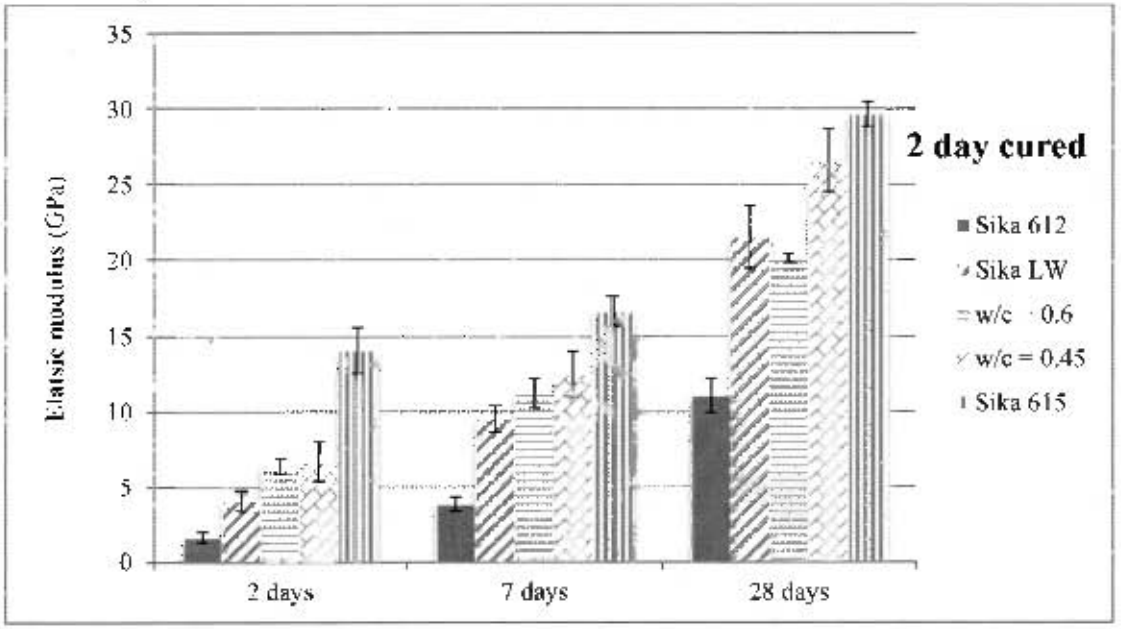

Figure 4.8: Elastic modulus tests of 2 day cured specimens.

Figure 4.9 presents the elastic modulus results for 7 day cured specimens. The 7 day cured specimens seem to follow a similar order as the 2 day cured specimens, with Sika 615 having the highest elastic modulus. Sika 612 had the lowest elastic modulus at all ages. Comparing laboratory made mixes alone, w/c = 0.45 specimens had higher elastic modulus values than w/c = 0.6 specimens at all ages.

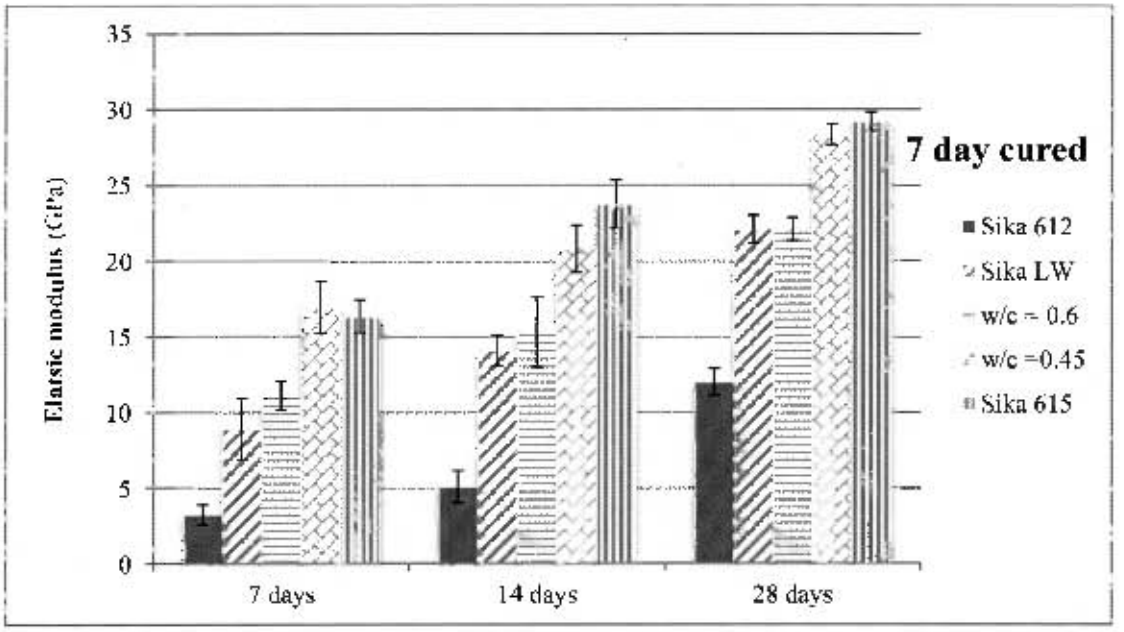

Figure 4.9: Elastic modulus tests of 7 day cured specimens.

4.2.3.2 Effect of Curing

The effect of curing on the 28 days elastic modulus of the repair mortars is shown in Figure 4.10. An increase in elastic modulus with increased curing period was observed in the laboratory made mixes. There was no detectable influence of curing on the 28 days elastic modulus of specimens made with the commercial mortars. Change in elastic modulus with increasing curing period for the commercial mortars was less than 1 GPa, which appears insignificant due to the large scatter observed in the results.

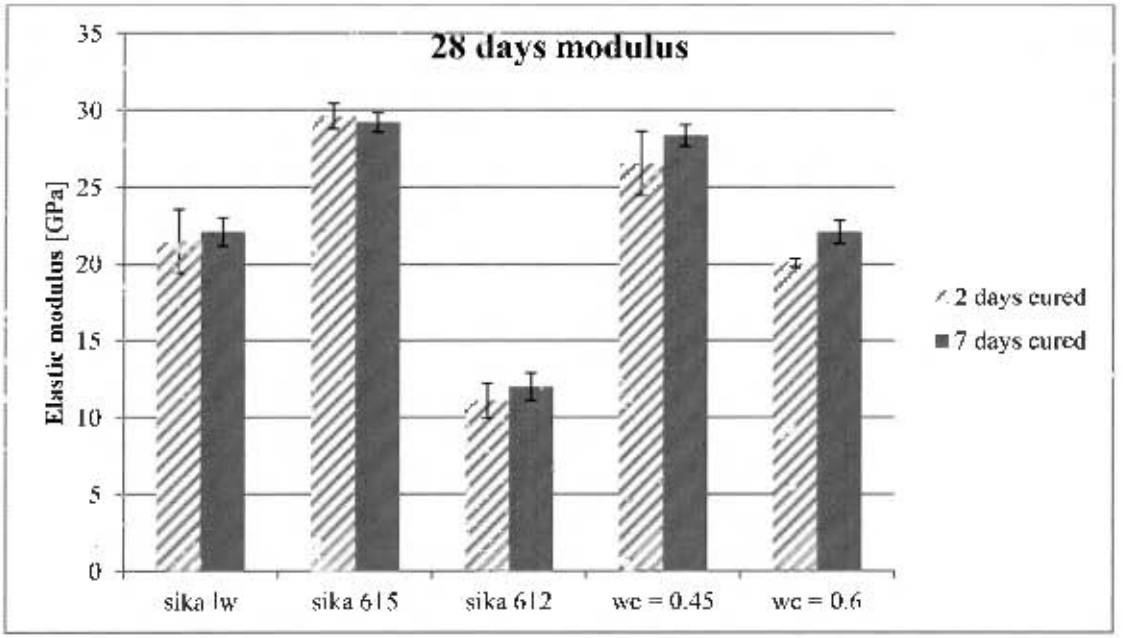

Figure 4.10: Effect of curing on 28 days elastic modulus.

4.2.4 Tensile relaxation

Tensile relaxation is the time dependent reduction in stress under a sustained strain. Previous research (Masuku, 2009; Beushausen, 2005; Pigeon *et al.*, 2000; Morimoto & Koyanagi 1995) has shown that relaxation is one of the main stress relief mechanisms against restrained shrinkage cracking. Therefore, in order to capture the effect of stress relaxation at an early age relaxation tests were carried out at ages 2 days and 7 days of mortar specimens. Also, tests were carried out at 28 days so as to capture the influence of relaxation in older specimens. The influence of curing-period was investigated by subjecting specimens to two curing regimes, viz. 2 days and 7 days curing-periods. Relaxation tests were carried out for each mix at ages 2, 7 and 28 days for the 2 day cured specimens and at 7 and 28 days for the 7 day cured specimens. These tests were carried out on dog bone specimens as detailed in Section 3.3.3. Tensile relaxation values are given as the difference between 100% and the percentage stress ratio. A typical relaxation curve is given in Figure 4.11. Note that relaxation tests were carried out for 72 hour periods as pointed out in Section 3.3.3. Two (2) specimens were used per each tensile relaxation test, and results are given in Appendix C.

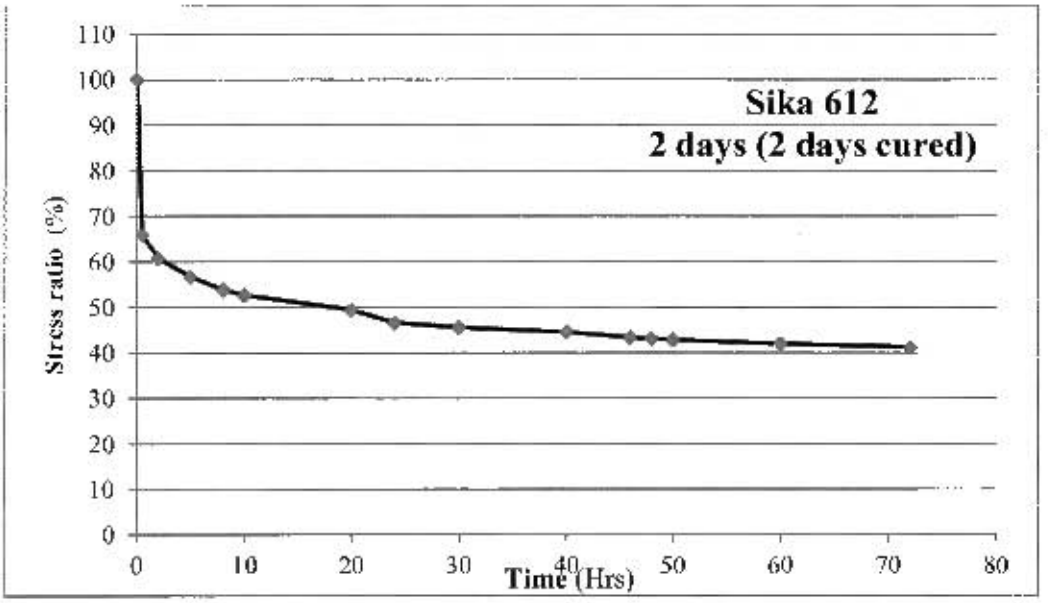

Figure 4.11: Typical relaxation curve.

4.2.4.1 Effect of mix type and age at loading

Results for tensile relaxation of specimens cured for 2 days are shown in Figure 4.12. Sika 612 specimens showed the highest margin of tensile relaxation at all ages compared to the other mortar specimens. 58% tensile relaxation was recorded in Sika 612 at the age of 2 days as compared to 46%, 44%, 40% and 34% recorded in 0.6 mix, Sika LW, 0.45 mix and Sika 615, respectively. A similar trend is observed at 7 days age of loading, with Sika 612 specimens having the highest margin of relaxation and Sika 615 specimens recording the lowest value. At 28 days age of loading, Sika 612 undergoes the same margin of relaxation as the 0.6 mix. It is observed that the margin of tensile relaxation decreases with an increase in age at loading. Younger specimens seem to undergo higher margins of relaxation than older specimens. This is consistent with the findings by Masuku (2009) that tensile relaxation decreases with an increase in age at loading. Relaxation reduces with increasing age because relaxation is dependent on the degree of hydration (Neville, 1996). Hydration is initially rapid but reduces gradually with time. According to Rusch *et al*, (1983), at later ages concrete would be more mature and therefore less capable of undergoing significant relaxation.

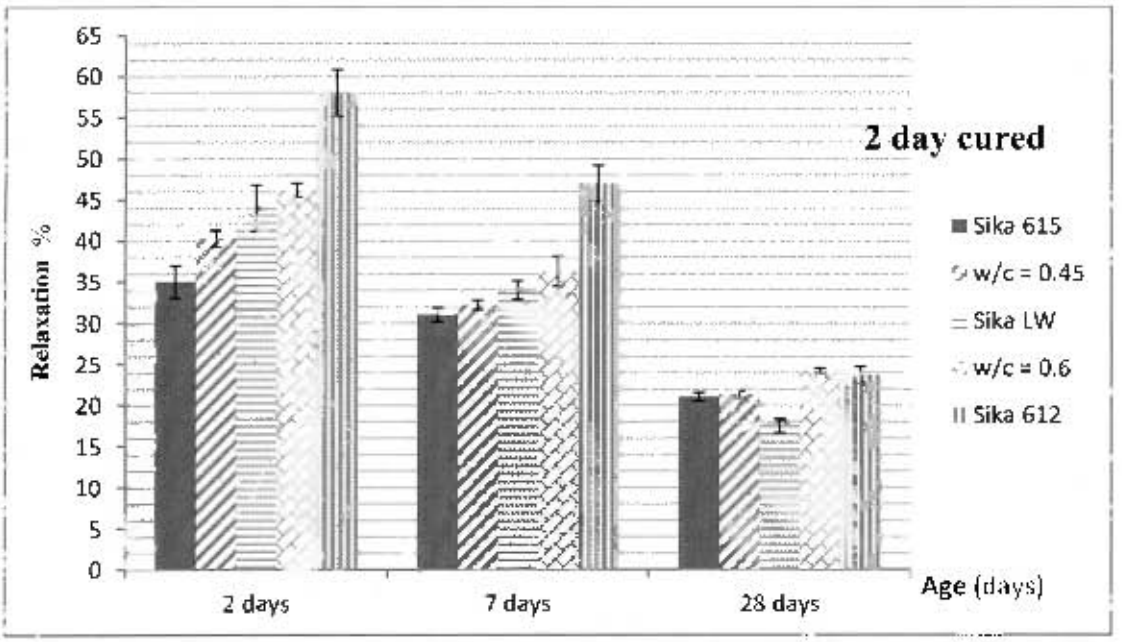

Figure 4.12: Tensile relaxation results of 2 day cured specimens.

Figure 4.13 presents the relaxation values for specimens cured for 7 days. At 7 days age of loading, Sika 612 had the highest margin of tensile relaxation. Again a similar trend to the one observed in 2 day cured specimens is observed, with Sika 612 having the highest relaxation margin (48%), followed by 0.6 mix (38%), Sika LW (36%), 0.45 mix (35%) and Sika 615 (31%). The age dependence of relaxation is again observed in Figure 4.13, with higher relaxation values recorded at 7 days than at 28 days age of loading. Considering laboratory mixes alone, it is observed that tensile relaxation is dependent on water-to-cement (w/c) ratio. 0.6 w/c ratio specimens had higher relaxation values at all ages compared to 0.45 w/c ratio specimens. This may be attributed to the porous nature of 0.6 w/c ratio specimens. Generally, high w/c ratio mix specimens tend to be more porous than low w/c ratio specimens. The porous nature of high w/c ratio mix specimens enables free movement of water through the pore spaces, and this result in sufficient redistribution of stresses (Rusch *et al.*, 1983). As a result greater tensile relaxation is achieved.

The above relaxation values, 34% - 58% for 2 day cured specimens and 31% - 48% for 7 day cured specimens, are in agreement with the relaxation values found by Masuku (2009). Masuku tested specimens made with w/c = 0.45, w/c = 0.6 and Sika LW, and found relaxation in the range 20% to 45%. These values all fall within the range of tensile relaxation values reported in

literature see Yokoyama *et al.* (1994), Gutsch & Rostasy (1995) and Alexander & Beushausen (2006).

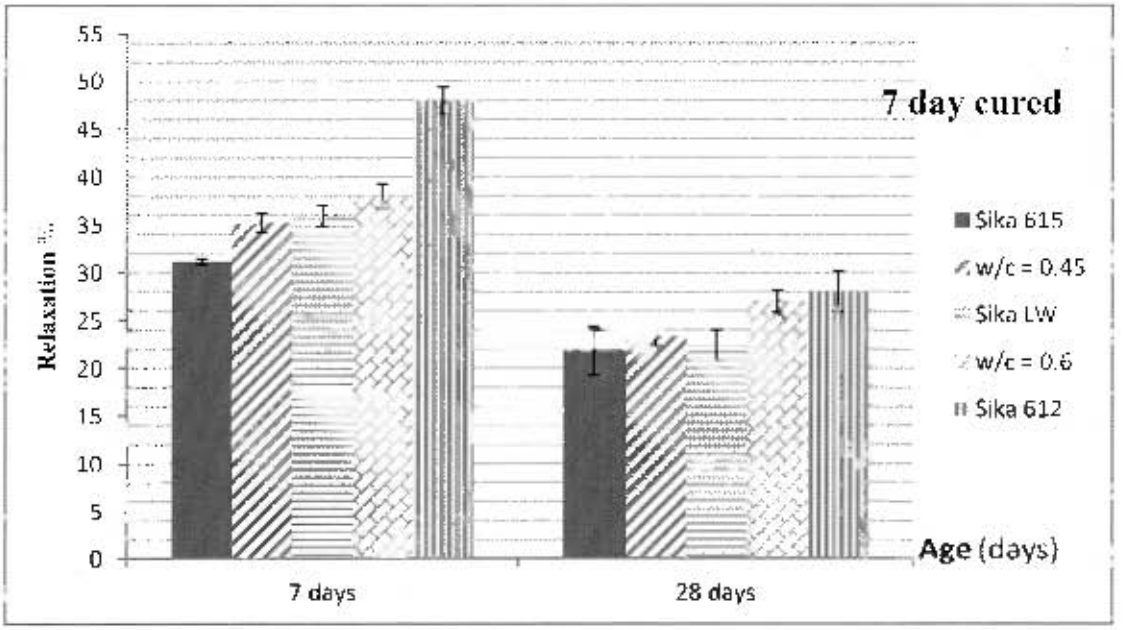

Figure 4.13: Tensile relaxation results of 7 day cured specimens.

Depending on the age of loading, tensile relaxation will reduce overlay stresses by approximately 20-58% (2 day cured specimens) and 20-48% (7 day cured specimens) in mixes tested. Masuku (2009) carried out tensile relaxation tests on concrete mortar specimens and found that, stress relaxation relieved overlay stress by 33-45% for 2 day cured specimens and 23-26% for 7 day cured specimens. Beushausen (2005) reported 40-50% stress relaxation in actual bonded concrete overlays. Pigeon *et al.* (2000) found relaxation in fully restrained specimens in the order of 67%. Morimoto & Koyanagi (1995) observed 20% relaxation after 96 hours. These findings show wide ranging differences in relaxation. Therefore it is noteworthy that a general comparison of relaxation values obtained using different concrete mixes and test equipment is problematic.

4.2.4.2 Effect of Curing

Figures 4.14(a)-4.14(e) show the effect of curing on tensile relaxation of concrete mortar specimens. There is an observed increase in tensile relaxation values with increased curing

period but due to the large scatter in the results, this cannot be affirmed. It appears curing has no real influence on tensile relaxation of the repair mortar specimens.

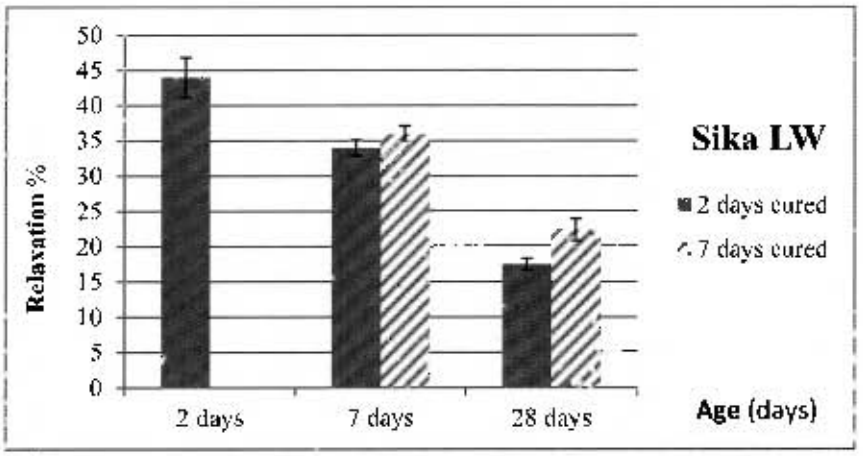

(a)

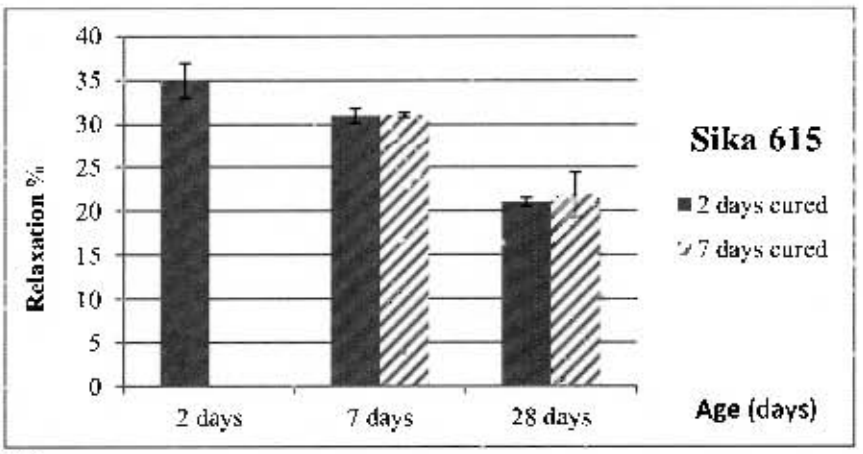

(b)

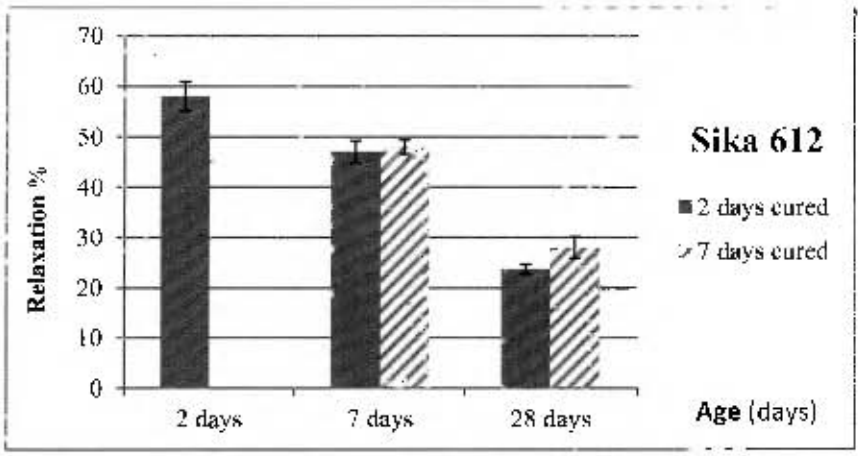

(c)

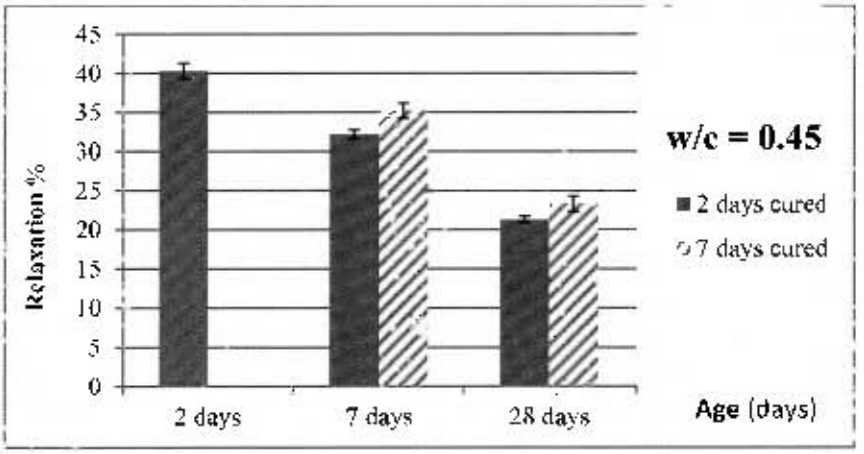

(d)

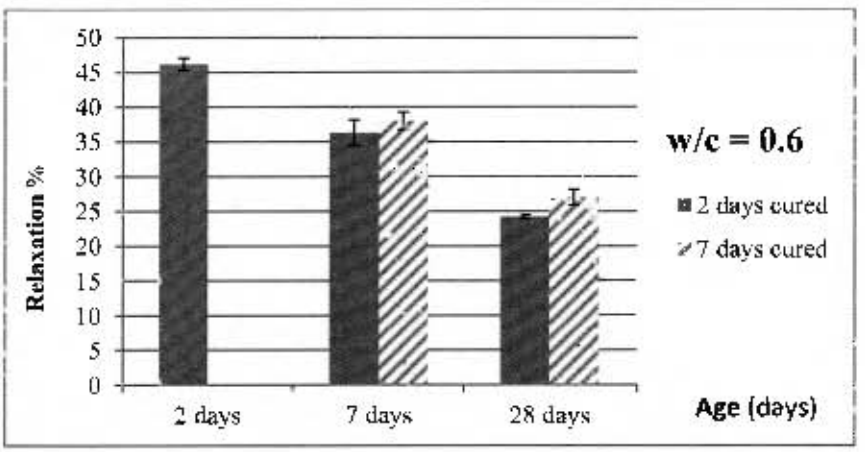

(e)

Figure 4.14: Effect of curing on tensile relaxation of mortar specimens.

4.2.5 Compressive strength

Compressive strength tests were carried out on 100 mm cubes as detailed in Section 3.3.5. These tests were conducted at the age of 2, 7, 10, 14, 21 and 28 days. Compressive strength tests were conducted for the purpose of material characterization only. This is because with respect to cracking, the tensile strength of the material is more important than the compressive strength (Section 2.8). Four (4) specimens were used per each compressive strength test, and results are given in Appendix C.

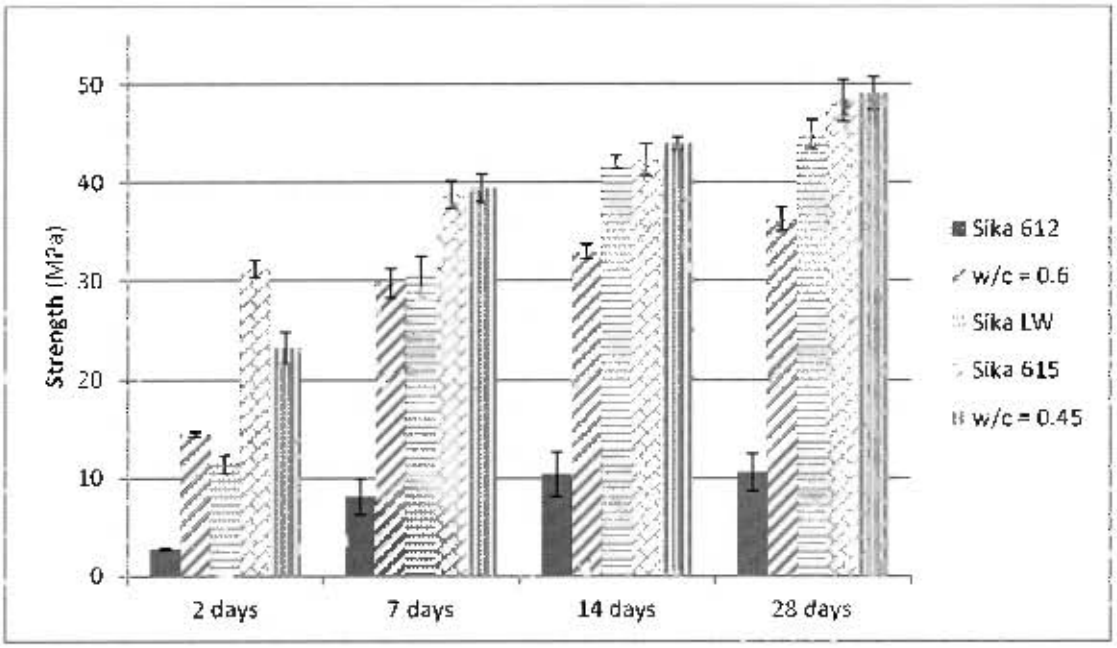

Figure 4.15: Comparison of compressive strength across the different mixes at ages 2, 7, 14 and 28 days.

Comparing the compressive strength values of the different mixes in Figure 4.15, it is observed that w/c = 0.45 mix and Sika 615 had the highest 28 day compressive strength, while Sika 612 had the lowest value. The lowest strength of 10 MPa for Sika 612 was about 20% of that of the 0.45 mix (49.8 MPa) at 28 days. It is also noted that the rate of strength gain was highest in Sika 615, which had attained about 67 % of its 28 day compressive strength in just 2 days. This was by far greater than the 25%, 26%, and 38% attained by Sika LW, Sika 612 and w/c = 0.6, respectively, at 2 days. The 28 days compressive strength of Sika 612 (10.6 MPa) was less than the values (45-55 MPa) stated on the manufacturer's data sheet (Sika MonoTop 612, 2008).

4.3 Ring test results

Ring tests were conducted to determine both the age at cracking and extent of cracking (crack area) in concrete repair mortars as detailed in Section 4.3.1. Age at cracking refers to the age of the specimen when cracking initiates. Extent of cracking was evaluated by calculating the total cracked area of the specimen two weeks after crack initiation. Crack area was calculated by multiplying the average width of the cracks by the total length of the cracks. The age at cracking and the crack area were used in the evaluation of performance of the repair mortars. Figure 4.16 shows a typical cracked specimen. The influence of curing-period was also investigated by subjecting ring specimens to 2 days and 7 days curing periods. The following sections summarize the results from the ring test.

Figure 4.16: Typical crack in ring specimens.

4.3.1 Age at cracking

Figure 4.17 shows age at cracking results for both 2 day cured and 7 day cured specimens. According to the figure, Sika 612 takes the longest time to crack (13 days) followed by w/c = 0.6 (10 days), Sika LW (7 days), w/c = 0.45 (7 days) and Sika 615 (5 days) for 2 day cured

specimens. Sika 612 took the longest time to crack probably because of its high margin of tensile relaxation, as well as low elastic modulus compared to the other mortar specimens. This is despite the fact that the highest free shrinkage strain was recorded in Sika 612 among the 2 day cured specimens. It appears the effect of low elastic modulus and high margin of tensile relaxation more than compensates for the effect of high shrinkage strain. Despite Sika 615 recording the lowest free shrinkage strain (together with w/c = 0.6), it took the shortest time for cracks to initiate. This may be because of the high values of elastic modulus and low margins of relaxation recorded in Sika 615 specimens. It is also interesting to note that Sika 615 specimens cracked first despite them recording the highest tensile strength (together with w/c = 0.45) of the 2 day cured specimens. Comparing the laboratory mix specimens, it is observed that w/c = 0.6 cracks at a much later age (10 days) than w/c = 0.45 (7 days). This may be attributed to the lower free shrinkage strain and higher relaxation margin recorded in w/c = 0.6 specimens than w/c = 0.45 specimens. In addition, w/c = 0.45 specimens had higher elastic modulus than w/c = 0.6 specimens. The combined effect of the above factors seems to have more influence than the fact that w/c = 0.45 specimens recorded higher tensile strength than w/c = 0.6 specimens.

For 7 day cured specimens, a similar trend to that observed for 2 day cured specimens is also observed. Once more Sika 612 recorded the longest period (16 days) to crack initiation followed by w/c= 0.6 (13 days), w/c = 0.45 (10 days), Sika LW (9 days) and Sika 615 (9 days). Interesting to note that Sika LW and Sika 615 specimens had the same age at cracking despite them having different material properties. Sika 615 had higher elastic modulus and tensile strength than Sika LW, while Sika LW underwent higher degree of relaxation and higher shrinkage strain than Sika 615. This suggests that crack resistance of repair mortars depends upon the combined influence of a number of factors other than just one factor. This agrees with Pigeon & Bissonnette (1999) who noted that crack resistance of concrete repair mortars is not just determined by one material property but the combined influence of various material properties and parameters. Figure 4.17 also shows the influence of curing on the age at cracking of repair mortar specimens. It is observed that an increase in curing period results in an increase in the age at cracking for all mortar types. Generally, this may be attributed to the increase in tensile strength with an increase in curing time. Curing may help in delaying the onset of cracking in bonded overlays.

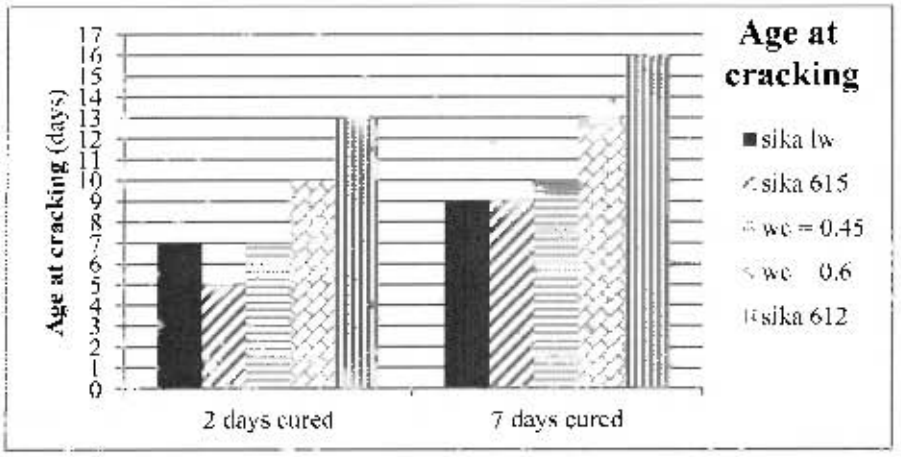

Figure 4.17: Results for age at cracking for both 2 day and 7 day cured specimens.

4.3.2 Crack area

The results of crack area are shown in Figure 4.18. Sika LW recorded the highest crack area for both 2 day and 7 day cured specimens, followed by Sika 615. In both instances, Sika 612 recorded the lowest crack area. Based on results in Figure 4.17 and Figure 4.18, there appears a correlation between crack area and the age at cracking (excluding results for w/c = 0.6). Mortar specimens that cracked first had a higher crack area than mortar specimens that cracked at a much later age, see Figure 4.19.

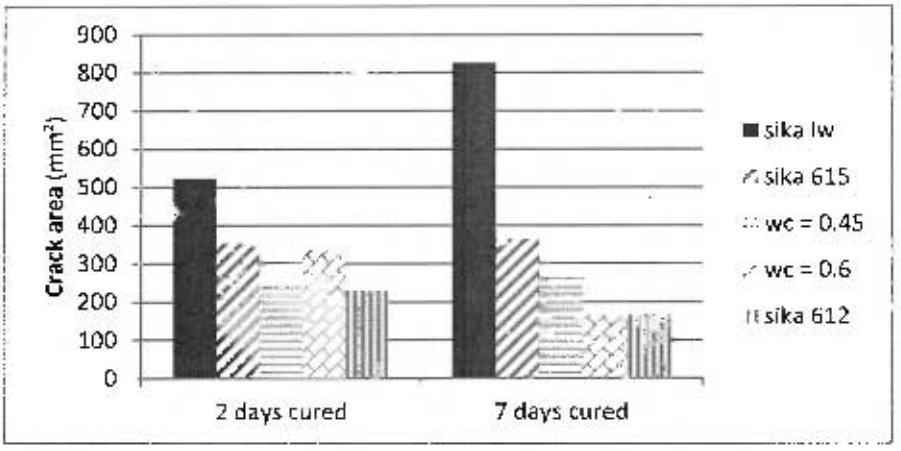

Figure 4.18: Results for crack area for both 2 day cured and 7 day cured specimens.

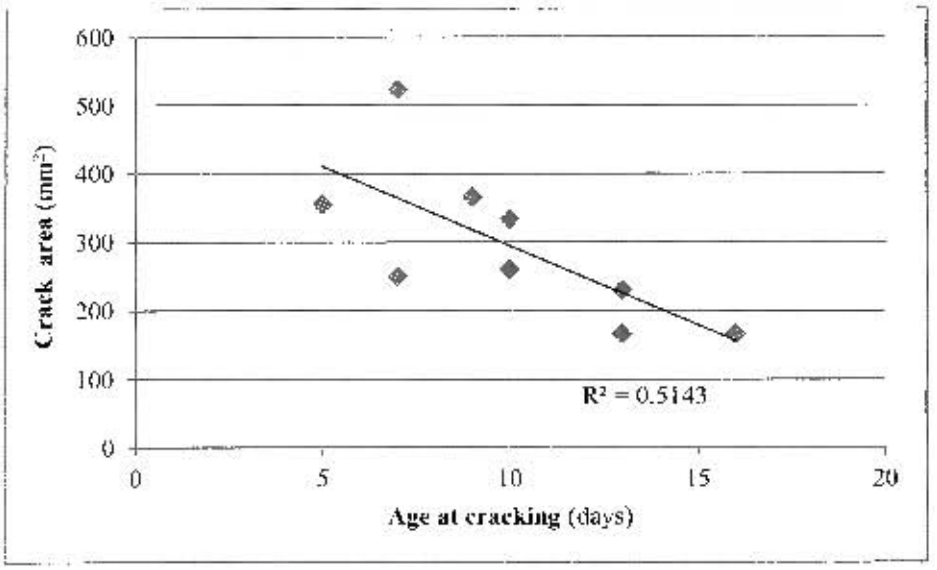

Figure 4.19: Crack area vs. age at cracking in ring test specimens.

4.4 Bonded overlay results

Bonded overlays were cast on beam specimens as detailed in Section 3.3.7. The main aim was to determine the age at cracking and crack area of the different repair mortars used in the research. Age at cracking refers to the age of the specimen when cracking initiates. Results from bonded overlays would enable an evaluation of ring test results (i.e. age at cracking) and also the results from analytical modeling (Chapter 5). Figure 4.20 shows an example of cracked bonded overlay specimens. In order to investigate the effect of curing, bonded overlays specimens were subjected to two curing regimes viz. 2 day and 7 day curing. The following sections give the results from the overlay tests.

Figure 4.20: Typical cracks on bonded overlay specimens.

4.4.1 Age at cracking

Age at cracking for both 2 day and 7 day cured specimens is given in Figure 4.21. For 2 day cured specimens, Sika 612 took the longest time to crack (24 days) followed by w/c = 0.6 (17 days), w/c = 0.45 (15 days), Sika 615 (14 days) and Sika LW (10 days). A similar order in age at cracking is observed in 7 day cured specimens, with Sika 612 recording the longest time to crack initiation. Sika LW had the shortest time to cracking in both instances. As pointed out earlier, the large margin of tensile relaxation and low values of elastic modulus in Sika 612 are probably responsible for its long period to cracking. Tensile relaxation appears to have a very big influence on age at cracking. Both Sika LW and Sika 612 had very high values of free shrinkage strain and low values of tensile strength, yet Sika LW recorded the shortest time to cracking while Sika 612 had the longest time to cracking. The possible explanation could be the fact that Sika 612 underwent relatively higher margin of relaxation than Sika LW (see Section 4.2.4). These results are in agreement with the findings by Pigeon & Bissonnette (1999) and Weiss *et al.*

(1998) who found that the response of thin overlays to drying shrinkage is highly influenced by the tensile creep capacity of the repair material.

Figure 4.21 shows that there is an increase in age at cracking with increased curing period. There was an increase in age at cracking of 4 days (Sika 612), 3 days (w/c = 0.45) and 2 days (w/c = 0.6). Sika LW and Sika 615 recorded no changes in age at cracking with increased curing time. For the laboratory mixes, this may be attributed to the increase in tensile strength with curing period. Also the increase in tensile relaxation with curing duration (Section 4.2.4.2) may have an influence.

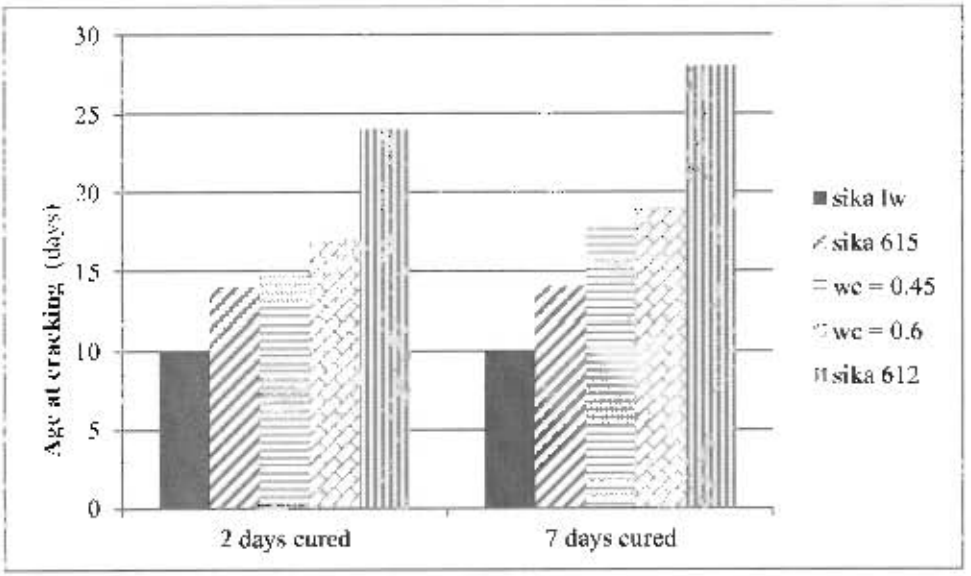

Figure 4.21: Results for age at cracking in bonded overlays.

4.4.2 Crack area

The results of crack area are given in Figure 4.22. According to the figure, Sika LW recorded the highest crack area followed by Sika 615, w/c = 0.45, Sika 612 and w/c = 0.6. Curing does not seem to have a specific influence on crack area because a reduction in crack area (Sika LW, Sika 615 and w/c = 0.45) and an increase in crack area (Sika 612 and w/c = 0.6) with increased curing time were observed. The mortar specimens that had low values of age at cracking (Figure 4.21) recorded the highest crack area except Sika 612 and w/c = 0.6, see Figure 4.23.

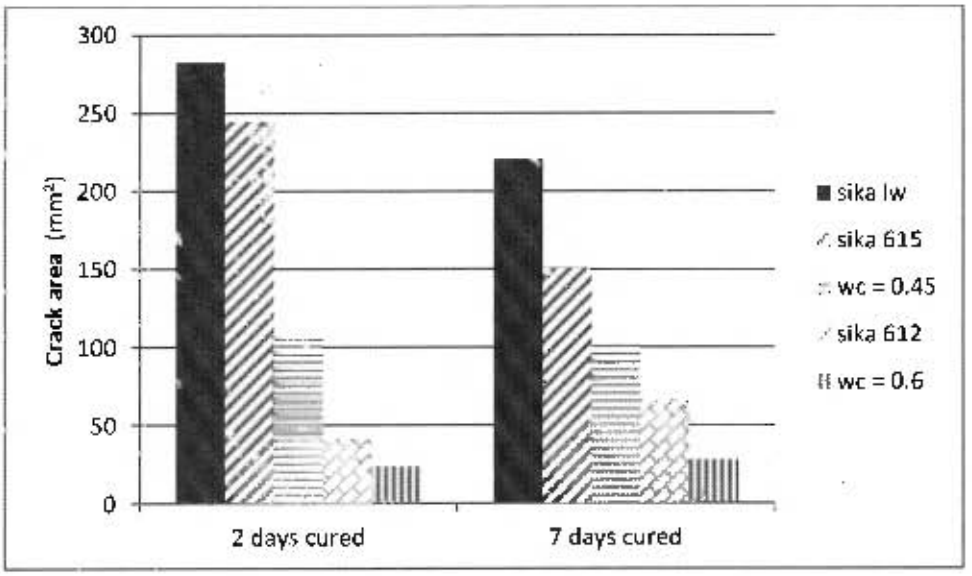

Figure 4.22: Results for crack area in bonded overlays.

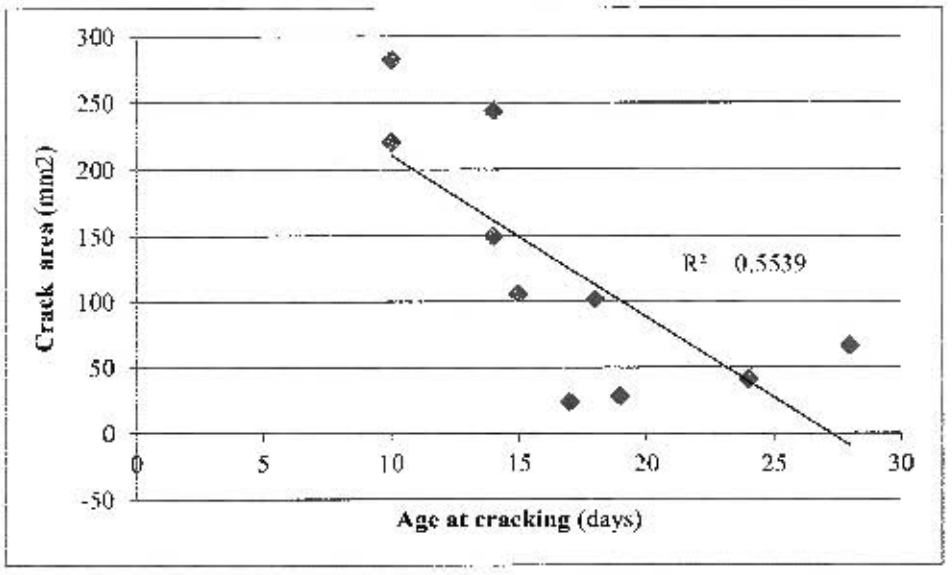

Figure 4.23: Crack area vs. age at cracking in bonded overlays.

4.5 Conclusion

Crack resistance of concrete repair mortars depends upon the interaction of many factors. To understand how these factors influence cracking of repair mortars/overlays, material property tests were carried out and results discussed in the preceding sections. In addition, the age at cracking and extent of cracking (crack area) were also determined using the ring test and bonded overlays. The following conclusions can be made based on the results and analysis presented in this chapter:

- Shrinkage alone, in spite of it being very important, does not determine the cracking behaviour of bonded overlays. Both Sika LW and Sika 612 had very high values of free shrinkage strain, yet Sika LW recorded the shortest time to cracking while Sika 612 recorded the longest time to cracking. This suggests that crack resistance of repair mortars depends upon the combined influence of a number of factors other than just one factor. Also Sika LW and Sika 615 specimens had the same age at cracking despite them having different material properties. Sika 615 had higher elastic modulus and tensile strength than Sika LW, while Sika LW underwent higher degree of relaxation and higher shrinkage strain than Sika 615. Cracking behaviour of repair mortars depends upon the combined influence of shrinkage, elastic modulus, tensile relaxation and tensile strength. This agrees with Pigeon *et al.,* (2000), who noted that crack resistance of repair mortars is a combined influence of various material properties and parameters.

- Tensile relaxation is correlated to age at cracking. Depending on the age of loading, tensile relaxation will reduce overlay stresses by approximately 20-58% (2 day cured specimens) and 20-48% (7 day cured specimens) in the mixes tested. These values seem to be in agreement with published literature (Masuku, 2009; Beushausen, 2005; Pigeon *et al.,* 2000). The degree of tensile relaxation depends upon the age of loading. High values of relaxation were observed in younger specimens than in older specimens.

- An increase in curing period was observed to delay the onset of cracking in both ring test specimens and bonded overlays tested in this study. This was attributed to the effect that curing had on free shrinkage strain and tensile strength. In addition to delaying free

shrinkage strain, curing was observed to increase the tensile strength of the repair mortar specimens. The combined influence of these factors appears to override the effect of increased elastic modulus with an increase in curing period.

A comparison of results from the ring test, results of the bonded overlays and also of the analytical modeling of age at cracking is done in Chapter Five.

CHAPTER FIVE: ANALYTICAL MODELING OF RESULTS

5.1 Introduction

This chapter presents an analytical method used in predicting the age at cracking of the bonded overlays used in the study. The chapter starts off by giving the theoretical basis behind the analytical method, and also the different assumptions made regarding the parameters used in the analysis. Also a comparison of results between the results from the analytical method to the results from the bonded overlays and the ring test is made. This comparison makes it possible for the research question to be answered. The chapter closes by summarizing the main conclusion drawn from the comparison of the different results.

5.2 Basis for the analytical modeling approach

The analytical modeling approach used in this study is based on the time development of the relevant material properties from the time curing is discontinued. Figure 5.1 shows a schematic of the main idea behind the approach. The tensile strength, the elastic stress resulting from restrained shrinkage and the stress remaining after tensile relaxation are all plotted against the age of concrete. The point on the graph at which the elastic stress exceeds the tensile strength depicts the age at which cracking would occur if the effect of stress relaxation were ignored. However, due to tensile relaxation of the material, the elastic stress only exceeds the tensile strength of the material at a later age. Hence, tensile relaxation imparts stress relief to the material which helps in delaying the age at cracking. The elastic stress remaining after the effect of tensile relaxation is deemed the remaining stress, and the point on the graph at which the remaining stress exceeds the tensile strength of the material depicts the predicted age at cracking of the material.

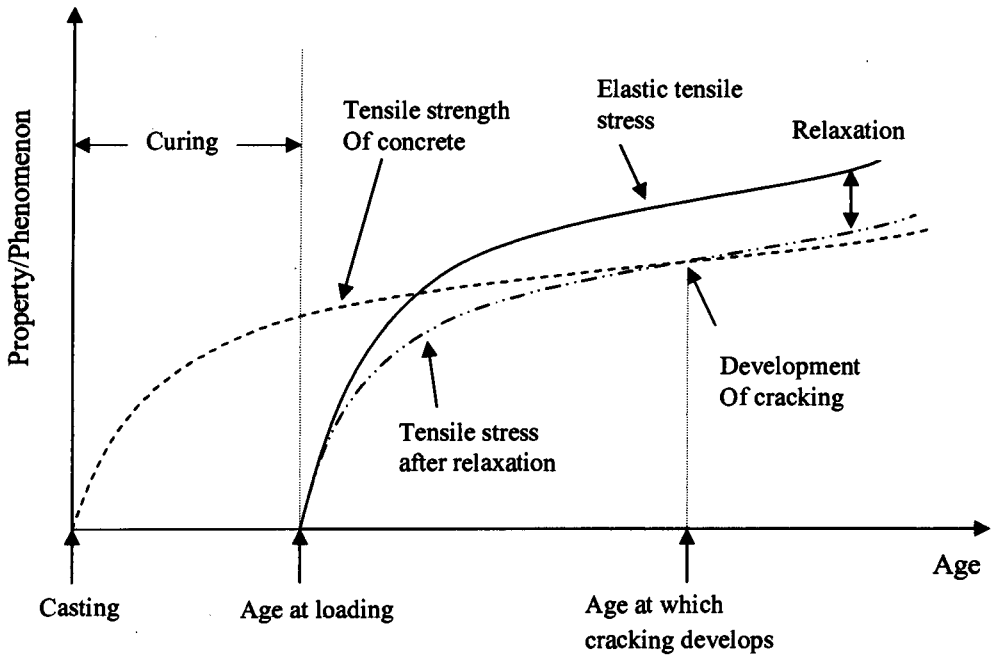

Figure 5.1: Schematic of the main idea behind the analytical modeling of age at cracking in bonded overlays

Since there was no direct method of measuring the elastic stress in the material, the elastic stress had to be estimated from the product of the restrained shrinkage strains and the modulus of elasticity of the material. The analytical modeling procedure, therefore, involved estimating the time development of the elastic stress and comparing it to the time development of the tensile strength of the material. To estimate the time development of the elastic stress, a step-by-step method was employed. This method involves dividing the total time into a number of intervals, and then calculating the stress increment resulting from the change in shrinkage strain in each interval. The principle of superposition which states that "the stress produced by a strain increment applied at any time t_o is not affected by any strain applied either earlier or later" makes this possible (Gilbert, 1988; Ghali *et al.*, 2006).

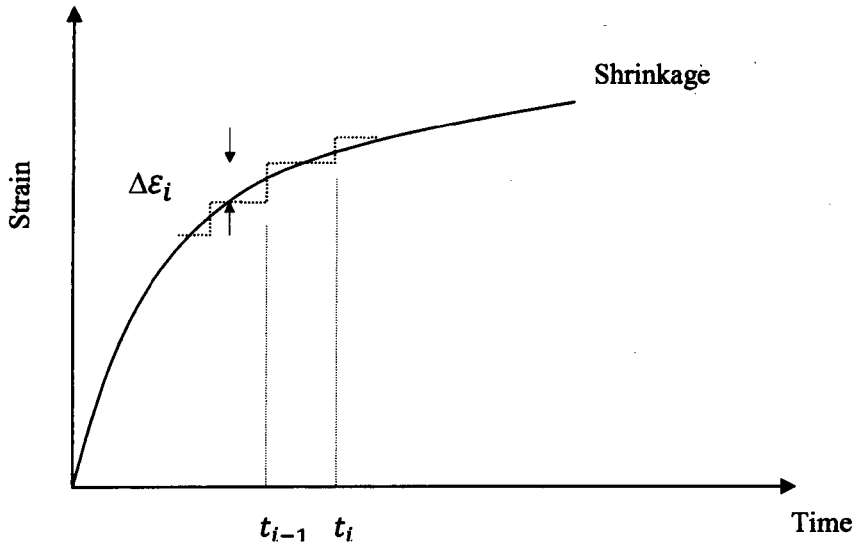

Figure 5.2: Time-varying strain history.

Thus, according to the principle of superposition, the elastic stress σ_i in concrete at any time t_i subjected to a time varying strain history like the one shown in Figure 5.2 is given by,

$$\sigma_i = \sigma_{i-1} + \Delta\varepsilon_i \; E_i \qquad [5.1]$$

where σ_i = stress at time t_i

σ_{i-1} = stress at time t_{i-1}

$\Delta\varepsilon_i$ = change in shrinkage strain in the interval $t_{i-1} - t_i$

E_i = mean elastic modulus in the interval $t_{i-1} - t_i$

For the continuously varying strain history shown in Figure 5.2, the strain increment which occurs during the i-th time interval, $\Delta\varepsilon_i$, is assumed to be applied at the middle of the interval. The mean elastic modulus is also taken at the middle of the interval. The above procedure can also be used to estimate the remaining stress $\ddot{\sigma}_i$ i.e. the stress remaining after accounting for the effects of tensile relaxation. This is achieved by introducing a relaxation factor ψ_i , and rewriting the above equation as follows,

$$\ddot{\sigma}_i = \ddot{\sigma}_{i-1} + \Delta\varepsilon_i \; E_i \; \psi_i \qquad [5.2]$$

where $\ddot{\sigma}_i$ = remaining stress at time t_i

$\ddot{\sigma}_{i-1}$ = remaining stress at time t_{i-1}

$\Delta\varepsilon_i$ = change in shrinkage strain in the interval $t_{i-1} - t_i$

E_i = mean elastic modulus in the interval $t_{i-1} - t_i$

ψ_i = factor accounting for the magnitude of the mean relaxation in the interval $t_{i-1} - t_i$

The relaxation factor ψ_i is also calculated at the middle of the interval, just like the elastic modulus. The calculation of the elastic modulus and tensile relaxation are discussed further in the next section (Section 5.3). The calculated elastic stress and the remaining stress, together with the tensile strength of the concrete, are then plotted against time (concrete age) to predict the age at cracking. The greater the number of time intervals, the more accurate is the estimations. According to Gilbert (1988), this method is perfectly general and can be used to predict behaviour due to any stress or strain history using any desired creep and shrinkage curves.

5.3 Main experimental parameters

The main experimental parameters used in the analytical modeling are the tensile strength, the elastic modulus, the tensile relaxation and the restrained shrinkage strain. Since these material properties were tested at specific ages i.e. at 2, 7, 14, 21 and 28 for 2 day-cured specimens and at 7, 10, 14, 21 and 28 for 7 day-cured specimens, regression functions were needed to interpolate values at the days when the properties were not tested. A literature survey (Straub, 1930; Meyers *et al.*, 1970; Gilbert, 1988; Gutsch & Rostasy, 1994; Weiss *et al.*, 1998; Masuku, 2009; Yoshitake *et al.*, 2011) indicates that different functions have been used in the past to model observed trends in concrete material properties. These functions have ranged from logarithmic functions, algebraic functions, power functions, exponential functions, hyperbolic functions to a combination of these.

Weiss *et al.,* (1998) used an exponential function (Equation 5.3) to obtain regression fits for elastic modulus of normal strength concrete. The shape of this equation was based on a form suggested by Muller (1994), although it was modified so as to better correlate with experimental data. Figure 5.3(a) shows how this equation fitted with experimental data. Yoshitake *et al.,* (2011) used a hyperbolic function (Equation 5.4) in predicting the tensile modulus at early age of normal mortar. Their equation included two coefficients that accounted for the effect of water-to-cement ratio and age of the mortar specimens. Figure 5.3(c) shows a fit of the equation with experimental data. Gutsch & Rostasy (1995) used an exponential function to model relaxation, while Masuku (2009) employed an algebraic function (Equation 5.5) in predicting long term tensile relaxation of mortar specimens. He investigated the effect of age at loading and mix type (see Section 2.4). The equation showed good fit with experimental data, Figure 5.3(b). Generally, the choice of a function used to interpolate time-dependent material properties with physically observed trends depends upon the experimental data.

$$E_\sigma(\xi) = E_c * \exp\left[A - (B/(\xi/t_1))^{0.5}\right] \quad [5.3]$$

where $E_\sigma(\xi)$ = elastic modulus from regression

E_c = 28-day elastic modulus

A and B = regression constants

ξ = time

t_1 = time of loading

$$E_t(T) = 4.3\frac{C}{W} + \frac{21T}{T+1.5} \quad [5.4]$$

where $\frac{C}{W}$ = inverse water-to-cement ratio

T = time (days)

$$\psi(t) = 100 - \sigma_t/\sigma_0 = 100 - A \cdot t^{(B)}\ (\%) \quad [5.5]$$

where $\psi(t)$ = relaxation function

σ_t = stress at time t

σ_0 = initial stress

A, B = empirical constants

t = time (hours)

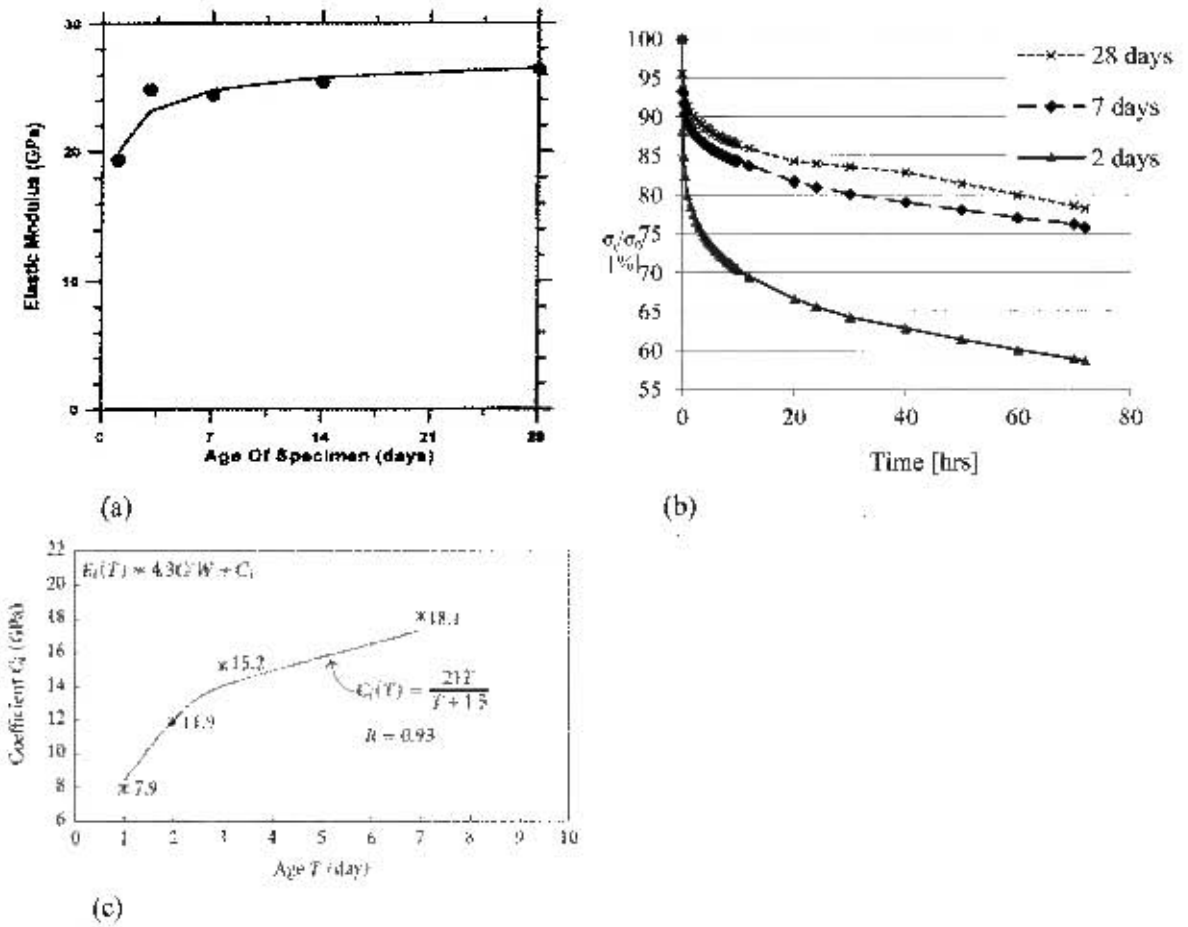

Figure 5.3: Material property regression: (a) Elastic modulus, after Weiss *et al.*, (1998); (b) Tensile relaxation, after Masuku (2009) and (c) Elastic modulus, after Yoshitake *et al.*, (2011)

In this study logarithmic based regression functions (Equations 5.6-5.8) were used as they showed good fit with the experimental data. Curves obtained from these functions were used in the analytical modeling. Typical curves are shown in Figure 5.4(a) for elastic modulus, Figure 5.4(b) for tensile strength and Figure 5.4(c) for tensile relaxation. The rest of the curves are given in Appendix A.

$$E_i(t_i) = \mathrm{A}\ln(t_i) + \mathrm{B} \quad [5.6]$$

$$F_{Vi}(t_i) = \mathrm{C}\ln(t_i) + \mathrm{D} \quad [5.7]$$

$$\beta_i(t_i) = \mathrm{N}\ln(t_i) + \mathrm{M} \quad [5.8]$$

$$\psi_i(t_i) = (100 - \beta_i(t_i)) * \frac{1}{100} \quad [5.9]$$

where $E_i(t_i)$ – mean elastic modulus in the interval $t_{i-1} - t_i$

$\beta_i(t_i)$ = mean relaxation in the interval $t_{i-1} - t_i$

$F_{Yi}(t_i)$ = tensile strength at time t_i

A, B, C, D, N and M = constants depending on regression analysis

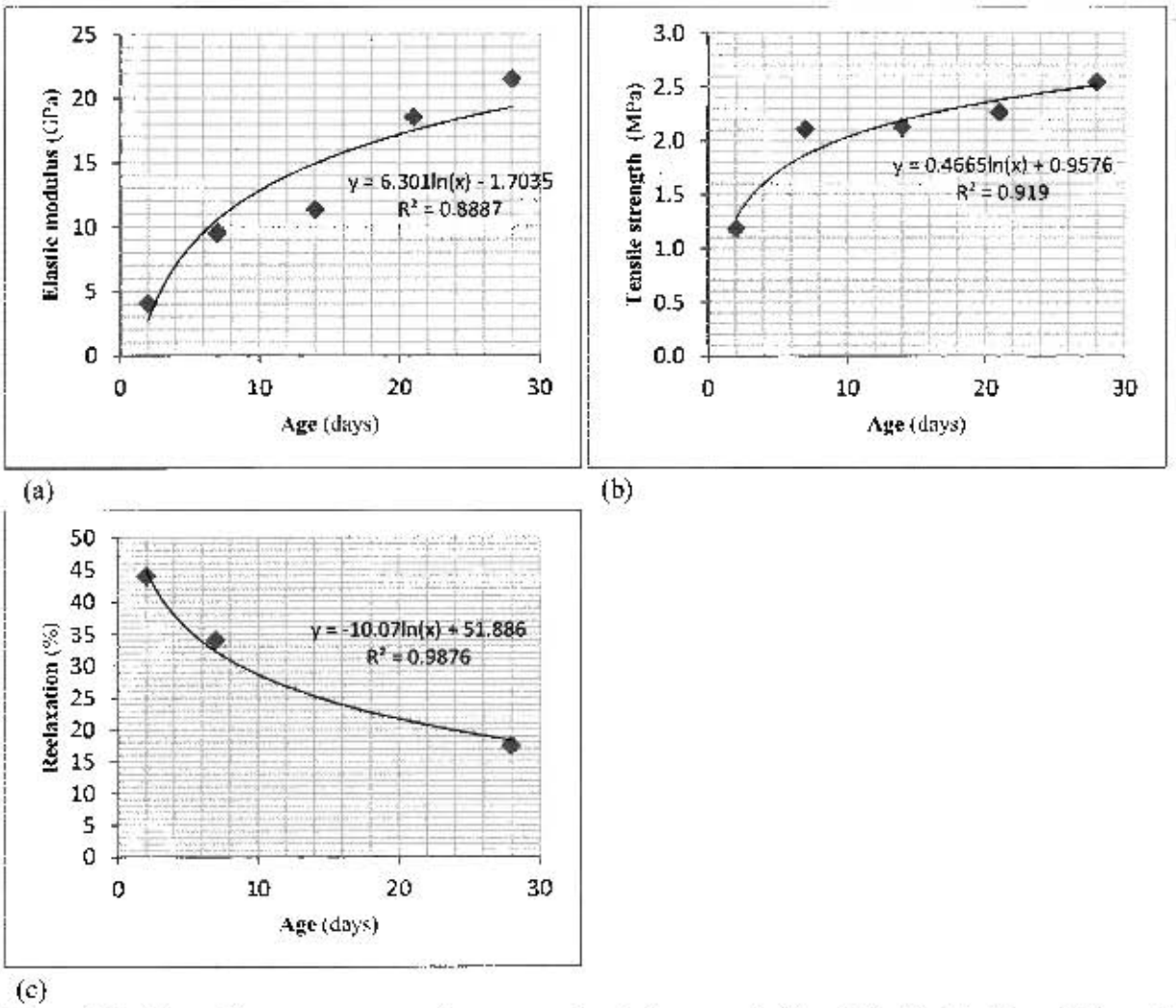

Figure 5.4: Material property regression curves for 2 days cured Sika LW: (a) Elastic modulus, (b) Tensile strength, and (c) Tensile relaxation.

5.4 Assumptions made regarding the main parameters

In order to simplify the prediction of age at cracking in bonded overlays, a number of assumptions regarding the material properties and other factors had to be made. These assumptions are necessary because a lot of factors affect the crack resistance of overlays in a complex way, and it is not possible to account for all the possible effects. The following sections give the main assumptions taken in the analytical modeling of age at cracking.

5.4.1 No shrinkage during curing

To facilitate calculation of stresses resulting from restraint, shrinkage is assumed to occur only from the period after curing. This may be represented as in Figure 5.5.

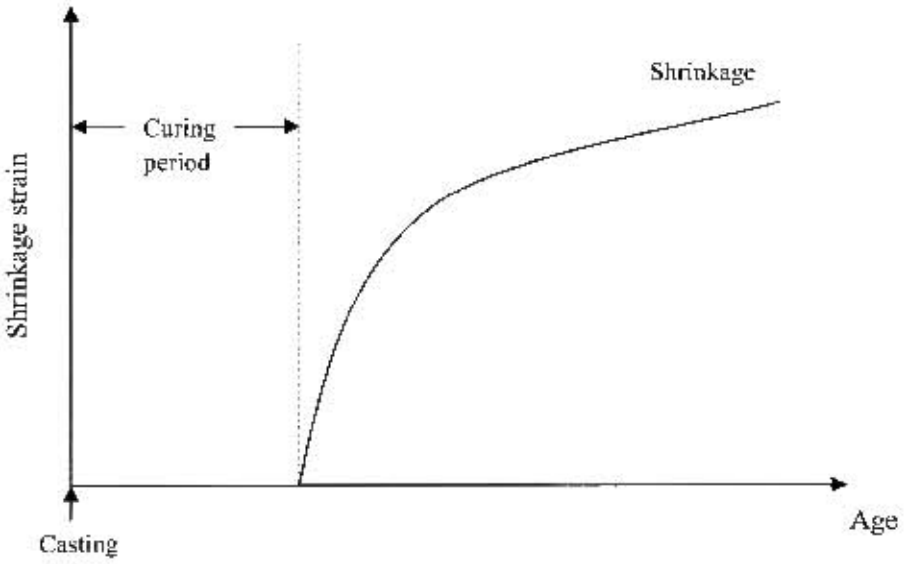

Figure 5.5: Schematic showing commencement of shrinkage.

During curing, shrinkage may occur due to autogenous shrinkage. However, Alexander (2001) states that shrinkage during curing is noteworthy particularly in concrete with a low w/c ratio (i.e. <0.40), which is not appreciable for the majority of mixes used in practice. Therefore, in this study it is assumed that the autogenous shrinkage that occurs during curing is negligible. And that no plastic shrinkage occurs during curing. A more sophisticated approach however, should consider autogenous shrinkage effects.

5.4.2 Tensile relaxation is instantaneous

Previous tensile relaxation studies (Masuku, 2009; Beushausen & Alexander, 2006; Harimoto & Koyanagi, 1994; and Gutsch & Rostasy, 1994) have shown that a large amount of tensile stress relaxation takes place at early ages of loading. The above authors found tensile stress relaxation to develop rapidly after loading. Relaxation results obtained in this study confirmed the findings above (Section 4.2.4).

Stress relaxation develops at a much faster rate than stresses resulting from ongoing overlay shrinkage. Therefore, in order to facilitate analytical modeling of overlay stresses, it appears appropriate to account for overlay stress relaxation in a simple manner. For the analysis of stresses it is assumed that tensile stress relaxation occurs instantaneously after loading (Figure 5.6) (Masuku, 2009; Beushausen & Alexander, 2006).

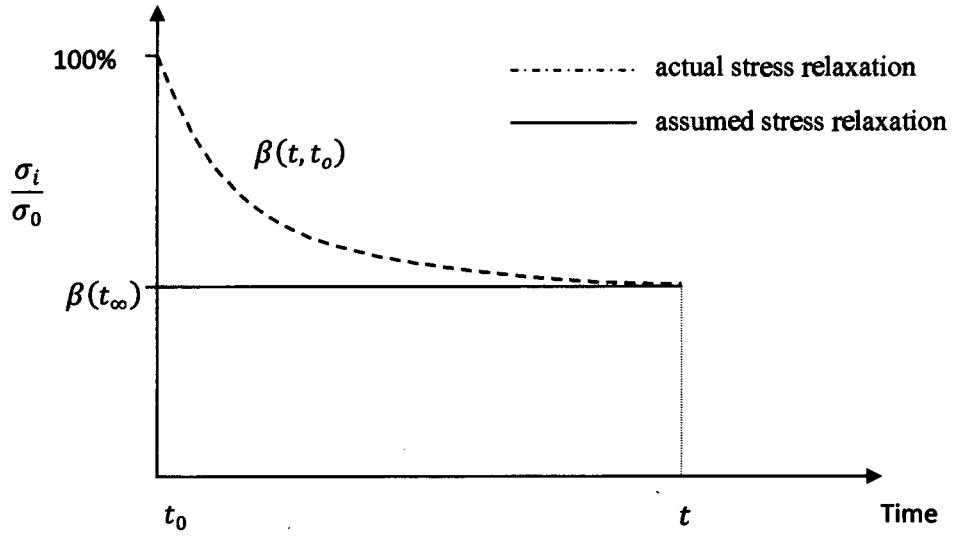

Figure 5.6: Schematic of simplified approach for the consideration of overlay stress relaxation.

From Figure 5.6 the relaxation function may be taken as a constant value. In this case the 72 hour relaxation is taken as ultimate value and applied in the modeling.

5.4.3 Restraint is proportional to free shrinkage

Previous research by Beushausen (2005), showed restraint in bonded concrete overlays to be roughly 60% of overlay free shrinkage (see Section 2.7.3). In this study restrained shrinkage strains are, therefore, calculated as 60% of the free shrinkage strains. Hence, in calculating the change in shrinkage strain $\Delta\varepsilon_i$ (Section 5.2), a factor accounting for 60% is applied to the change in free shrinkage strain i.e.

$$\Delta\varepsilon_i = 0.6\,\Delta\,\varepsilon_{FSS\,i} \qquad [5.10]$$

where $\Delta\varepsilon_i$ = change in restrained shrinkage strain in the interval $t_{i-1} - t_i$

$\Delta\,\varepsilon_{FSS\,i}$ = change in free shrinkage strain in the interval $t_{i-1} - t_i$

5.5 Application of model

In this section, the performance of the repair mortars is investigated using the above-mentioned method. Since specimens were cured for 2 days and 7 days, the model shows time development of elastic stress and remaining stress starting from the age of 2 days for 2-day cured specimens and 7 days for 7-day cured specimens. It is assumed that shrinkage induced stresses only start after the end of curing (see Section 5.4.1). The model shows the time development of tensile and remaining stress for a period of 28 days because material properties data for each mortar type (per curing regime) was taken for a period of 28 days. In addition, almost all the repair mortars cracked within a period of 28 days. The 28 days period was divided into 2-day time intervals to enable the calculation of stresses, as given in Section 5.2. Intervals of 2 days were chosen because they provided reasonable accuracy.

5.5.1 2 day Sika LW

Table 5.1 shows the material properties data of Sika LW specimens cured for 2 days.

Table 5.1: Material properties for 2 day cured Sika LW specimens.

Period (days)	Change in free shrinkage strain (10)	Mean elastic modulus [GPa]	Tensile strength [MPa]	Mean tensile relaxation [%]	Elastic stress [MPa]	Remaining stress [MPa]
0-2	0.0	1.0	1.3	45.0	0.0	0.0
2-4	260.0	4.0	1.5	41.0	0.6	0.4
4-6	250.0	8.0	1.7	36.0	1.8	1.1
6-8	140.0	10.5	1.9	32.0	2.7	1.7
8-10	130.0	12.0	2.0	29.5	3.6	2.4
10-12	110.0	13.5	2.1	27.5	4.5	3.0
12-14	20.0	14.5	2.2	26.0	4.7	3.2
14-16	20.0	15.5	2.3	24.5	4.9	3.3
16-18	30.0	16.0	2.3	23.5	5.2	3.5
18-20	60.0	17.0	2.3	22.0	5.8	4.0
20-22	25.0	17.5	2.4	21.0	6.1	4.2
22-24	5.0	18.0	2.4	20.5	6.1	4.3
24-26	20.0	18.5	2.5	19.5	6.3	4.4
26-28	5.0	19.0	2.5	18.5	6.4	4.5

A plot of data given in Table 5.1 is shown in Figure 5.7. According to the figure, it takes about 9 days for cracks to initiate in Sika LW cured for 2 days. This corresponds to 7 days after curing. It is observed that tensile relaxation delays the onset of cracking by 3 days. Sika LW cracks at a relatively young age of 9 days. This is likely because the rate of increase in shrinkage is higher than the rate of gain in tensile strength. A combined effect of increase in shrinkage and elastic modulus causes a build-up of shrinkage induced stresses. Since tensile relaxation is not enough to relieve the resulting stresses, cracking results.

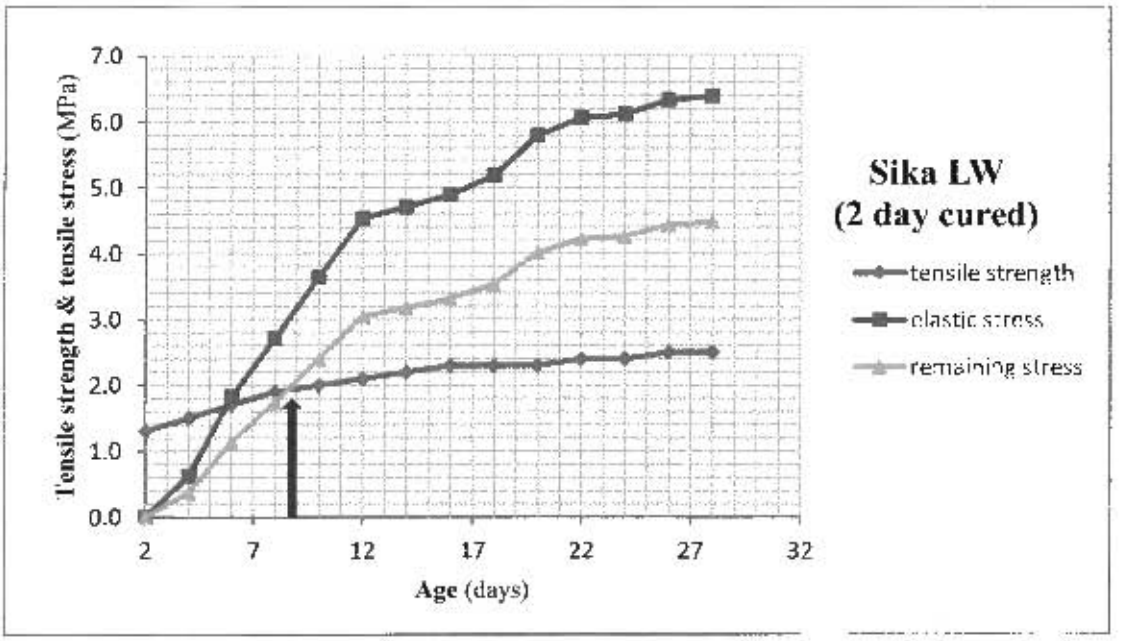

Figure 5.7: Overlay strength and stress development for 2-day cured Sika LW specimens.
(Arrow indicates the age at crack initiation)

5.5.2 7 day Sika LW

The material properties data of Sika LW specimens cured for 7 days is given in Table B.2 in Appendix B. The data given in Table B.2 is plotted in Figure 5.8. According to the figure, it takes about 9 days for Sika LW cured for 7 days to start cracking. This represents 2 days after the end of curing. Comparing Figures 5.7 and 5.8 it is observed that both the 2 day-cured and the 7 day-cured Sika LW crack at the same age. However, the 2 day-cured specimens take 7 days after curing for cracks to initiate. This may be attributed to the high level of tensile relaxation experienced at the young age (see Section 4.2.4).

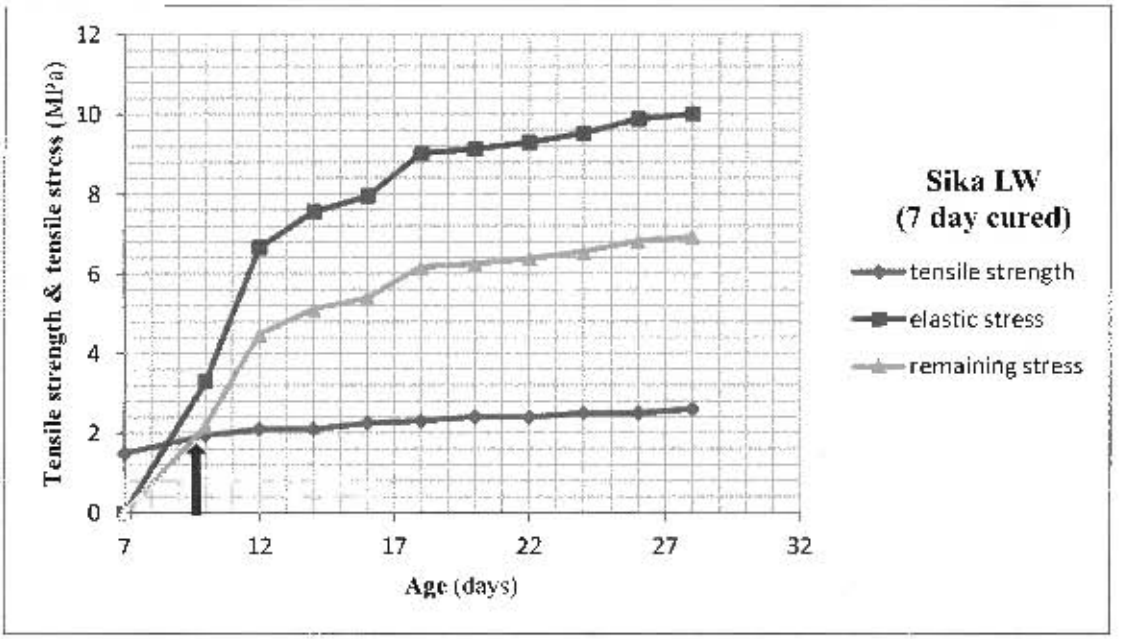

Figure 5.8: Overlay strength and stress development for 7-day cured Sika LW specimens. *(Arrow indicates the age at crack initiation)*

5.5.3 2 day Sika 615

Table B.3 in Appendix B gives the material properties data of Sika 615 specimens cured for 2 days. A plot of the data in Table B.3 is given in Figure 5.9. It takes 14 days for cracks to initiate in Sika 615 cured for 2 days. This represents 12 days after the end of curing. This is greater than the 7 days it takes for cracks to initiate in 2 day-cured Sika LW. In spite of the fact that 2 day-cured Sika 615 has a lower tensile relaxation and a much higher elastic modulus than 2 day-cured Sika LW, it cracks at a later age than 2 day-cured Sika LW. This may be attributed to the high strength gain experienced by Sika 615.

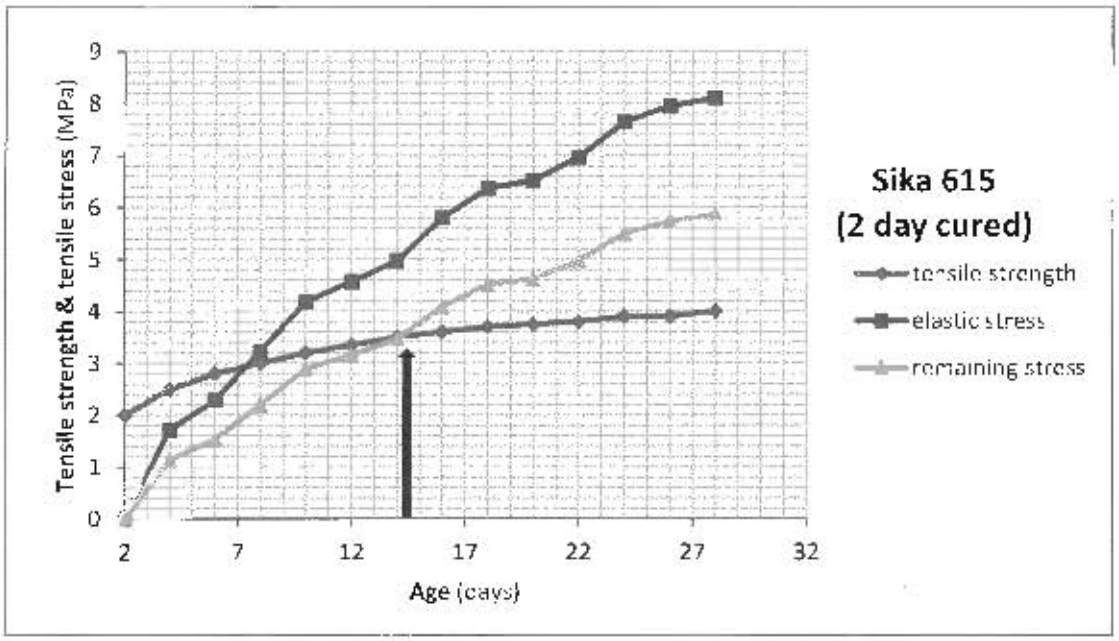

Figure 5.9: Overlay strength and stress development for 2-day cured Sika 615 specimens. *(Arrow indicates the age at crack initiation)*

5.5.4 7 day Sika 615

Material properties data of Sika 615 specimens cured for 7 days is given in Table B.4 in Appendix B. Figure 5.10 shows a plot of the data given in Table B.4. It is observed that Sika 615 cured for 7 days cracks at approximately the age of 13 days. This corresponds to 6 days after curing. Comparing with the 2 day-cured Sika 615, it takes 7 day-cured Sika 615 specimens half the time for cracks to initiate than it takes 2 day-cured Sika 615 specimens. This may be attributed to the higher tensile strength at every age in the 2 day-cured specimens (see Section 5.2.2). Other factors being equal (i.e. elastic modulus, tensile relaxation etc), high tensile strength delays the onset of cracking.

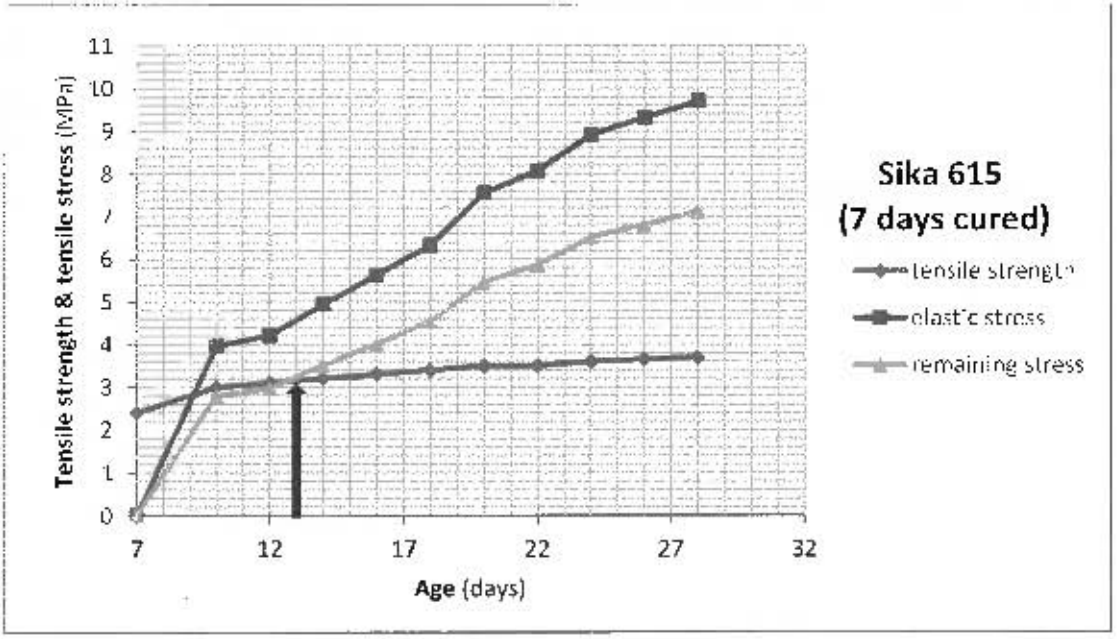

Figure 5.10: Overlay strength and stress development for 7-day cured Sika 615 specimens. *(Arrow indicates the age at crack initiation)*

5.5.5 2 day Sika 612

Material properties data of Sika 612 specimens cured for 2 days is given in Table B.5 in Appendix B. A plot of the data given in Table B.5 is given in Figure 5.11. According to Figure 5.9, Sika 612 cured for 2 days does not undergo cracking within the 28 days period of testing. It is observed that the tensile strength of Sika 612 is greater than the remaining stress, hence, no cracking occurs within the testing period. This is in spite of the fact that 2 day-cured Sika 612 undergoes the greatest drying shrinkage (excluding 7 day-cured Sika 612) among all the repair mortars. The absence of cracking within the 28 days testing period may be attributed to the fact that 2 days-cured Sika 612 had the lowest elastic modulus among all the mortars and also underwent the greatest amount of tensile relaxation (see Sections 5.2.3 and 5.2.4). The combined effect of a high degree of relaxation and low elastic modulus leads to high resistance to crack initiation.

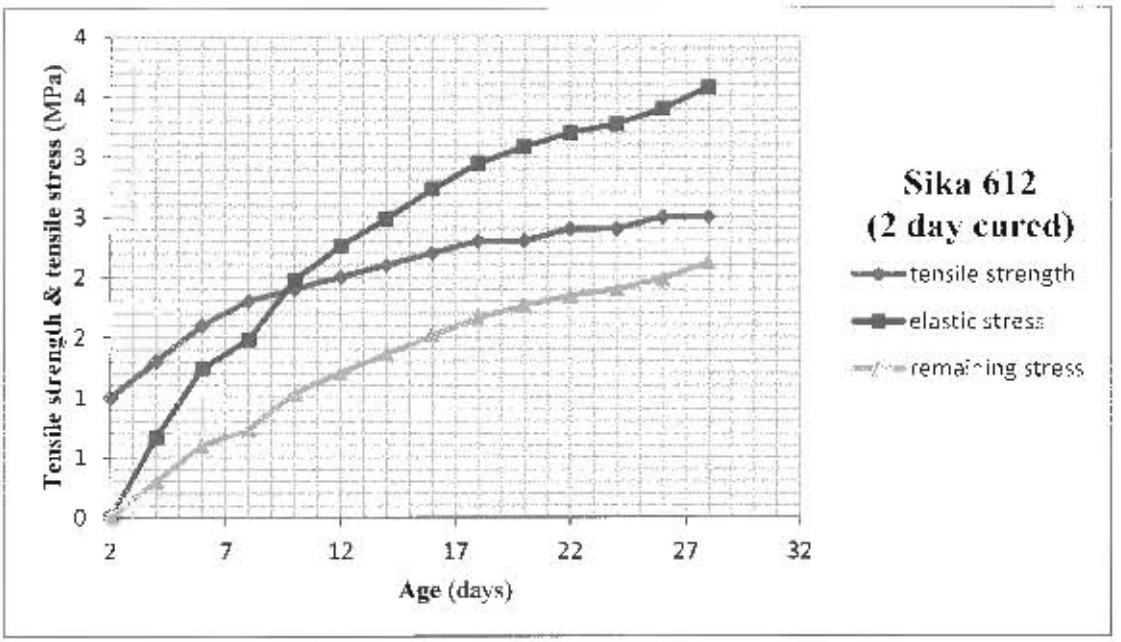

Figure 5.11: Overlay strength and stress development for 2-day cured Sika 612.

5.5.6 7 day Sika 612

Table B.6 in Appendix B shows the material properties data of Sika 612 specimens cured for 7 days. The data given in Table B.6 is plotted in Figure 5.12. The figure shows that 7 day-cured Sika 612 is likely to crack at the age of 12 days. This corresponds to 5 days after the end of curing. It is interesting to note the contrasting performance between 7 days-cured Sika 612 and that of 2 day-cured. While 7 day-cured Sika 612 cracks just after 12 days, 2 day-cured Sika 612 does not crack within the testing period. This may be explained by the fact that 7 day-cured Sika 612 undergoes higher shrinkage than 2 day-cured Sika 612. In addition, the degree of tensile relaxation is much higher at the early age that is associated with 2 day-cured Sika 612. Furthermore, 7 day-cured Sika 612 has a higher elastic modulus at the age of loading (end of curing) than 2 day-cured Sika 612.

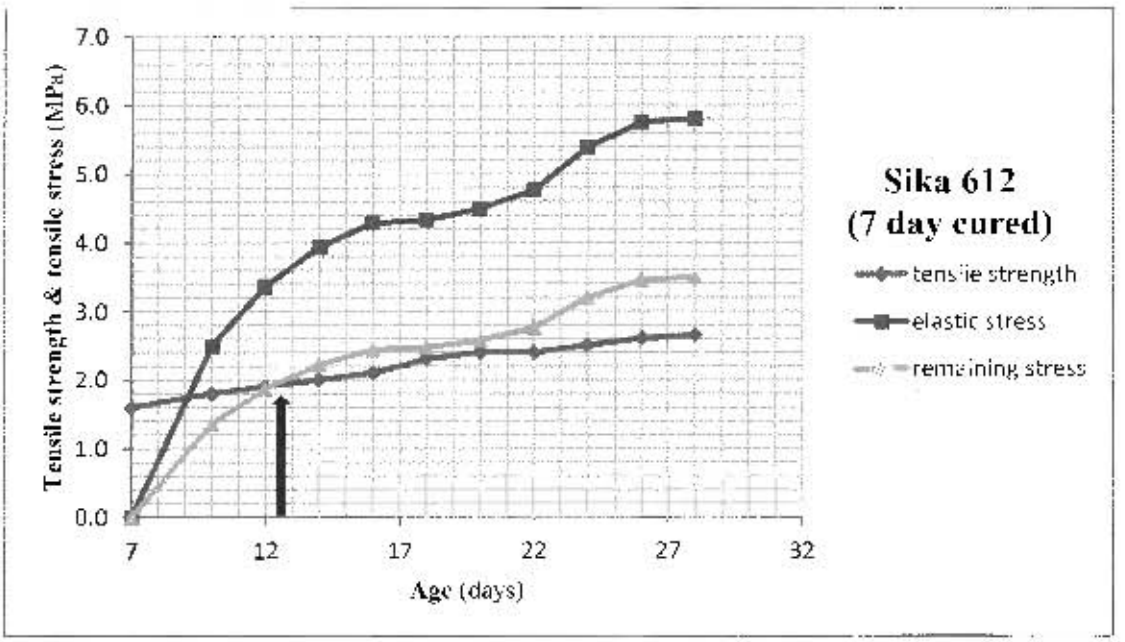

Figure 5.12: Overlay strength and stress development for 7-day cured Sika 612 specimens. *(Arrow indicates the age at crack initiation)*

5.5.7 2 day w/c = 0.45

Material properties data of w/c = 0.45 specimens cured for 2 days is given in Table B.7 in Appendix B. Figure 5.13 shows a plot of the data given in Table B.7. From the figure, it is observed that the 0.45 mix cured for 2 days cracks at the age of 14 days. This represents 12 days after the end of curing. Therefore, 2 day-cured 0.45 mix cracks at the same age as 2 day-cured Sika 615. This may be because, even though 0.45 mix underwent higher shrinkage than Sika 615, Sika 615 had a higher elastic modulus than 0.45 mix. Thus, the two effects seem to even out. Note that both mixes had similar values of tensile strength and tensile relaxation.

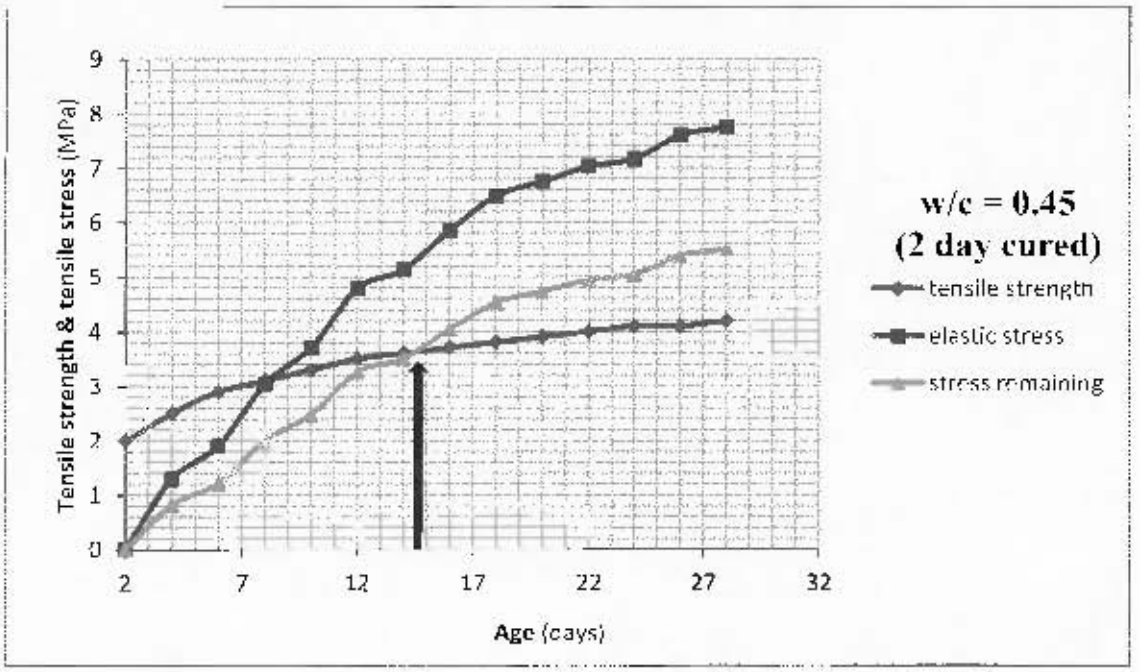

Figure 5.13: Overlay strength and stress development for 2-day cured w/c = 0.45 specimens. *(Arrow indicates the age at crack initiation)*

5.5.8 7 day w/c = 0.45

Material properties data of w/c = 0.45 mix specimens cured for 7 days is given in Table B.8 in Appendix B. Figure 5.14 gives a plot of the data shown in Table B.8. According to the figure, 7 day-cured 0.45 mix cracks at the age of 15 days. This corresponds to 8 days after the end of curing. Compared to the 2 day-cured 0.45 mix, the 7 day-cured mix cracks at an age that is 1 day later than that of the 2 day-cured mix. This may be attributed to the fact that the tensile strength of concrete increases with an increase in the duration of curing. Subsequently, the onset of cracking is delayed. It is also observed that 7 day-cured 0.45 mix performs better than 7 day-cured Sika LW, Sika 615 and Sika 612. The 7 day-cured 0.45 mix had the highest tensile strength of all the repair mortars.

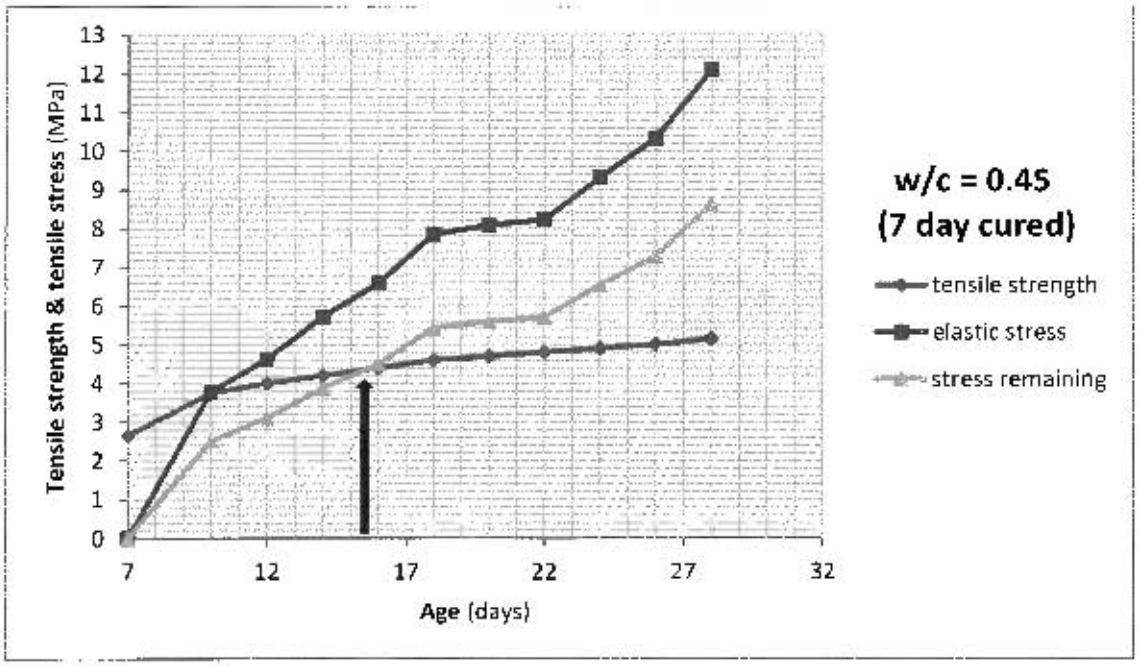

Figure 5.14: Overlay strength and stress development for 7-day cured w/c = 0.45 specimens. *(Arrow indicates the age at crack initiation)*

5.5.9 2 day w/c = 0.6

Table B.9 in Appendix B gives the material properties data of w/c = 0.6 specimens cured for 2 days. Figure 5.15 shows a plot of the data given in Table 5.9. From the figure, 2 day-cured 0.6 mix cracks at the age of 17 days. This represents 15 days after the end of curing. Of all the 2 day-cured specimens (excluding Sika 612), the 0.6 mix takes the longest time to crack. This may be because the 2 day-cured 0.6 mix underwent the lowest shrinkage of all the mortars. In addition, apart from 2 day-cured Sika 612, the 0.6 mix recorded the highest degree of tensile relaxation.

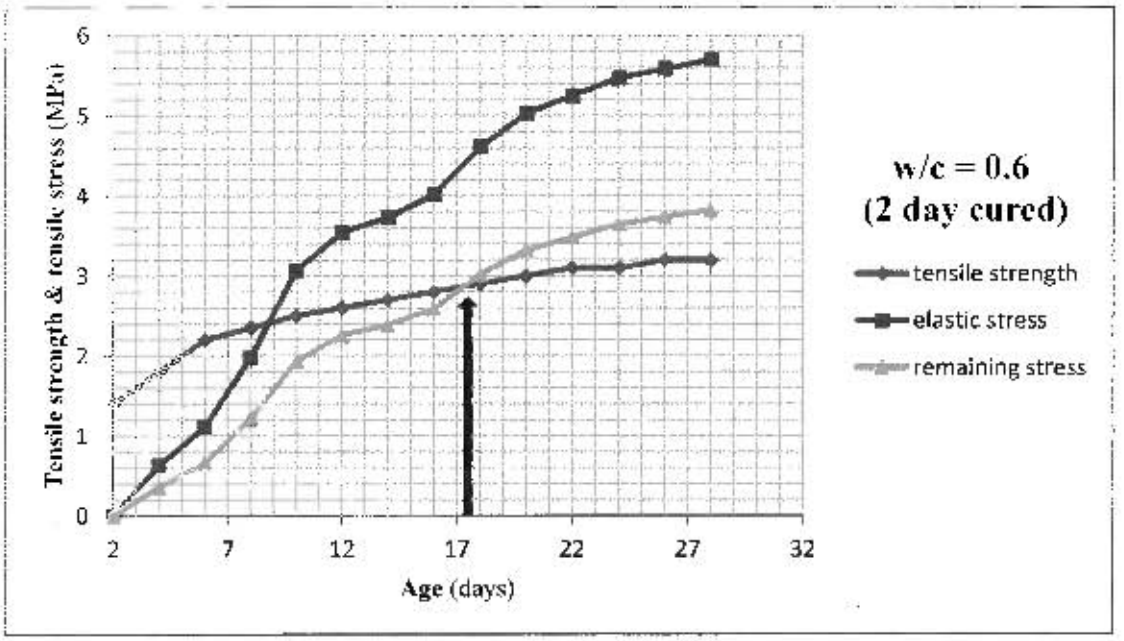

Figure 5.15: Overlay strength and stress development for 2-day cured w/c = 0.6 specimens. *(Arrow indicates the age at crack initiation)*

5.5.10 7 day w/c = 0.6

Material properties data of w/c = 0.6 mix specimens cured for 7 days is given in Table B.10 in Appendix B. Figure 5.16 shows a plot of the data given in Table B.10. According to Figure 5.16, w/c = 0.6 mix specimens cured for 7 days crack at an age of 20 days. This corresponds to 13 days after the end of curing. Of all the 7 day-cured specimens, the 7 day-cured 0.6 mix takes the longest time to crack. This may be attributed to the combined effect of low shrinkage and high relaxation. Compared to the 2 day-cured 0.6 mix, the 7 day-cured mix cracks at an age that is 2 days later than that of the 2 day-cured mix. This may be due to an increase in tensile strength with increased duration of curing. Subsequently, the onset of cracking is delayed.

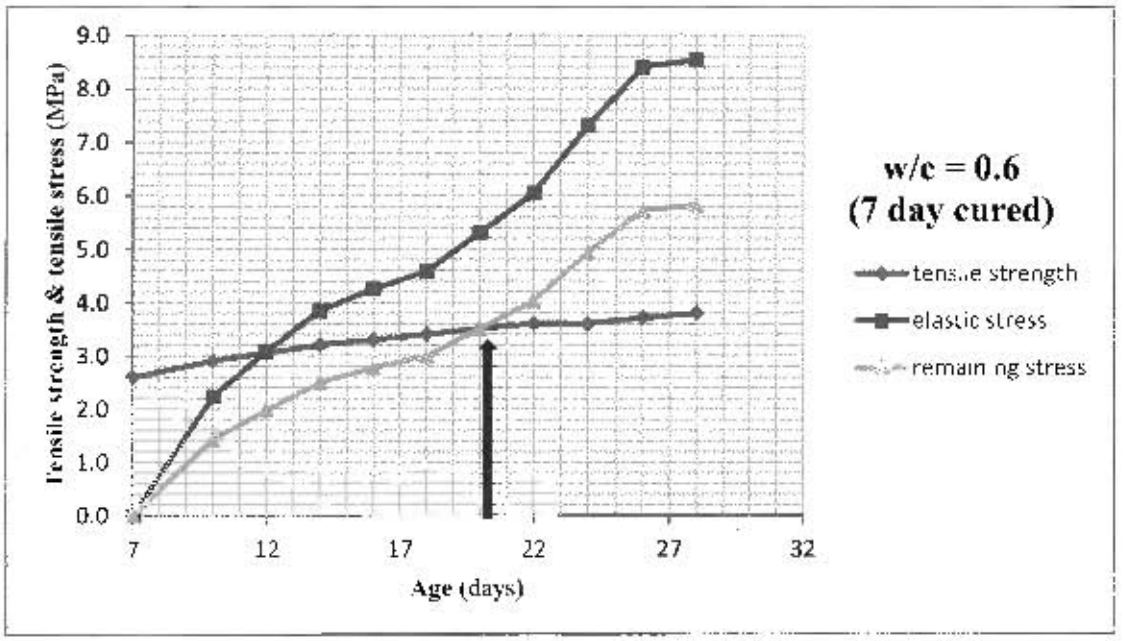

Figure 5.16: Overlay strength and stress development for 7-day cured w/c = 0.6 specimens. *(Arrow indicates the age at crack initiation)*

5.6 Comparison of model with experimental results

Table 5.11 presents a comparison of results i.e. age at cracking between analytical modeling and experimental tests.

Table 5.2: Comparison of analytical modeling and experimental results (age at cracking, days).

Test type	Sika LW		Sika 615		Sika 612		w/c = 0.45		w/c = 0.6	
	2 days	7 days	2 days	7 days	2 days	7 days	2 days	7 days	2 days	7 days
Ring test	7	9	5	9	13	16	7	10	10	13
Bonded overlays	10	10	14	14	24	28	15	18	17	19
Analytical modeling	9	9	14	13	NA	12	14	15	17	20

Figure 5.17 shows a comparison of age at cracking for specimens cured for 2 days, while Figure 5.18 gives a comparison for specimens cured for 7 days. Excluding the results for Sika 612, Figure 5.17 and Figure 5.18 show a very favorable agreement between results of the analytical

modeling and results of bonded overlays. For 2 days cured specimens, there is an exact match between results from modeling and bonded overlays for w/c = 0.6 and Sika 615 specimens. While for Sika LW and w/c = 0.45 specimens, results of analytical modeling lie within one day of the bonded overlays results. For 7 day cured specimens (Figure 5.18), the results of the analytical modeling lie within three days of the bonded overlay results (excluding Sika 612). Considering the number of assumptions made in the analytical modeling (Section 5.4), there is a favorable agreement between analytical modeling and bonded overlays.

A large comparison between ring test results and the other results in both Figure 5.17 and Figure 5.18 indicates differences. For the 2 day cured specimens, Figure 5.15 shows that the ring test results were off by 3 days (Sika LW), 9 days (Sika 615), 11 days (Sika 612), 8 days (w/c = 0.45) and 7 days (w/c = 0.6) from the bonded overlays results. For the 7 days cured specimens, Figure 5.16 shows that the ring test results were off by 1 day (Sika LW), 5 days (Sika 615), 12 days (Sika 612), 8 days (w/c = 0.45) and 6 days (w/c = 0.6) from the bonded overlays results. These differences are to be expected because restrained shrinkage strain values between the ring test and bonded overlays are different. This difference arises because the degree of restraint to shrinkage is different between the two cases. The huge differences in age at cracking indicate that the ring tests will not give the actual age at cracking for concrete repair mortars.

Results for Sika 612 from analytical modeling and bonded overlay do not seem to agree. The modeling predicts no cracking for the 2 day cured specimens and 12 days age at cracking for the 7 day cured specimens. These are very different to the 24 days and 28 days age at cracking obtained from bonded overlays. In Sections 4.2.3 and 4.2.5 it was also noted that the 28 days elastic modulus (12-13 GPa) and compressive strength (10.6 MPa) of Sika 612 lie way below the values given in the product data sheet (25 GPa for elastic modulus and 45-55 MPa for compressive strength). No tangible explanation could be found for this.

Tables 5.3 and 5.4 give ranking of the repair mortars according to age at cracking. Mortars that cracked first are given a lower ranking in the tables while mortars that took long to crack are placed high up at the top of the tables. Ignoring the results for Sika 612, it is observed that there is general agreement on the order in which repair mortars crack among the three tests for both 2

day cured and 7 day cured specimens. In all cases, the w/c = 0.6 mix placed well at the top of the tables while Sika LW had the lowest ranking. Agreement on order of cracking between results of the ring test and results of the other two tests suggests that the ring test will give the correct order of cracking when comparing different materials for cracking resistance.

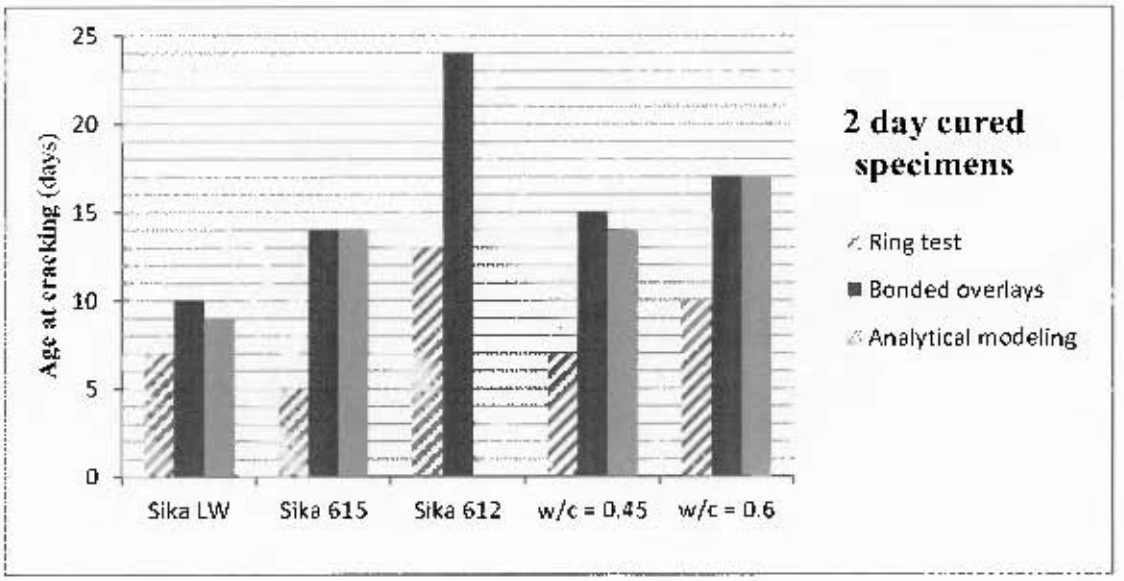

Figure 5.17: Comparison of age at cracking for 2 day cured specimens.

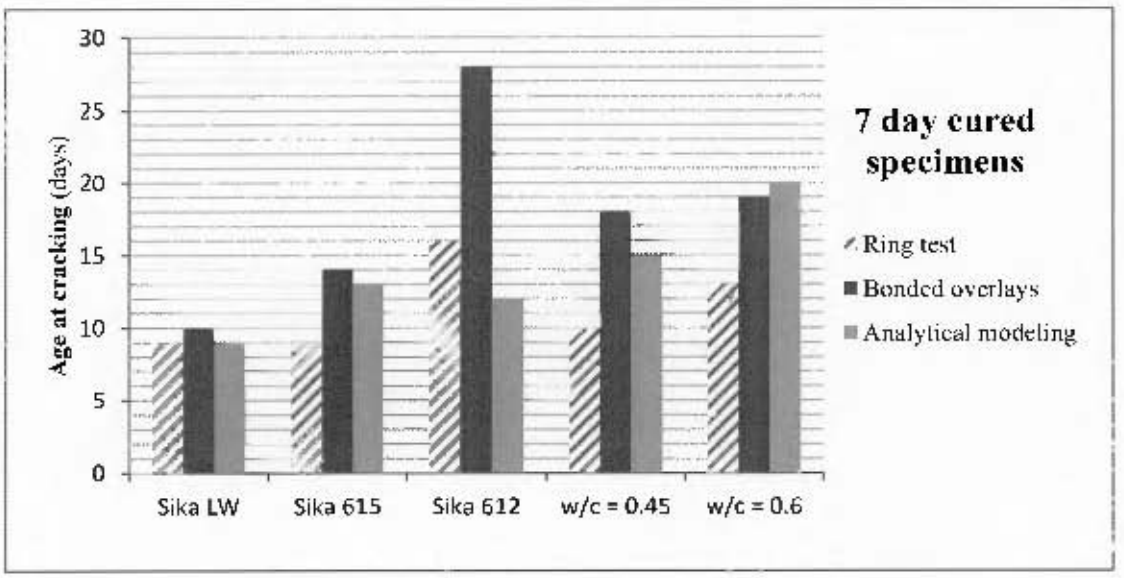

Figure 5.18: Comparison of age at cracking for 7 day cured specimens.

Table 5.3: Mortar ranking according to age at cracking for 2 day cured specimens.
(Figure in brackets indicate age at cracking)

Ranking	Ring test	Bonded overlay	Analytical modeling
1	Sika 612 (13)	Sika 612 (24)	Sika 612
2	w/c = 0.6 (10)	w/c = 0.6 (17)	w/c = 0.6 (17)
3	w/c = 0.45 (7) Sika LW (7)	w/c = 0.45 (15)	w/c = 0.45 (14) Sika 615 (14)
4	Sika 615 (5)	Sika 615 (14)	Sika LW (9)
5		Sika LW (10)	

Table 5.4: Mortar ranking according to age at cracking for 7 day cured specimens.
(Figure in brackets indicate age at cracking)

Ranking	Ring test	Bonded overlay	Analytical modeling
1	Sika 612 (28)	Sika 612 (28)	w/c = 0.6 (20)
2	w/c = 0.6 (13)	w/c = 0.6 (19)	w/c = 0.45 (15)
3	w/c = 0.45 (10)	w/c = 0.45 (18)	Sika 615 (13)
4	Sika 615 (9) Sika LW (9)	Sika 615 (14)	Sika 612 (12)
5		Sika LW (10)	Sika LW (9)

5.7 Conclusion

A simple analytical model based on the superposition principle was used to predict the onset of cracking in bonded concrete overlays. The model was based on time development of key material parameters i.e. tensile relaxation, restrained shrinkage strain, elastic modulus and tensile strength. The following conclusions can be made based on the results and analysis presented in this chapter:

- Age at cracking of bonded concrete overlays can be successfully predicted based on the time development of the different material properties. Results from the analytical model showed a very favorable agreement with actual results from the bonded overlays. All the model results were within 3 days, utmost, of the actual results (excluding results for Sika 612). This is quite favorable considering the number of assumptions made in the analytical modeling of results (see Section 5.4).

- The ring test will not give the actual age at cracking but will give the correct order of cracking when comparing different materials for crack resistance. Comparison of results from the ring test and bonded overlays indicated huge differences for age at cracking (see Figures 5.17 and 5.18). Nevertheless, the order of cracking for both 2 day cured and 7 day cured specimens were similar for both the ring test and bonded overlays (see Tables 5.3 and 5.4).

The above conclusions suggest that the ring test would suffice when assessing different materials on which one would perform better, but would not be enough in assessing materials for age at cracking. In order to assess age at cracking of overlays, information on the time development of the different material parameters is needed.

CHAPTER SIX: SUMMARY, CONCLUSIONS AND RECOMMENDATIONS

6.1 Introduction

The number of concrete infrastructure needing repair and rehabilitation is increasing worldwide. The bonded overlay technique, which involves removal of a damaged concrete layer on an existing concrete member and replacing it with a new layer is one of the most widely used techniques. It is used for both structural and non-structural repairs in concrete members or elements such as slabs on grade, pavements, toppings and linings, etc.

The performance of overlays is weakened by such effects as early age surface cracking, spalling or interface debonding. Early age surface cracking due to restrained deformation is a major problem arising in bonded overlays. Overlay resistance to crack initiation, development and propagation depends on a number of time-dependent properties of the concrete. To be able to predict the onset of cracking requires knowledge of the different material properties and also how they interact with each other.

This research sought to model and predict age at cracking of bonded overlays based on experimentally established material properties and the ring test. The main aim was to investigate whether the performance, with particular focus on age at cracking, of bonded overlays can be adequately predicted from tests such as ring test, free shrinkage strain, tensile strength test, tensile relaxation etc., and if so, which of these tests would suffice for prediction of overlay performance.

Age at cracking refers to the age at which cracking occurs and its importance cannot be overstated. Firstly, cracking in itself is unsightly in cosmetic repairs and may lead to loss of structural integrity in structural repairs. Secondly, age at cracking could indicate the age at which concrete may become exposed to potential harmful substances such as chlorides, carbon dioxide etc. The ingress of these harmful substances could cause further deterioration resulting in eventual failure of the overlay-substrate composite. The investigation covered in this study

serves as an important contribution towards efforts aimed at harnessing early age shrinkage cracking of concrete repair mortars.

6.2 Summary of main conclusions

Based on the materials and the results obtained in this research, the following conclusions were made:

6.2.1 Effect of material properties

The crack resistance of repair mortars depends upon the combined influence of a number of factors rather than just one factor. Free shrinkage strain alone, in spite of it being very important, does not determine the cracking behavior of bonded overlays. Both Sika LW and Sika 612 had very high values of free shrinkage strain, yet Sika LW recorded the shortest time to cracking while Sika 612 recorded the longest time to cracking. Also Sika LW and Sika 615 specimens had the same age at cracking despite them having different material properties. Sika 615 had higher elastic modulus and tensile strength than Sika LW, while Sika LW underwent higher degree of relaxation and higher shrinkage strain than Sika 615.

Tensile relaxation appears to have a very big influence on age at cracking. Depending on the age of loading, tensile relaxation will reduce overlay stresses by approximately 20-58% (2 day cured specimens) and 20-48% (7 day cured specimens) in the mixes tested. These values are in agreement with published literature (Masuku, 2009; Beushausen, 2005; Pigeon *et. al* 2000). The degree of tensile relaxation depends upon the age of loading. Higher values of relaxation were observed in younger specimens than in older specimens.

Shrinkage and tensile strength are often used as the main material parameters considered in judging the potential cracking performance of overlays and repair patches. This research has shown that shrinkage and strength values in isolation cannot determine the cracking behaviour of cement mortars. Cracking behavior of repair mortars depends upon the combined influence of shrinkage, elastic modulus, tensile relaxation and tensile strength. This agrees with Pigeon & Bissonnette (1999), who noted that crack resistance of repair mortars is a combined influence of various material properties and parameters. According to Hengjing *et al.* (2008) early age

cracking in concrete should be studied by combining the influence of shrinkage, shrinkage stress and creep.

In practice, advantage could be taken of the above results during selection of repair materials. Before any material is selected for use, it would have to meet a criterion chosen based on all the material parameters i.e. tensile strength, elastic modulus, restrained shrinkage and tensile relaxation. By taking into consideration all the different material parameters instead of just shrinkage and tensile strength, the potential resistance of the material against restrained shrinkage cracking could be enhanced. Obviously the development and implementation of such a criterion would require a much more comprehensive and rigorous testing program than was carried out in this study, hence it is beyond the scope of this thesis.

6.2.2 Effect of curing on cracking performance

An increase in curing period was observed to delay the onset of cracking in both ring test specimens and bonded overlays tested in this study. This was attributed to the effect that curing had on free shrinkage strain and tensile strength. In addition to delaying free shrinkage strain, curing was observed to increase the tensile strength of the repair mortar specimens. The combined influence of these factors appears to override the effect of increased elastic modulus with an increase in curing period.

The above effect of curing on onset of cracking implies that extending the curing period could prove beneficial in practice. By extending the curing period, the onset of cracking could be delayed or even prevented thus improving the performance of the overlay. This would result in long overlay service life and hence, enhanced durability.

6.2.3 Analytical modeling of age at cracking

In order to simplify analytical modeling, it was assumed that: no shrinkage occurs during the curing period, tensile relaxation is instantaneous from the onset of loading and that restraint is

equivalent to 60% of free shrinkage strain (Beushausen, 2005). Results from the modeling showed that:

- Age at cracking of bonded concrete overlays can be successfully predicted based on the time development of the different material properties. Results from the analytical model showed a very favorable agreement with actual results from the bonded overlays. All the model results were within 3 days, utmost, of the actual results (excluding results for Sika 612). This is quite favorable considering the number of assumptions made in the analytical modeling of results (see Section 5.4).

- The ring test will not give the actual age at cracking but will give the correct order of cracking when comparing different materials for crack resistance. Comparison of results from the ring test and bonded overlays indicated large differences for age at cracking (see Figures 5.15 and 5.16). Nevertheless, the order of cracking for 2 day cured and 7 day cured specimens were similar for both the ring test and bonded overlays (see Tables 5.3 and 5.4).

The above conclusions suggest that the ring test would suffice when assessing different materials on which one would perform better but would not be enough in assessing materials for age at cracking. In order to assess age at cracking of bonded overlays to restrained shrinkage cracking, information on the time development of the tensile strength, elastic modulus, tensile relaxation and shrinkage is needed.

The results of the analytical model are based on laboratory results of material parameters and the assumptions made i.e. no shrinkage occur during curing, tensile relaxation is instantaneous and degree of restraint is 60%, therefore they may not be representative of a real life repair. In an actual real life repair shrinkage might take place during curing through autogenous effects and the degree of restraint may be different to 60% depending on the overlay-substrate bond. However, provided actual restraint and shrinkage are estimated through field investigations, the above analytical model could prove useful in assessing and comparing materials for cracking performance.

6.3 Recommendations

This research identified some of the main aspects affecting bonded concrete overlay crack resistance. However more research needs to be conducted to come up with comprehensive results. The following recommendations are made:

- More research needs to be carried out on a comprehensive list of repair materials. While results from this study are significant, tests were carried out on a small number (5) of repair materials. Therefore, there is need to test a more comprehensive list.
- Future research could also look into the possibility of adapting the analytical model into a FEM model for predicting age at cracking.

REFERENCES

AASHTO PP34 - 98 1998. Standard Practice for Estimating the Cracking Tendency of Concrete.

ACI Committee 224. 2007. *Causes, Evaluation, and Repair of Cracks in Concrete Structures (ACI 224.1R-07).* American Concrete Institute.

ACI Committee 364 2002. Evaluation and Minimization of Bruising (Micro-cracking) in Concrete Repairs (ACI 364.7T-02(11)).

ACI Committee 364 2006. *Cement-based repair material.* [Online]. Available: http://www.concrete.org/FAQ/afmviewfaq.asp?faqid=52 (2010)

Alexander, M.G. 1994. Deformation properties of blended cement concretes containing blastfurnace slag and condensed silica fume. *Advances in cement research.* 6(22):73-81.

Alexander, M.G. 2001. Deformation and volume change of hardened concrete. In *Fulton's Concrete Technology.* G. Owens, Ed. 8th ed. Midrand, South Africa: Cement and Concrete Institute.

Alexander, M.G. & Beushausen, H.D. 2009. Deformation and Volume Change of Hardened Concrete. In *Fulton's Concrete Technology.* G. Owens, Ed. Ninth ed. South Africa: Cement and Concrete Institute. 111.

Altoubat, S.A. & Lange, D.A. 2001. Creep, Shrinkage, and Cracking of Restrained Concrete at Early Age. *ACI materials journal.* 98(4):323.

Amba, J.C., Balayssac, J.P. & Detriche, C.H. 2010. Characterization of differential shrinkage of bonded mortar overlays subjected to drying. *Materials and structures.* 43.

Asad, M., Baluchi, M.H. & Al-Ghadib, A.H. 1997. Drying shrinkage stresses in concrete patch repair systems. *Magazine of concrete research.* 49:283-293.

ASCE 2009. *2009 Report Card for America's Infrastructure.* Washington DC: American Society of Civil Engineers (ASCE).

ASTM 2004. Standard Test Method for Determining Age at Cracking and Induced Tensile Stress Characteristics of Concrete and Mortar under Restrained Shrinkage. C 1581 - 04:1.

Ballim, Y. 2004. A numerical model and associated calorimeter for predicting temperature profiles in mass concrete. *Cement and concrete composites.* 26:695-703.

Ballim, Y. & Graham, P.C. 2003. A maturity approach to the rate of heat evolution in concrete. *Magazine of concrete research.* 55(3):249-256.

Ballim, Y. & Graham, P.C. 2004. Early-age heat evolution of clinker cements in relation to microstructure and composition: implications for temperature development in large concrete elements. *Cement and concrete composites.* 26:417-426.

Ballim, Y. & Graham, P.C. 2009. The effects of supplementary cementing materials in modifying the heat of hydration of concrete. *Materials and structures.* 42:803-811.

Banthia, N., Azzabi, M. & Pigeon, M. 1993. Restrained shrinkage cracking in fiber-reinforced cementitious composites. *Materials and structures.* 26:405-413.

Banthia, N. & Gupta, R. 2006. Influence of polypropylene fiber geometry on plastic shrinkage cracking in concrete. *Cement and concrete research.* 36:1263-1267.

Banthia, N. & Gupta, R. 2009. Plastic shrinkage cracking in cementitious repairs and overlays. *Materials and structures.* 42:567.

Banthia, N., Yan, C. & Mindess, S. 1996. Restrained shrinkage cracking in fiber reinforced concrete : A novel testing technique. *Cement and concrete research.* 26(1):9-14.

Baroghel-Bouny, V. & Godin, J. 2001. Experimental study on drying shrinkage of ordinary and high-performance cementitious materials. *Concrete science and engineering.* :13-22.

Bentur, A. & Kovler, K. 2003. Evaluation of early age cracking characteristics in cementitious systems. *Materials and structures.* 36:183-190.

Berke, N.S. & Dallaire, M.P. 1994. The effect low addition rates of polypropylene fibers on plastic shrinkage cracking and mechanical properties of concrete. *Fiber Reinforced Concrete : Developments and Innovations.* 1994. J.I. Danile & S.P. Shah, Eds. Washington DC: American Concrete Institute. 19.

Beushausen, H.D. & Alexander, M.G. 2006. Failure mechanisms and tensile relaxation of bonded concrete overlays subjected to differential shrinkage. *Cement and concrete research.* 36:1908-1914.

Beushausen, H.D., Alexander, M.G. & Ballim, Y. 2012. Early-age properties, strength development and heat of hydration of concrete containing various South African slags at different replacement ratios. *Construction and building materials.* 29:533-540.

Beushausen, H.D. 2005. Performance of bonded concrete overlays subjected to differential shrinkage. University of Cape Town, South Africa.

Beushausen, H.D. & Alexander, M.G. 2007. Localised strain and stress in bonded concrete overlays subjected to differential shrinkage. *Materials and structures.* :189-199.

Bissonnette, B., & Pigeon, M. 1995. Tensile creep at early ages of ordinary silica fume and fiber reinforced concretes, Cement and Concrete Research. 25 (5) (1995) 1075 – 1085.

Brown, M.D., Sellers,G., Folliard,K. J.& Fowler, D.W. 2003. Restrained shrinkage cracking of concrete bridge decks: State-of-the-Art Review. *FHWA/TX-0-4098-1.*

Cabrera, J.G. & Al-Hasan, A.S. 1997. Performance properties of concrete repair materials. *Construction and building materials.* 11(5-6):283.

Care, S. & Nicolle, O. 2005. Caracterisation des gradients de microstructure des materiaux cimentaires induits par les couplages hydratation-transfert d'eau: application aux structures de beton arme reparees. *17th congres francais de mecanique,troyes.*

Carlson, R.W. & Reading, T.J. 1988. Model Study of Shrinkage Cracking in Concrete Building Walls. *ACI structural journal.* 85(4):395-404.

Carlsward, J. 2006. Shrinkage cracking of fiber reinforced self-compacting concrete overlays- Test methods and theoretical modeling. PhD Thesis, University of Lulea University of Technology, Sweden.

Chen, T. C., Ferraro, C. C., Yin, W. Q., Ishee, C. A. & Ifju, P.G. 2010. A novel two-dimensional method to measure surface shrinkage in cementitious materials. *Cement and concrete research.* 40:687-698.

Collepardi, S., Coppola, L., Troli, R. & Collepardi, M. 1997. Mechanical properties of modified reactive powder concrete. *Superplasticizers and other chemical admixtures in concrete.* M. VM, Ed. ACI SP. 1.

Delatte, M., Mack, E. & Cleary, J. 2007. *Evaluation of High Absorptive Materials to Improve Internal Curing of Low Permeability Concrete.* Ohio: Ohio Department of Transport.

Deshpande, S., Darwin, D. & Browning, J. 2007. *Evaluating free shrinkage of concrete for control of cracking in bridge decks.* Lawrence, Kansas: The University of Kansas Center for Research,Inc.

Emmons, P.H. & Vaysburd, A.M. 1995. *Performance Criteria for Concrete Repair Materials ,Phase I.* Washington DC: US Army Corps of Engineers.

Feldman, R.F. & Sereda, P.J. 1968. A model for hydrated Portland cement paste as deduced from sorption-length change and mechanical properties. *Matériaux et construct.* 1:509-520.

Garas, V.Y., Kahn, L.F. & Kurtis, K.E. 2009. Short-term tensile creep and shrinkage of ultra-high performance concrete. *Cement and concrete composites.* :147-152.

German Federal Ministry of Transport, Highway Construction Department 1990. Technical Test Regulations for Concrete Substitution Systems made of Cement Mortar/Concrete with a Plastic Additive (PCC). *TP BE-PCC.*

Ghali, A., Favre, R. & Eldbadry, M. 2006. *Concrete Structures: Stresses and deformations.* Third edition e-copy ed. London: Taylor & Francis e-library.

Gilbert, R.I. 1988. *Time Effects in Concrete Structures.* Netherlands: ELSEVIER.

Granju, J., Sabathier,V., Turatsinze,A., & Toumi,A.. 2004. Interface Between an Old Concrete and a Bonded Overlay:Debonding Mechanism. *Interface science.* 12:381-388.

Grieve, G.R.H. 1991. The influence of two South African fly ashes on the engineering properties of concrete. PhD. University of the Witwatersrand, Johannesburg.

Grzybowski, M. & Shah, S.P. 1990. Shrinkage Cracking of Fiber Reinforced Concrete. *ACI materials journal.* 87(2):138.

Gutsch, A.W. 2002. Properties of early age concrete: Experiments and modelling. *Material and structures.* 35:76-79.

Gutsch, A. & Rostasy, F.S. 1995. Young concrete under high tensile stress-Creep, Relaxation and Cracking. *Thermal Cracking in Concrete at Early Ages.* 1994, October 10-12. R. Springenschmid, Ed. London, UK: E & FN Spon. 111.

Holt, E. 2002. Very Early Age Autogenous Shrinkage: Governed by Chemical Shrinkage or Self-Desiccation? In *Self-Desiccation and its Importance in Concrete Technology.* B. Persson & G. Fagerlund, Eds. Lund: Lund Institute of Technology, Lund University. 1.

Jae Heum Moon & Jason Weiss 2006. Estimating residual stress in the restrained ring test under circumferential drying. *Cement and concrete composites.* 28:486-496.

Kheder, G. 1997. A mathematical model for the prediction of volume change cracking in end-restrained concrete memebers. *Materials and structures.* 30:174-181.

Kovler, K. 1994. Testing system for determining the mechanical behaviour of early age concrete under restrained and free uniaxial shrinkage. *Materials and structures.* 27(170):324-330.

Kraai, P.P. 1985. Proposed Test to Determine the Cracking Potential due to Drying Shrinkage of Concrete. *Concrete construction.* 30(9):775-778.

Krauss, P.D. & Rogalla, E.A. 1996. *Transverse cracking in newly constructed bridge decks.* National Cooperative Highway Research Program (NCHRP), Transportation Research Board.

Lerch, W. 1957. Plastic shrinkage. *ACI materials journal.* 28(8):797-802.

Letsch, R.H. 1991. Shrinkage and temperature stresses in PC and PCC due to hindered deformation. *International Symposium on Concrete Polymer Composites.* Bo Chum, Germany: 53.

Loser, R. & Leemann, A. 2009. Shrinkage and restrained shrinkage cracking of self-compacting concrete compared to conventionally vibrated concrete. *Materials and structures.* 42:71-82.

Masuku, C. 2009. Tensile relaxation of bonded concrete overlays. MSc. University of Cape Town.

Mehta, K.P. & Monteiro, P.J.M. 2006a. Dimension Stability. In *Concrete: Microstructure, Properties, and Materials.* Third ed. United States of America: McGraw-Hill Companies. 85.

Mehta, K.P. & Monteiro, P.J.M. 2006b. Micro-structure of Concrete. In *Concrete: Microstructure, Properties, and Materials.* Third ed. United States of America: McGraw-Hill Companies. 21.

Mehta, K.P. & Monteiro, P.J.M. 2006c. Strength. In *Concrete: Microstructure, Properties, and Materials.* Third ed. United States of America: McGraw-Hill Companies. 49.

Meyers, B.L., Branson, D.E., Schumann, C.G. & Christiason, M.L. 1970. *The Prediction of Creep and Shrinkage Properties of Concrete.* Iowa: Iowa Highway Commission.

Mindess, S., Young, J.F. & Darwin, D. 2003. *Concrete.* Second ed. Upper Saddle River, NJ 07458: Prentice Hall,Pearson Education Inc.

Mizobuchi, T., Yokozeki, K. & Nobuta, Y. 2000. Experimental estimation of thermal cracking using the modified temperature testing machine. *Proceedings of an international workshop on control of cracking in early age concrete.* 1999. Sendai, Japan: .

Mora-Ruacho, J., Gettu, R. & Aguado, A. 2009. Influence of shrinkage-reducing admixtures on the reduction of plastic shrinkage cracking in concrete. *Cement and concrete composites.* 39:141.

Morgan, D.R. 1996. Compatibility of Concrete Repair Materials and Systems. *Construction and building materials.* 10(1):57.

Morimoto, H. & Koyanagi, W. 1995. Estimation of stress relaxation in concrete at early ages. *Thermal Cracking in Concrete at Early Ages.* 1994, October 10-12. R. Springenschmid, Ed. London, UK: E & FN Spon. 95.

Muller, H.S. 1994. New prediction models for creep and shrinkage of concrete. *ACI SP.* 135(1):1-19.

Nantung, T. 2011. Curing, Shrinkage, and Cracking of Ternary Concrete Mixes. *HPC bridge views.* May/June(67):9-12.

Neville, A.M. 1996. *Properties of Concrete.* England: Pearson Education Limited-Prentice Hall.

Newbolds, S.A. & Olek, J. 2002. *The influence of curing conditions on strength properties and maturity development of concrete.* West Lafayette: Purdue University.

NRMAC 1998. *Concrete in Practice: plastic shrinkage cracking.* NRMAC.

Paillere, A.M., Buil, M. & Serrano, J.J. 1989. Effect of Fiber Addition on the Autogenous Shrinkage of Silica Fume Concrete. *ACI materials journal.* 86(2):139-144.

Pane, I. & Hansen, W. 2002. Early age creep and relaxation of concrete containing blended cements. *Materials and structures.* 35:92.

Pease, B.J., Shah, H.R. & Weiss, W.J. 2005. Shrinkage behaviour and residual stress development in mortars containing shrinkage. *ACI SP.*

Pickett, G. 1956. Effect of aggregate on shrinkage of concrete and hypothesis concerning shrinkage. *Journal of the american concrete institute.* 27(5):581-590.

Pigeon, M. & Bissonnette, B. 1999. Tensile Creep and Cracking Potential. *Concrete international.* 31-35.

Pigeon, M., Toma,G., Delagrave,A., Bissonnette,B., Marchand,J., & Prince,J.C. 2000. Equipment for the analysis of the behaviour of concrete under restrained shrinkage at early ages. *Magazine of concrete research.* 52(4):297-302.

Powers, T.C. 1968. The thermodynamics of volume change and creep. *Materiaux et constructions.* 1(6):487-507.

Radlinska, A., Pease, B. & Weiss, J. 2007. A preliminary numerical investigation on the influence of material variability in the early-age cracking behaviour of restrained concrete. *Materials and structures.* :375-386.

Ravina, D. & Shalon, R. 1968. Plastic shrinkage cracking. *ACI materials journal.* 65(22):282-292.

Reza, A., Parviz, G. & Jamal, A. 2005. Prediction of restrained shrinkage based on restraint factors in patching repair mortar. *Cement and concrete research.* 35:1909-1913.

RILEM TC 119- TCE 1997. Avoidance of thermal cracking in concrete at early ages - Recommendations. *Materials and structures.* 30:451-461.

Ruetz, W. 1965. A hypothesis for the creep of hardened cement paste and the influence of simultaneous shrinkage. *The structure of concrete, proceedings of an international conference.* :319-344.

Rusch, H., Jungwirth, D. & Hilsdorf, H. 1983. *Creep and Shrinkage: Their effect on the behaviour of concrete structures.* New York, USA: .

Schneider, U. 2007. Recommendation of RILEM TC 200-HTC: Mechanical concrete properties at high temperatures-modelling and application. Part 11: Relaxation. *Materials and structures.* 40:449.

See, H.T., Attiogbe, E.K. & Miltenberger, M.A. 2003. Shrinkage Cracking Characteristics of Concrete Using Ring Specimens. *ACI materials journal.* 100(3):239.

Shaeles, C.P. & Hover, K.C. 1988. Influence of Mix Proportions and Construction Operations on Plastic Shrinkage Cracking in Thin Slabs. *ACI materials journal.* 85(6):495-504.

Shah, S.P. & Weiss, J. 2006. Quantifying shrinkage cracking in fibre reinforced concrete using the ring test. *Materials and structures.* (39):887-899.

Shah, S.P., Weiss, W.J. & Yang, W. 1998. Shrinkage Cracking-can it be prevented? *Concrete international.* 20(4):51-55.

Sika. 2008. Sika MonoTop 612 Data Sheet.

Sika. 2008. Sika MonoTop 615 HB.

Sika. 2011. *Sika product manual.* 2011th ed. South Africa: Sika South Africa.

Standards South Africa 2006. SANS 5863:2006 Concrete tests: Compressive strength of hardened concrete. *South African National Standards.*

Straub, L.G. 1930. Plastic Flow in Concrete Aches. *Proceedings of the American Society of Civil Engineers, 56.*

Tarek, A. & Sanjayan, J.G. 2008. Factors contributing to early age shrinkage cracking of slag concretes subjected to 7-days moist curing. *Materials and structures.* :633-642.

Tritsch, N., Darwin, D. & Browning, J. 2005. *Evaluating shrinkage and cracking behavior of concrete using restrained ring and free shrinkage tests.* Kansas: The University of Kansas Center for Research.

Troxell, G.E., Davis, H.E. & Kelly, J.W. 1968. Influence of shrinkage and creep on concrete cracking. In *Composition and Properties of Concrete.* New York: McGraw-Hill. 342.

Troxell, G.E., Raphael, J.M. & Davis, R.E. 1958. Long-time creep and shrinkage tests of plain and reinforced concrete. *Proceedings American Society for Testing and Materials.* 58:1101-1120.

Uno, P.J. 1998. Plastic shrinkage cracking and evaporation formulas. *ACI materials journal.* 95(4):365-375.

Verbeck, G.J. 1958. Carbonation of hydrated Portland cement. *Research Departmentt Bulletin, Portland Cement Association.* :17-36.

Weiss, J., Yang, W. & Shah, S.P. 1998. Shrinkage Cracking of Restrained Concrete Slabs. *Journal of engineering mechanics.* July:765-774.

Weiss, W.J. & Shah, S.P. 2002. Restrained shrinkage cracking: The role of shrinkage reducing admixtures and specimen geometry. *Materials and structures.* 34(246):85-91.

West, M., Darwin, D. & Browning, J. 2010. *Effects of materials and curing period on shrinkage of concrete.* Lawrence, Kansas: The University of Kansas Center for Research.

Xi, Y.P., Shing, B.S, Abu-Hejleh, N., Asiz, A., Suwito, A., Xie, Z. H.& Ababneh, A. 2003. *Assessment of the cracking problem in newly constructed bridge decks in Colorado.* University of Colorado at Boulder.

Yokoyama, K., Hirashi,S., Kasai,Y., & Kishitani, K. 1994. Shrinkage and cracking of high strength concrete and flowing concrete at early ages. *4th CANMET/ACI International Conference on Superplasticizers and other Chemical Admixtures in Concrete.* 1994. V.M. Malhotra, Ed. ACI. 243.

Yoshitake, I., Rajabipour, F., Mimura,Y., & Scanlon, A. 2011. A prediction method of tensile young's modulus of concrete at early age. *Advances in civil engineering.* 2012.

Yuan, Y., Li, G. & Cai, Y. 2003. Modeling for prediction of restrained shrinkage effect in concrete repair. *Cement and concrete research.* 33:347-352.

Zhuang, J. 2009. Evaluation of concrete mix designs to mitigate early-age shrinkage cracking in bridge decks. MSc Thesis. Washington State University.

Zhutovsky, S., Kovler, K. & Bentur, A. 2004. Influence of cement paste matrix properties on the autogenous curing of high-performance concrete. *Cement and concrete composites.* 26:499-507.

APPENDICES

Appendix A: Material properties' regression curves

Tensile strength

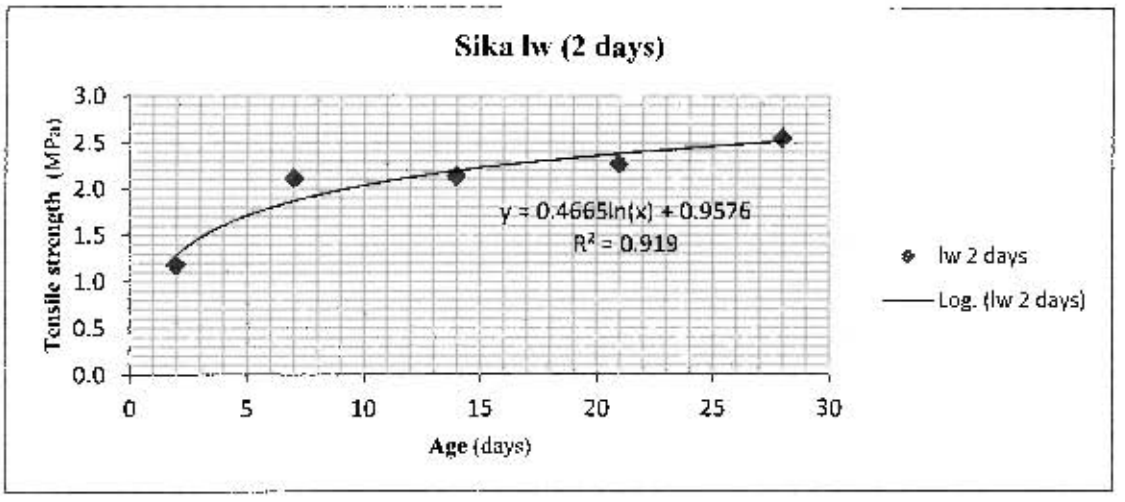

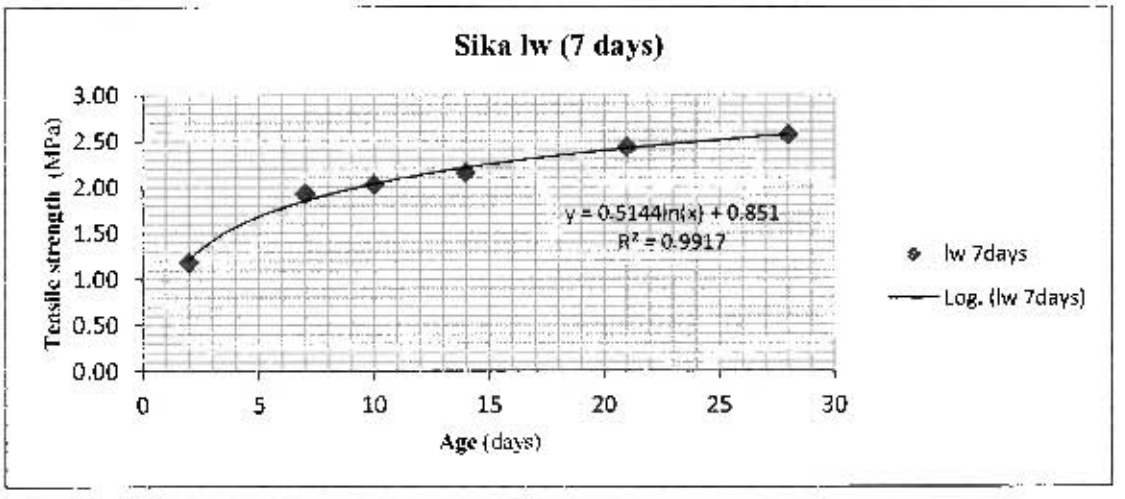

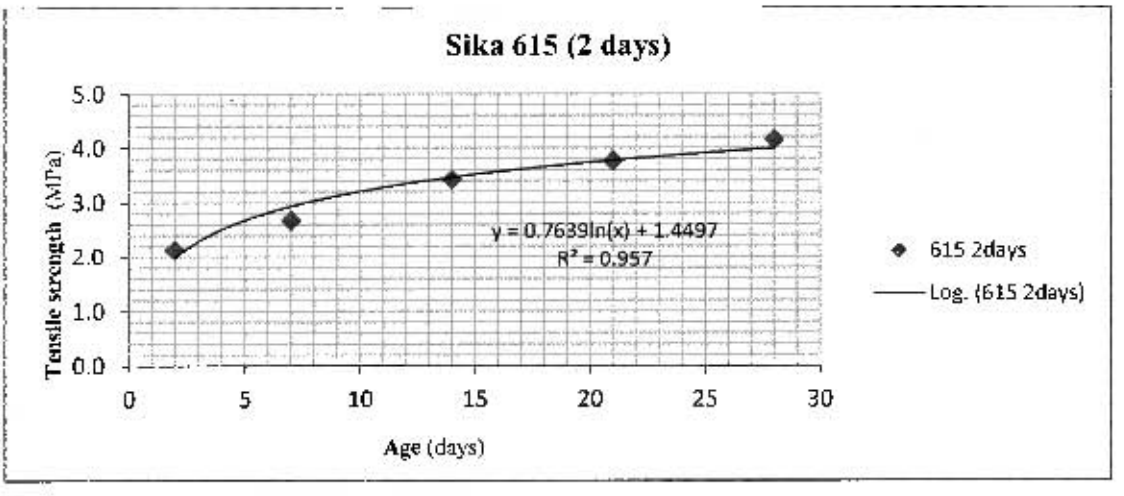

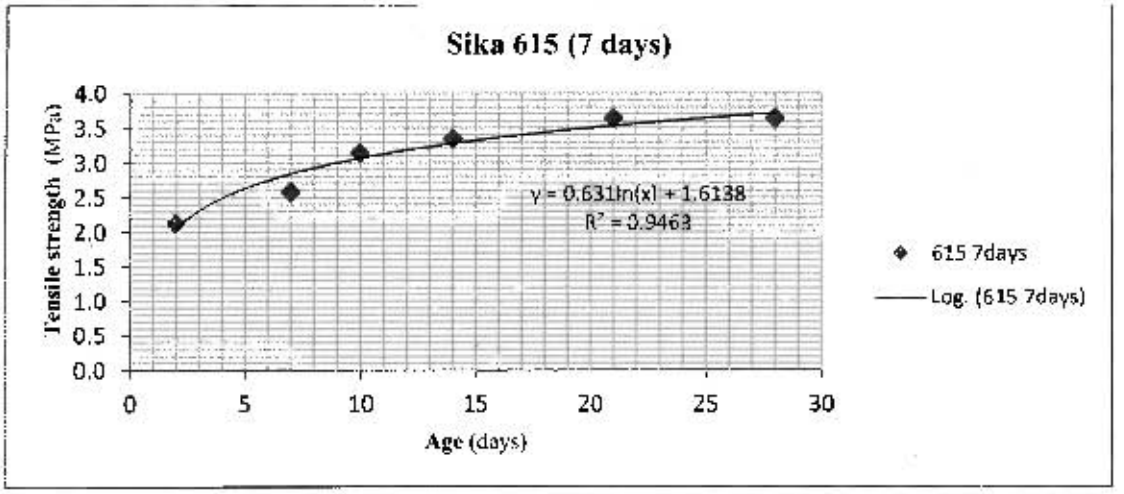
Sika 615 (7 days)
Tensile strength (MPa)
Age (days)
y = 0.631ln(x) + 1.6138
R² = 0.9463
615 7days
Log. (615 7days)

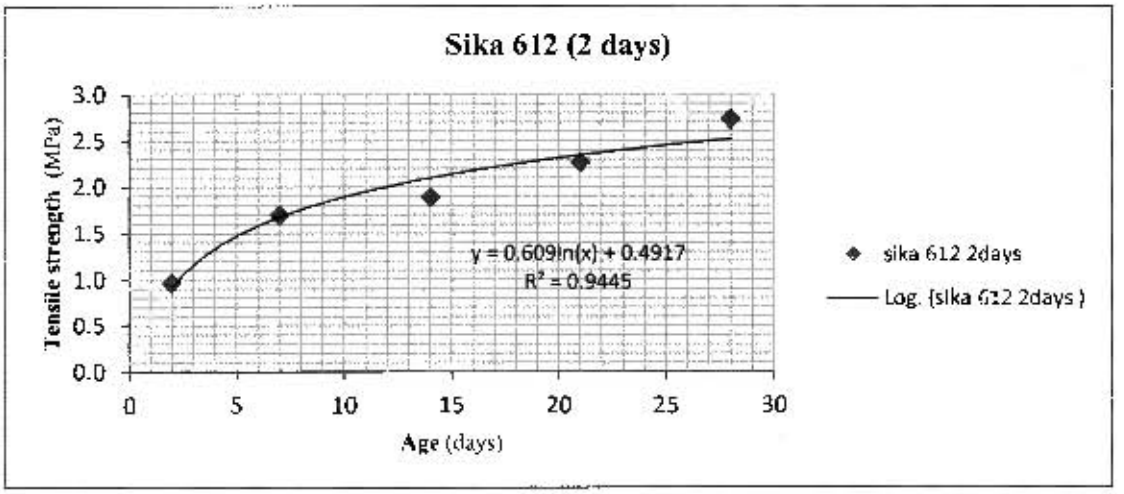
Sika 612 (2 days)
Tensile strength (MPa)
Age (days)
y = 0.609ln(x) + 0.4917
R² = 0.9445
sika 612 2days
Log. (sika 612 2days)

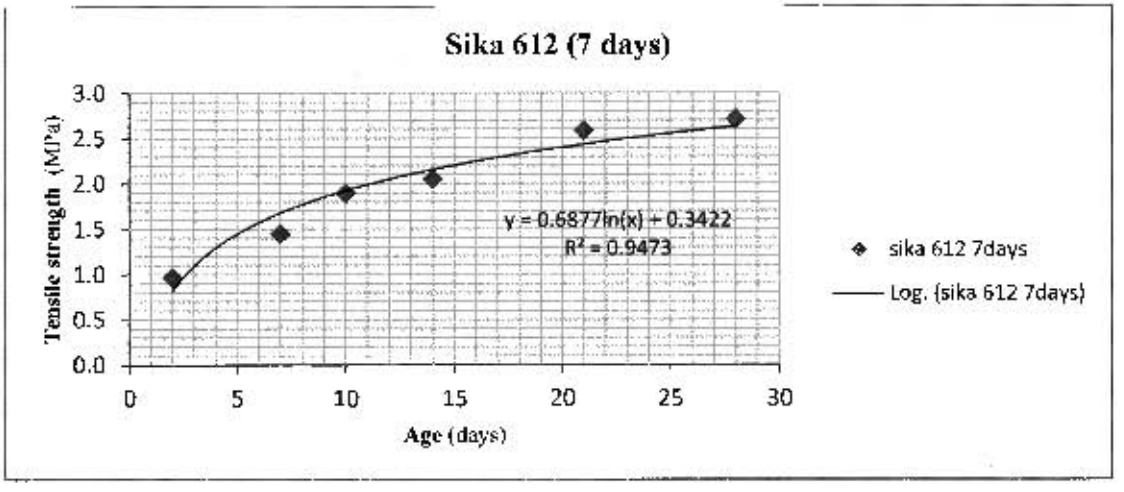
Sika 612 (7 days)
Tensile strength (MPa)
Age (days)
y = 0.6877ln(x) + 0.3422
R² = 0.9473
sika 612 7days
Log. (sika 612 7days)

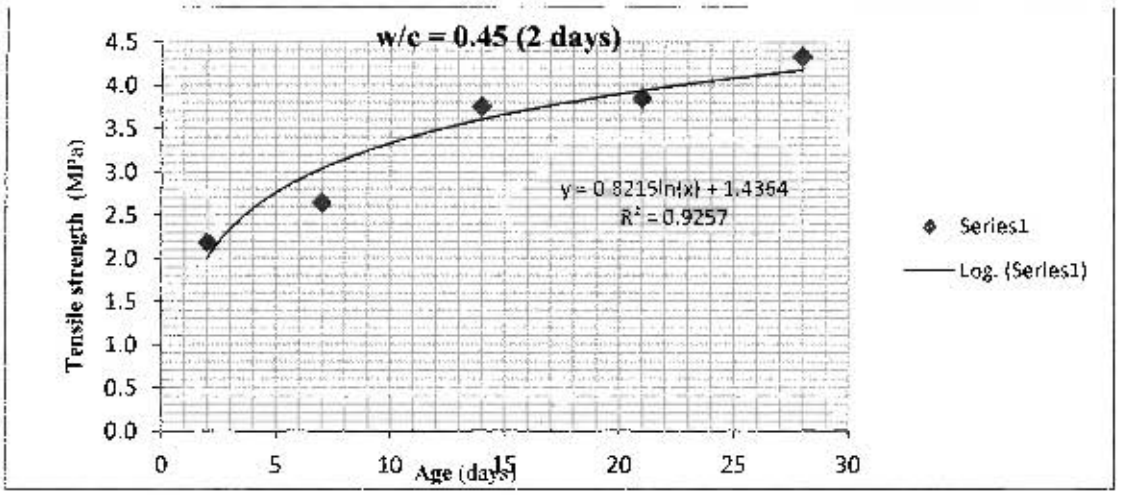
w/c = 0.45 (2 days)
Tensile strength (MPa)
Age (days)
y = 0.8215ln(x) + 1.4364
R² = 0.9257
Series1
Log. (Series1)

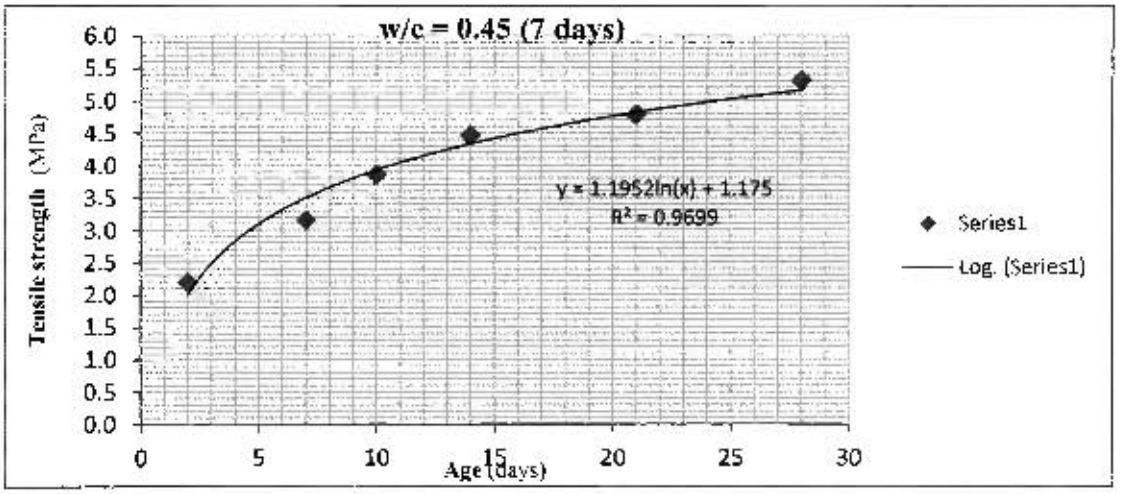
w/c = 0.45 (7 days)
Tensile strength (MPa)
Age (days)
y = 1.1952ln(x) + 1.175
R² = 0.9699
Series1
Log. (Series1)

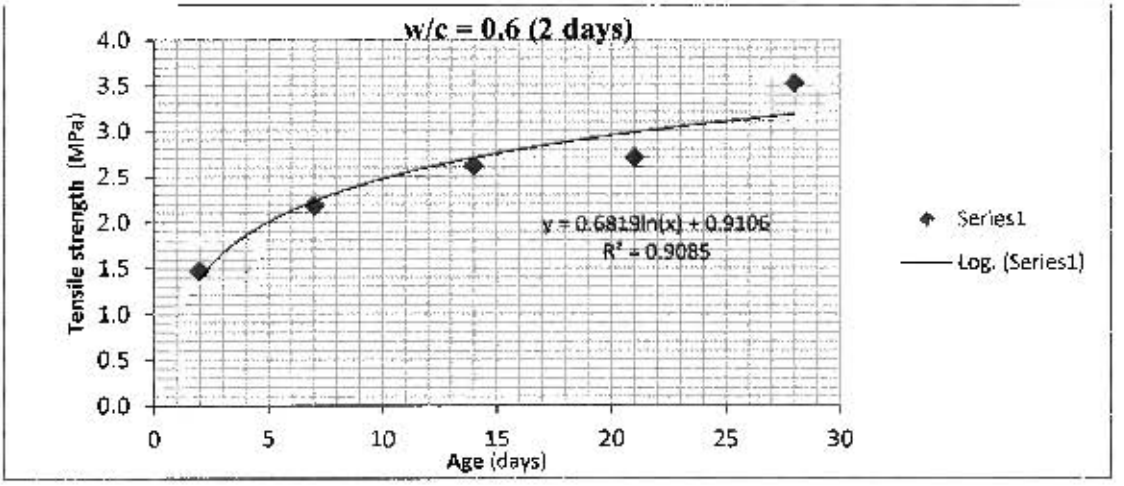
w/c = 0.6 (2 days)
Tensile strength (MPa)
Age (days)
y = 0.6819ln(x) + 0.9106
R² = 0.9085
Series1
Log. (Series1)

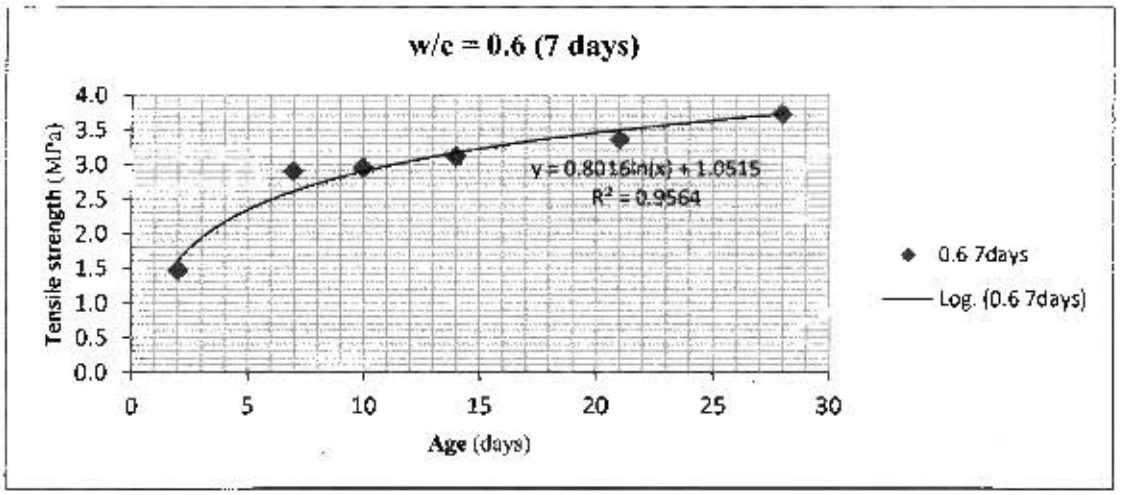

Elastic modulus

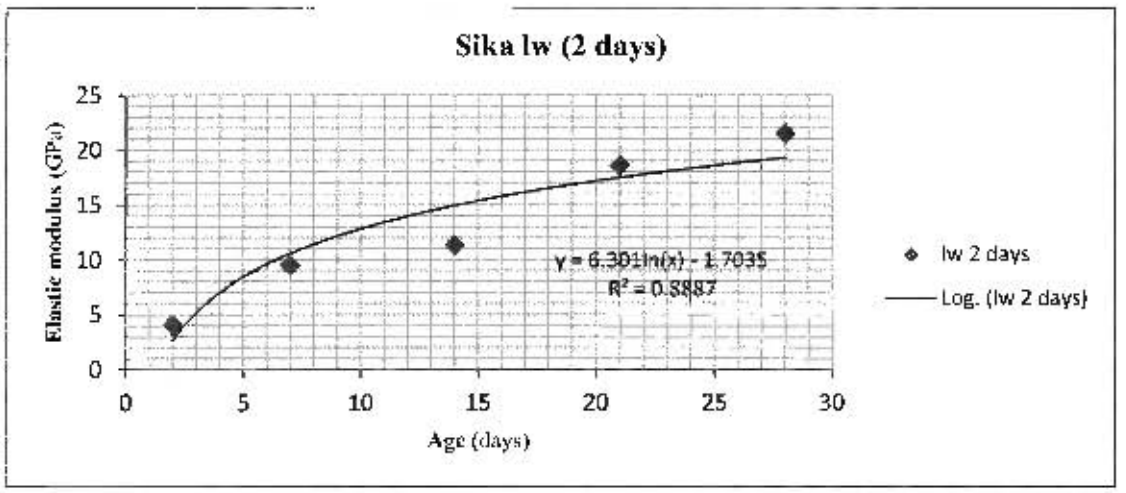

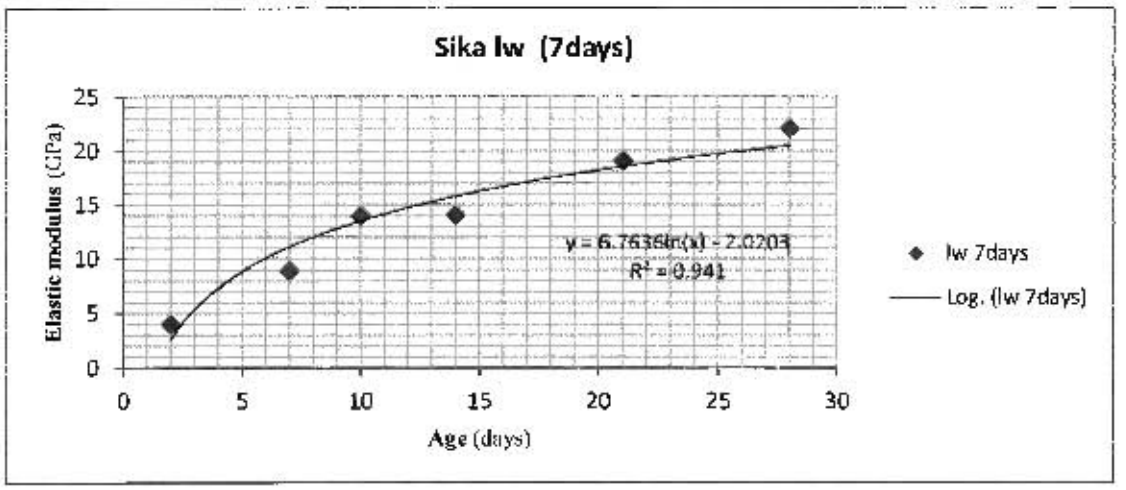

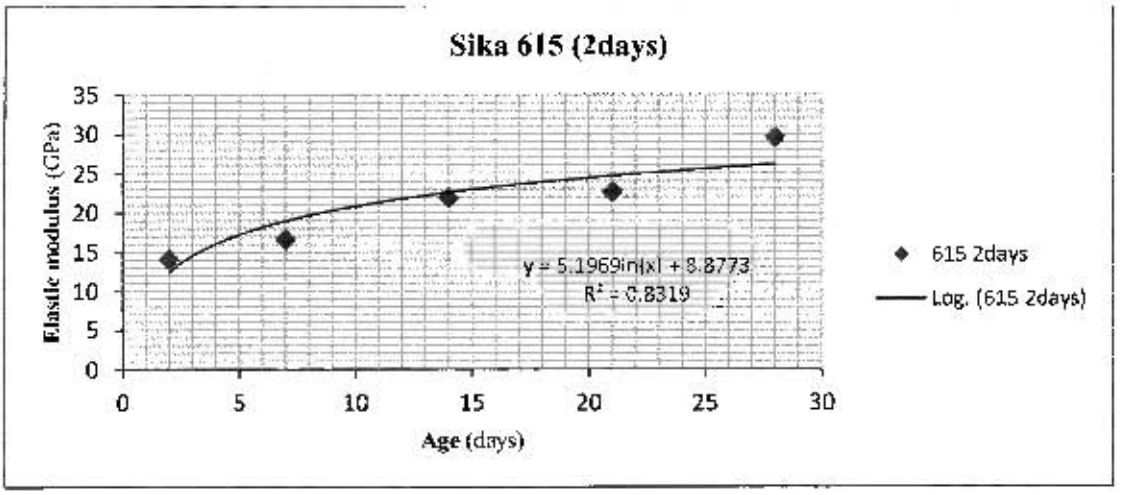
Sika 615 (2days)
Elastic modulus (GPa)
Age (days)
y = 5.1969ln(x) + 8.8773
R² = 0.8319
615 2days
Log. (615 2days)

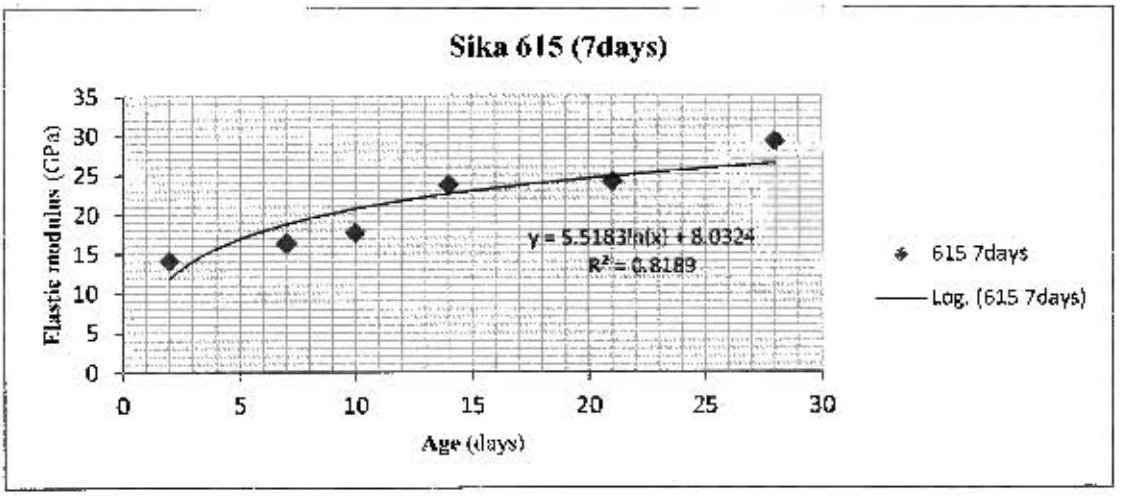
Sika 615 (7days)
Elastic modulus (GPa)
Age (days)
y = 5.5183ln(x) + 8.0324
R² = 0.8189
615 7days
Log. (615 7days)

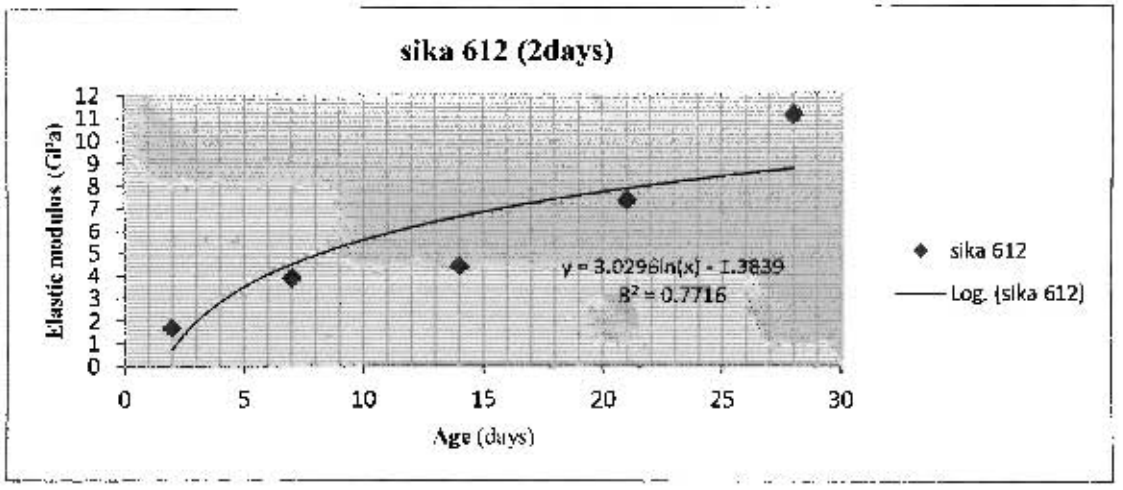
sika 612 (2days)
Elastic modulus (GPa)
Age (days)
y = 3.0296ln(x) - 1.3839
R² = 0.7716
sika 612
Log. (sika 612)

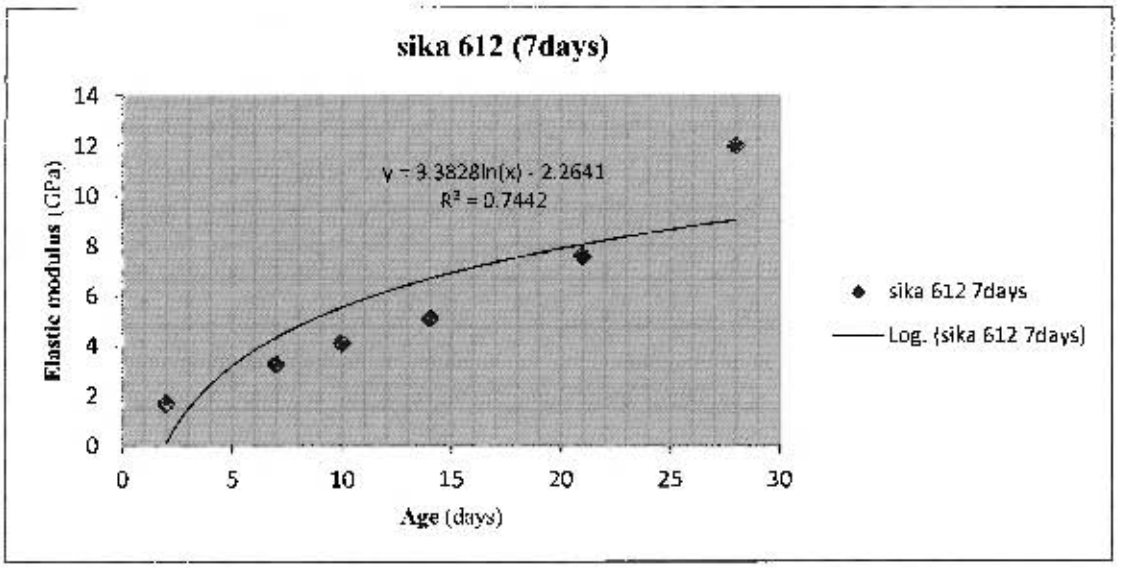
sika 612 (7days)
y = 3.3828ln(x) - 2.2641
R² = 0.7442
Elastic modulus (GPa)
Age (days)
sika 612 7days
Log. (sika 612 7days)

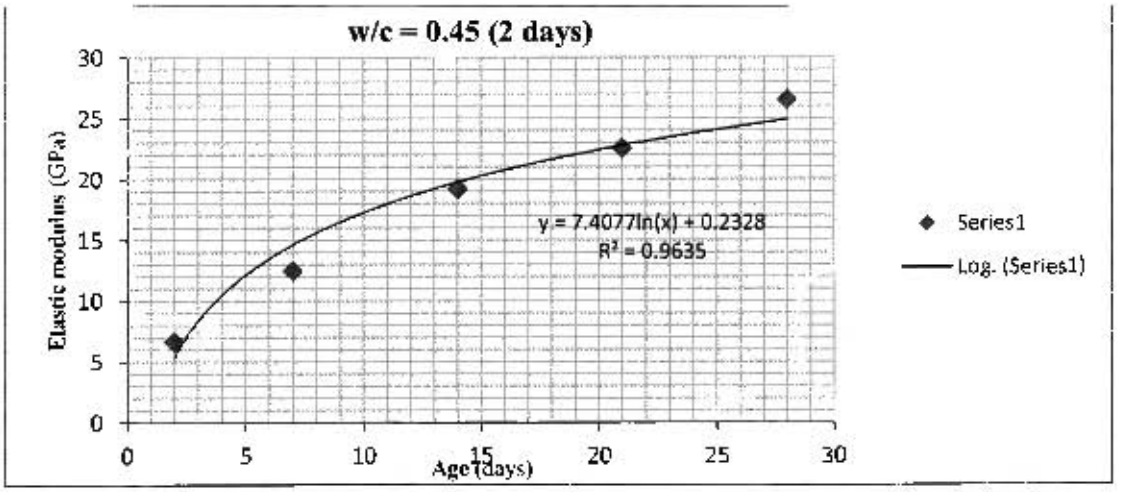
w/c = 0.45 (2 days)
y = 7.4077ln(x) + 0.2328
R² = 0.9635
Elastic modulus (GPa)
Age (days)
Series1
Log. (Series1)

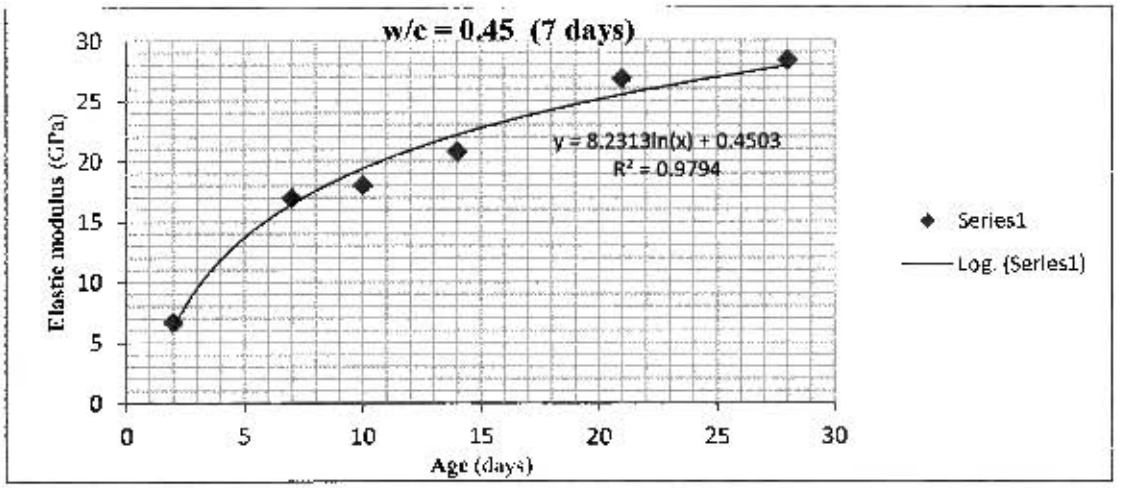
w/c = 0.45 (7 days)
y = 8.2313ln(x) + 0.4503
R² = 0.9794
Elastic modulus (GPa)
Age (days)
Series1
Log. (Series1)

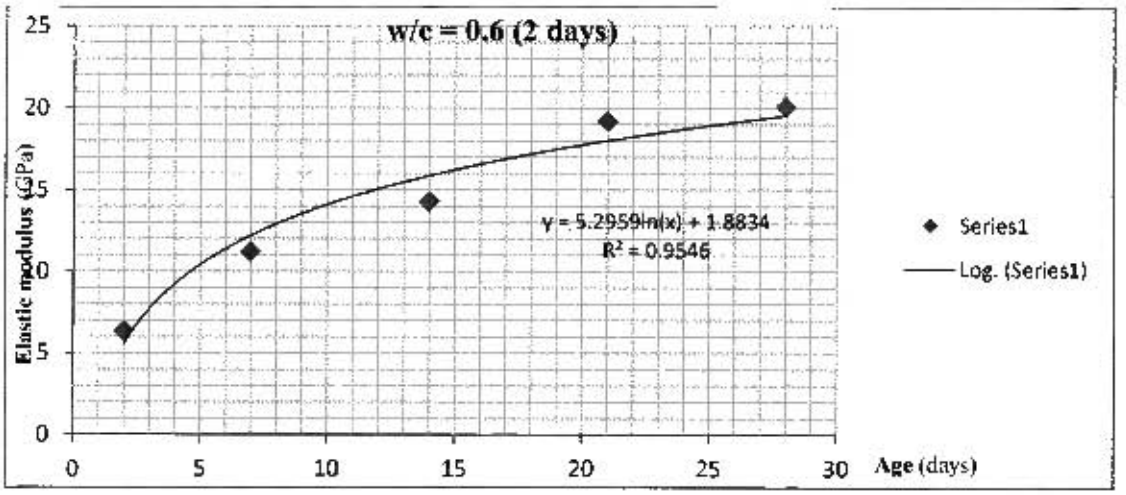

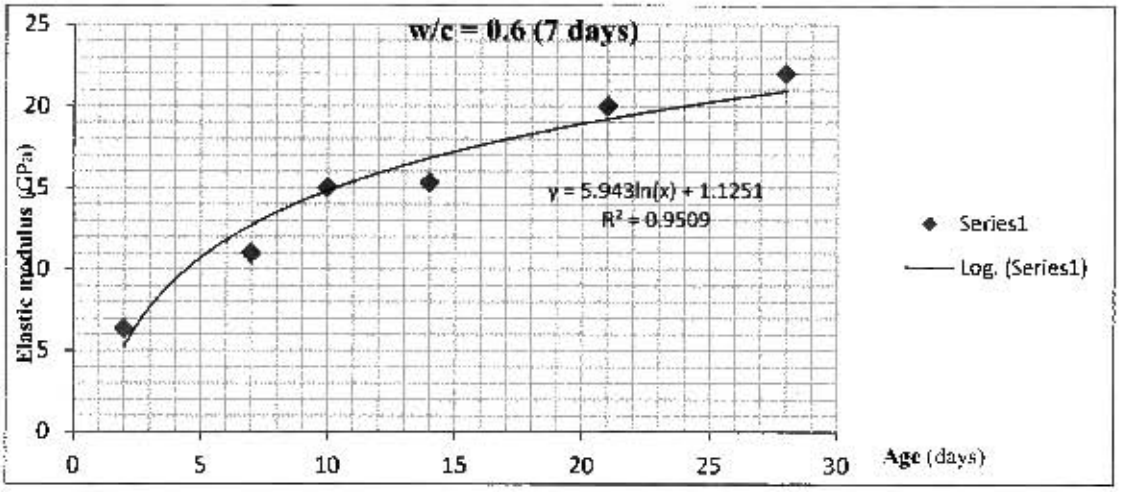

Tensile relaxation

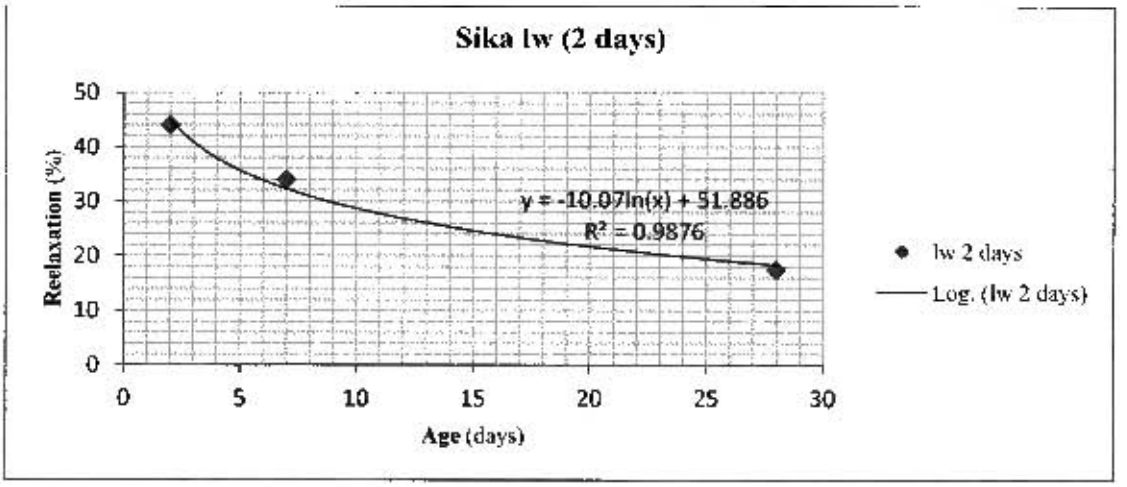

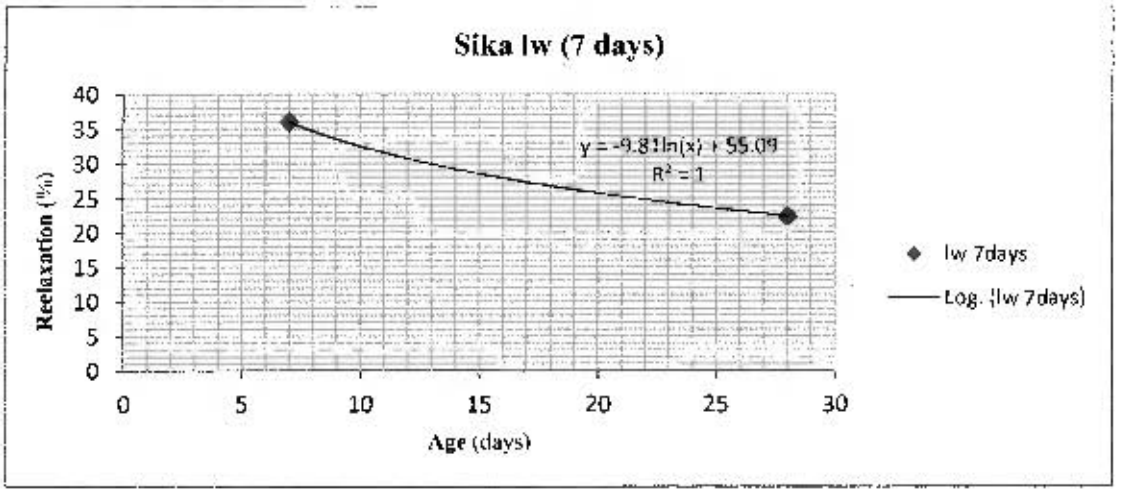
Sika Iw (7 days)
Reelaxation (%)
Age (days)
y = -9.81ln(x) + 55.09
R² = 1
Iw 7days
Log. (Iw 7days)

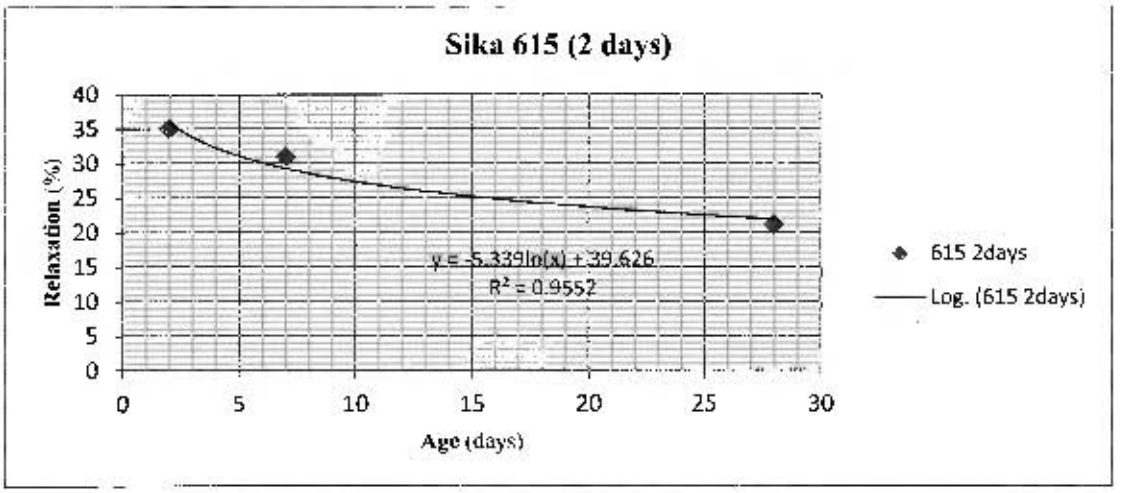
Sika 615 (2 days)
Relaxation (%)
Age (days)
y = -5.339ln(x) + 39.626
R² = 0.9552
615 2days
Log. (615 2days)

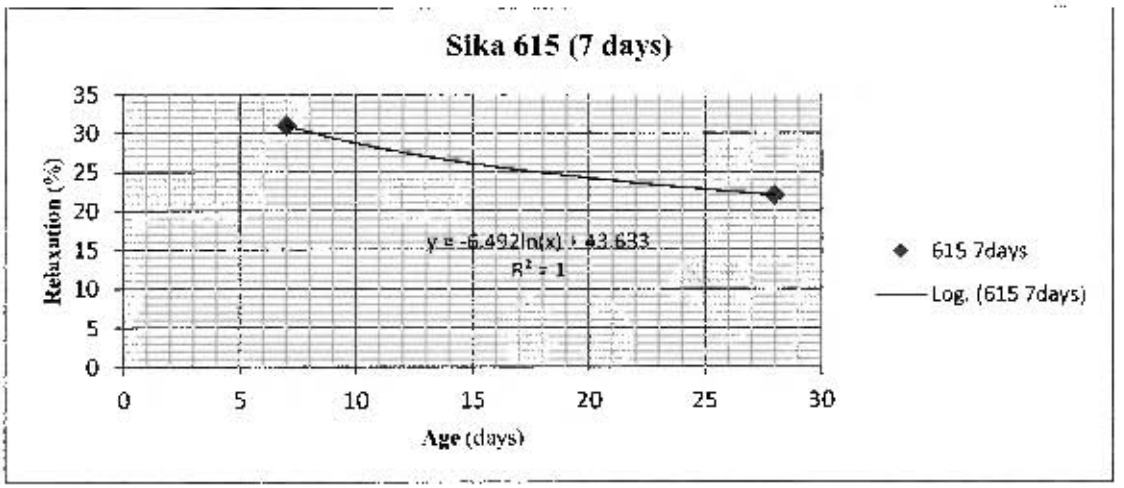
Sika 615 (7 days)
Relaxation (%)
Age (days)
y = -6.492ln(x) + 43.633
R² = 1
615 7days
Log. (615 7days)

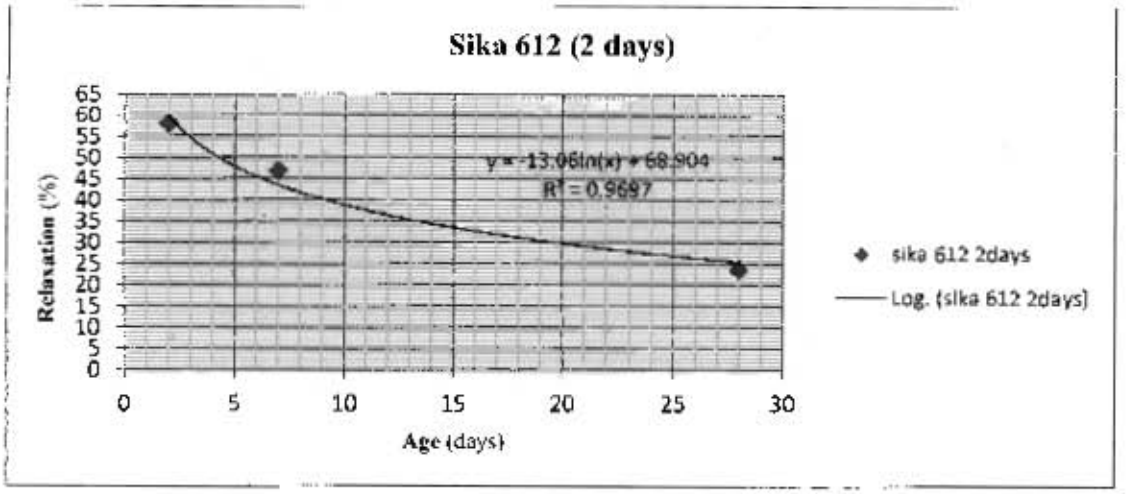
Sika 612 (2 days)
y = -13.06ln(x) + 68.904
R² = 0.9697
Relaxation (%)
Age (days)
sika 612 2days
Log. (sika 612 2days)

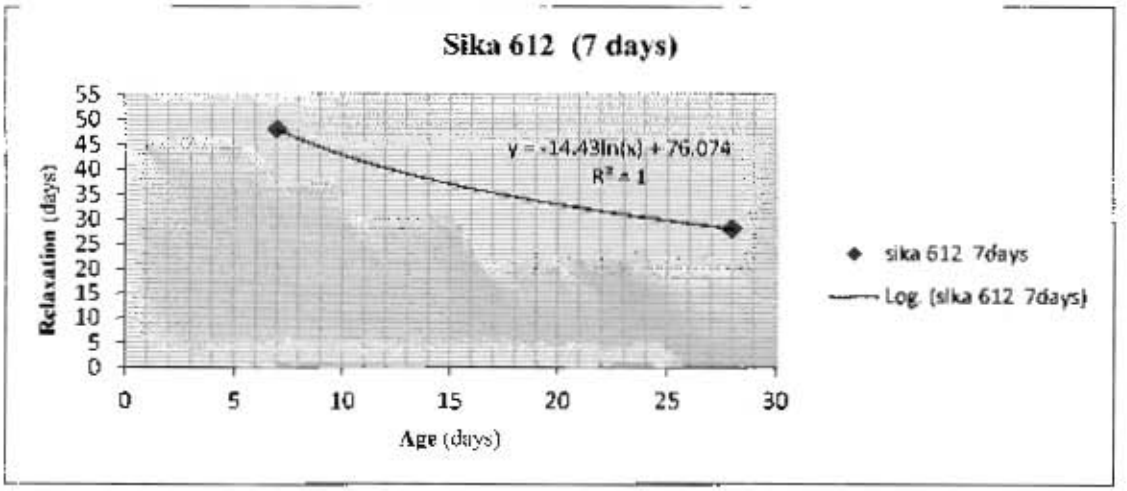
Sika 612 (7 days)
y = -14.43ln(x) + 76.074
R² = 1
Relaxation (days)
Age (days)
sika 612 7days
Log. (sika 612 7days)

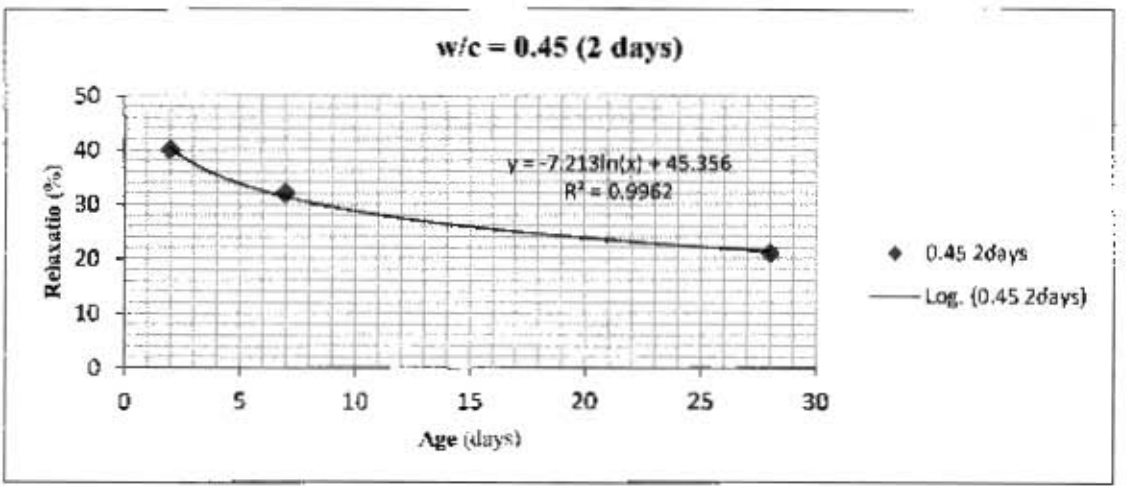
w/c = 0.45 (2 days)
y = -7.213ln(x) + 45.356
R² = 0.9962
Relaxatio (%)
Age (days)
0.45 2days
Log. (0.45 2days)

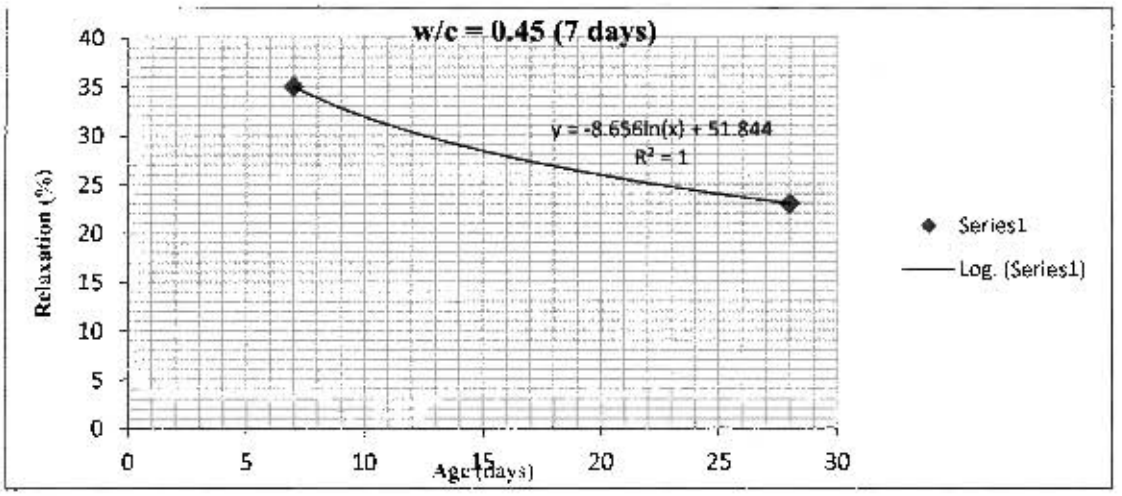
w/c = 0.45 (7 days)
y = -8.656ln(x) + 51.844
R² = 1
Relaxation (%)
Age (days)
Series1
Log. (Series1)

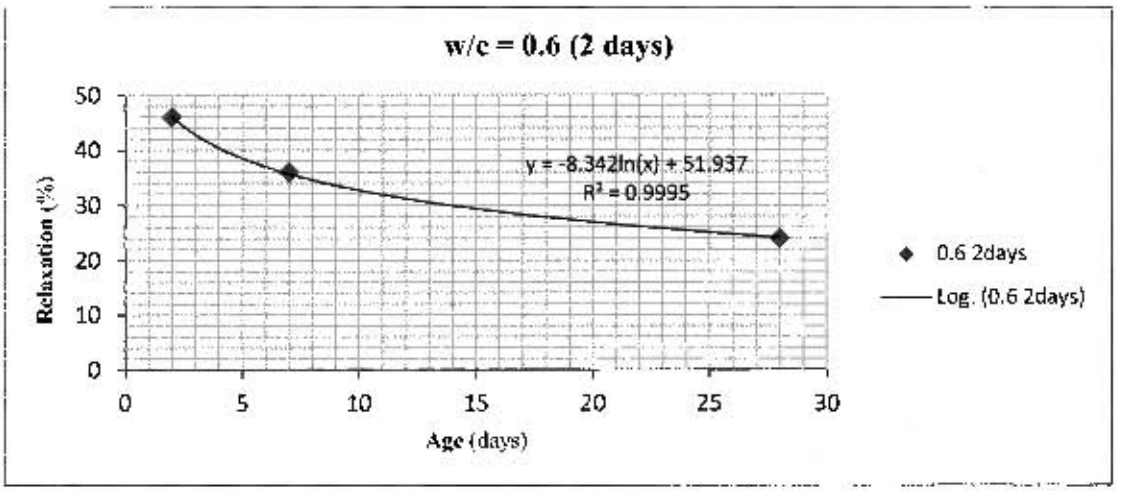
w/c = 0.6 (2 days)
y = -8.342ln(x) + 51.937
R² = 0.9995
Relaxation (%)
Age (days)
0.6 2days
Log. (0.6 2days)

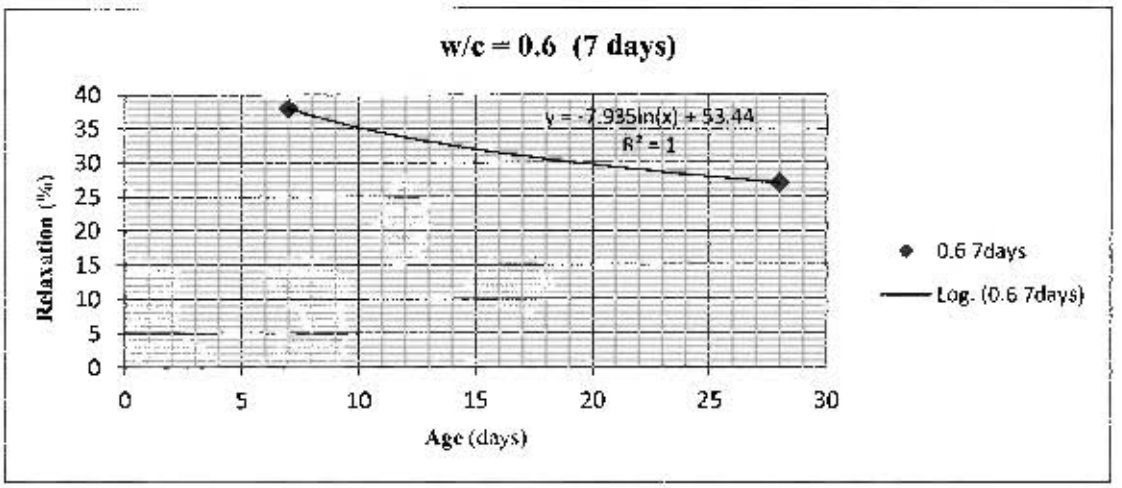
w/c = 0.6 (7 days)
y = -7.935ln(x) + 53.44
R² = 1
Relaxation (%)
Age (days)
0.6 7days
Log. (0.6 7days)

Appendix B: Material properties' tables

Table B.1: Material properties for 2 days cured Sika LW specimens.

Period (days)	Change in free shrinkage strain (10)	Mean elastic modulus [GPa]	Tensile strength [MPa]	Mean tensile relaxation [%]	Elastic stress [MPa]	Remaining stress [MPa]
0-2	0.0	1.0	1.3	45.0	0.0	0.0
2-4	260.0	4.0	1.5	41.0	0.6	0.4
4-6	250.0	8.0	1.7	36.0	1.8	1.1
6-8	140.0	10.5	1.9	32.0	2.7	1.7
8-10	130.0	12.0	2.0	29.5	3.6	2.4
10-12	110.0	13.5	2.1	27.5	4.5	3.0
12-14	20.0	14.5	2.2	26.0	4.7	3.2
14-16	20.0	15.5	2.3	24.5	4.9	3.3
16-18	30.0	16.0	2.3	23.5	5.2	3.5
18-20	60.0	17.0	2.3	22.0	5.8	4.0
20-22	25.0	17.5	2.4	21.0	6.1	4.2
22-24	5.0	18.0	2.4	20.5	6.1	4.3
24-26	20.0	18.5	2.5	19.5	6.3	4.4
26-28	5.0	19.0	2.5	18.5	6.4	4.5

Table B.2: Material properties for 7 days cured Sika LW specimens.

Period (days)	Change in free shrinkage strain (10)	Mean elastic modulus [GPa]	Tensile strength [MPa]	Mean tensile relaxation [%]	Elastic stress [MPa]	Remaining stress [MPa]
0-7	0.0	6.0	1.5	36.0	0.0	0.0
7-10	440.0	12.5	2.0	34.0	3.3	2.2
10-12	400.0	14.0	2.1	31.5	6.7	4.5
12-14	100.0	15.0	2.1	30.0	7.6	5.1

14-16	40.0	16.0	2.3	28.5	7.9	5.4
16-18	105.0	17.0	2.3	27.0	9.0	6.2
18-20	10.0	18.0	2.4	26.0	9.1	6.2
20-22	15.0	18.5	2.4	25.0	9.3	6.4
22-24	20.0	19.0	2.5	24.0	9.5	6.5
24-26	30.0	20.0	2.5	23.5	9.9	6.8
26-28	10.0	20.5	2.6	22.0	10.0	6.9

Table B.3: Material properties for 2 days cured Sika 615 specimens.

Period (days)	Change in free shrinkage strain (10)	Mean elastic modulus [GPa]	Tensile strength [MPa]	Mean tensile relaxation [%]	Elastic stress [MPa]	Remaining stress [MPa]
0-2	0.0	12.0	2.0	35.0	0.0	0.0
2-4	205.0	14.0	2.5	34.0	1.7	1.1
4-6	55.0	17.0	2.8	31.0	2.3	1.5
6-8	85.0	18.5	3.0	29.0	3.2	2.2
8-10	80.0	20.0	3.2	28.0	4.2	2.9
10-12	30.0	21.0	3.4	26.5	4.6	3.2
12-14	30.0	22.5	3.5	26.0	5.0	3.5
14-16	60.0	23.0	3.6	25.0	5.8	4.1
16-18	40.0	24.0	3.7	24.5	6.4	4.5
18-20	10.0	24.5	3.8	24.0	6.5	4.6
20-22	30.0	25.0	3.8	23.5	7.0	5.0
22-24	45.0	25.0	3.9	23.0	7.6	5.5
24-26	20.0	25.5	3.9	22.5	8.0	5.7
26-28	10.0	26.0	4.0	22.0	8.1	5.9

Table B.4: Material properties for 7 days cured Sika 615 specimens.

Period (days)	Change in free shrinkage strain (10)	Mean elastic modulus [GPa]	Tensile strength [MPa]	Mean tensile relaxation [%]	Elastic stress [MPa]	Remaining stress [MPa]
0-7	0.0	18.0	2.4	31.0	0.0	0.0
7-10	330.0	20.0	3.0	29.5	4.0	2.8
10-12	20.0	21.0	3.1	28.0	4.2	3.0
12-14	55.0	22.0	3.2	27.0	4.9	3.5
14-16	50.0	23.0	3.3	26.0	5.6	4.0
16-18	50.0	23.5	3.4	25.0	6.3	4.5
18-20	85.0	24.0	3.5	24.5	7.6	5.5
20-22	35.0	25.0	3.5	24.0	8.1	5.9
22-24	55.0	25.5	3.6	23.5	8.9	6.5
24-26	25.0	26.0	3.7	22.5	9.3	6.8
26-28	25.0	26.0	3.7	22.0	9.7	7.1

Table B.5: Material properties for 2 days cured Sika 612 specimens.

Period (days)	Change in free shrinkage strain (10)	Mean elastic modulus [GPa]	Tensile strength [MPa]	Mean tensile relaxation [%]	Elastic stress [MPa]	Remaining stress [MPa]
0-2	0.0	1.0	1.0	60.0	0.0	0.0
2-4	620.0	1.8	1.3	55.0	0.7	0.3
4-6	280.0	3.4	1.6	48.0	1.2	0.6
6-8	90.0	4.4	1.8	44.0	1.5	0.7
8-10	160.0	5.2	1.9	40.0	2.0	1.0
10-12	80.0	5.8	2.0	37.0	2.3	1.2
12-14	60.0	6.4	2.1	35.0	2.5	1.4
14-16	60.0	6.8	2.2	34.0	2.7	1.5

16-18	50.0	7.2	2.3	32.0	2.9	1.7
18-20	30.0	7.5	2.3	30.0	3.1	1.8
20-22	25.0	7.8	2.4	29.0	3.2	1.8
22-24	15.0	8.1	2.4	28.0	3.3	1.9
24-26	25.0	8.4	2.5	27.0	3.4	2.0
26-28	35.0	8.6	2.5	26.0	3.6	2.1

Table B.6: Material properties for 7 days cured Sika 612 specimens.

Period *(days)*	Change in free shrinkage strain (10)	Mean elastic modulus [GPa]	Tensile strength [MPa]	Mean tensile relaxation [%]	Elastic stress [MPa]	Remaining stress [MPa]
0-7	0.0	2.0	1.6	48.0	0.0	0.0
7-10	830.0	5.0	1.8	45.5	2.5	1.4
10-12	250.0	5.8	1.9	41.5	3.4	1.9
12-14	150.0	6.4	2.0	39.0	3.9	2.2
14-16	85.0	6.9	2.1	37.0	4.3	2.4
16-18	10.0	7.3	2.3	35.0	4.3	2.5
18-20	35.0	7.7	2.4	34.0	4.5	2.6
20-22	55.0	8.1	2.4	32.0	4.8	2.8
22-24	125.0	8.4	2.5	31.0	5.4	3.2
24-26	70.0	8.7	2.6	29.0	5.8	3.5
26-28	10.0	9.0	2.7	28.0	5.8	3.5

Table B.7: Material properties for 2 days-cured w/c = 0.45 specimens.

Period (days)	Change in free shrinkage strain (10)	Mean elastic modulus [GPa]	Tensile strength [MPa]	Mean tensile relaxation [%]	Elastic stress [MPa]	Remaining stress [MPa]
0-2	0.0	5.0	2.0	40.0	0.0	0.0
2-4	270.0	8.0	2.5	37.5	1.3	0.8

4-6	85.0	12.0	2.9	33.5	1.9	1.2
6-8	130.0	14.5	3.1	31.0	3.0	2.0
8-10	70.0	16.0	3.3	29.0	3.7	2.5
10-12	100.0	18.0	3.5	28.0	4.8	3.3
12-14	30.0	19.0	3.6	27.0	5.1	3.5
14-16	60.0	20.0	3.7	25.0	5.9	4.0
16-18	50.0	21.0	3.8	24.0	6.5	4.5
18-20	20.0	22.0	3.9	24.0	6.7	4.7
20-22	20.0	23.0	4.0	23.0	7.0	4.9
22-24	10.0	23.5	4.1	22.0	7.2	5.0
24-26	30.0	24.0	4.1	21.0	7.6	5.4
26-28	10.0	24.5	4.2	21.0	7.7	5.5

Table B.8: Material properties for 7 days cured w/c = 0.45 specimens.

Period (days)	Change in free shrinkage strain (10)	Mean elastic modulus [GPa]	Tensile strength [MPa]	Mean tensile relaxation [%]	Elastic stress [MPa]	Remaining stress [MPa]
0-7	0.0	9.8	2.7	35.0	0.0	0.0
7-10	350.0	18.0	3.8	33.5	3.8	2.5
10-12	70.0	20.0	4.0	31.0	4.6	3.1
12-14	85.0	21.5	4.2	29.0	5.7	3.9
14-16	65.0	22.5	4.4	28.5	6.6	4.5
16-18	88.0	24.0	4.6	27.0	7.9	5.4
18-20	15.0	24.5	4.7	26.0	8.1	5.6
20-22	10.0	25.0	4.8	25.5	8.2	5.7
22-24	70.0	26.0	4.9	24.5	9.3	6.5
24-26	62.0	27.0	5.0	24.0	10.3	7.3
26-28	107.0	27.5	5.2	23.0	12.1	8.6

Table B.9: Material properties for 2 days cured w/c = 0.6 specimens.

Period (days)	Change in free shrinkage strain (10)	Mean elastic modulus [GPa]	Tensile strength [MPa]	Mean tensile relaxation [%]	Elastic stress [MPa]	Remaining stress [MPa]
0-2	0.0	4.0	1.4	46.0	0.0	0.0
2-4	150.0	7.0	1.8	43.0	0.6	0.4
4-6	80.0	10.0	2.2	38.5	1.1	0.7
6-8	120.0	12.0	2.4	36.0	2.0	1.2
8-10	140.0	13.0	2.5	34.0	3.1	1.9
10-12	55.0	14.5	2.6	32.0	3.5	2.3
12-14	20.0	15.5	2.7	30.5	3.7	2.4
14-16	30.0	16.0	2.8	29.0	4.0	2.6
16-18	60.0	16.5	2.9	28.0	4.6	3.0
18-20	40.0	17.5	3.0	27.0	5.0	3.3
20-22	20.0	18.0	3.1	26.0	5.2	3.5
22-24	20.0	18.5	3.1	25.5	5.5	3.6
24-26	10.0	19.0	3.2	25.0	5.6	3.7
26-28	10.0	19.5	3.2	24.0	5.7	3.8

Table B.10: Material properties for 7 days cured w/c = 0.6 specimens.

Period (days)	Change in free shrinkage strain (10)	Mean elastic modulus [GPa]	Tensile strength [MPa]	Mean tensile relaxation [%]	Elastic stress [MPa]	Remaining stress [MPa]
0-7	0.0	8.0	2.6	38.0	0.0	0.0
7-10	265.0	14.0	2.9	36.5	2.2	1.4
10-12	95.0	15.0	3.1	34.5	3.1	2.0
12-14	80.0	16.0	3.2	33.0	3.8	2.5
14-16	40.0	17.0	3.3	32.0	4.3	2.8

16-18	30.0	18.0	3.4	30.5	4.6	3.0
18-20	65.0	18.5	3.5	30.0	5.3	3.5
20-22	65.0	19.0	3.6	29.0	6.0	4.0
22-24	105.0	20.0	3.6	28.0	7.3	4.9
24-26	90.0	20.5	3.7	27.5	8.4	5.7
26-28	10.0	21.0	3.8	27.0	8.5	5.8

Appendix C: Laboratory Results

Tensile strength results

	Sika LW (2 days cured)					
Age (days)	**spec 1(N)**	**spec 2(N)**	**spec 3(N)**	**Average(N)**	**strength(MPa)**	**St Dev**
2	1925	1891	1862	1893	1.18	0.0195
7	3240	3499	3372	3371	2.11	0.0810
14	3405	3407	3395	3403	2.13	0.0041
21	3660	3641	3591	3631	2.27	0.0224
28	4068	4070	4075	4071	2.54	0.0023

	Sika LW (7 days cured)					
Age (days)	**spec 1(N)**	**spec 2(N)**	**spec 3(N)**	**Average(N)**	**strength(MPa)**	**St Dev**
7	2622	3106	3548	3092	1.93	0.2892
10	3245			3245	2.03	
14	3058	3502	3829	3463	2.16	0.2418
21	3893			3893	2.43	
28	4365	4099	3829	4098	2.56	0.1673

	Sika 615 (2 days cured)					
Age (days)	**spec 1(N)**	**spec 2(N)**	**spec 3(N)**	**Average(N)**	**strength(MPa)**	**St Dev**
2	3401	3500	3405	3435	2.15	0.0351
7	4310	4352	4263	4309	2.69	0.0279
14	6291	5542	4659	5497	3.44	0.5107
21	6098	5968	5954	6006	3.75	0.0496
28	6755	6602	6551	6636	4.15	0.0664

	Sika 615 (7 days cured)					
Age (days)	**spec 1(N)**	**spec 2(N)**	**spec 3(N)**	**Average(N)**	**strength(MPa)**	**St Dev**
7	3319	4100	4947	4122	2.58	0.5089
10	5340	5102	4720	5054	3.16	0.1953
14	5313	5300	5400	5338	3.34	0.0340
21	6000		5000	5500	3.44	0.4419
28	5360	5900	6300	5853	3.66	0.2947

	Sika 612 (2 days cured)					
Age (days)	**spec 1(N)**	**spec 2(N)**	**spec 3(N)**	**Average(N)**	**strength(MPa)**	**St Dev**
2	1406	1502	1685	1531	0.96	0.09
7	2644	2753	2788	2728	1.71	0.05
14	3113	3001	2941	3018	1.89	0.05
21	4044	3535	3217	3599	2.25	0.26
28	4422	4388	4323	4378	2.74	0.03

	Sika 612 (7 days cured)					
Age (days)	**spec 1(N)**	**spec 2(N)**	**spec 3(N)**	**Average(N)**	**strength(MPa)**	**St Dev**
2	2397	2306	2234	2312	1.45	0.05
7	2562	2931	3501	2998	1.87	0.29
14	3419	3301	3136	3285	2.05	0.08
21	3495	3400	3495	3463	2.16	0.03
28	3585	3998	4452	4012	2.51	0.27

	w/c = 0.45 (2 days cured)					
Age (days)	**spec 1(N)**	**spec 2(N)**	**spec 3(N)**	**Average(N)**	**strength(MPa)**	**St Dev**
2	3538	3501	3449	3496	2.19	0.0280
7	4911	4124	3544	4193	2.62	0.4288
14	6300	5925	5704	5976	3.74	0.1883
21	6337	6100	5976	6138	3.84	0.1147
28	6946	6899	6917	6921	4.33	0.0148

	w/c = 0.45 (7 days cured)					
Age (days)	**spec 1(N)**	**spec 2(N)**	**spec 3(N)**	**Average(N)**	**strength(MPa)**	**St Dev**
7	5346	5104	4752	5067	3.17	0.1867
10	5858	5905	6465	6076	3.80	0.2111
14	6609	7005	7669	7094	4.43	0.3348
21	8036	7509	7253	7599	4.75	0.2495
28	8891	8508	8075	8491	5.31	0.2552

	w/c = 0.6 (2 days cured)					
Age (days)	**spec 1(N)**	**spec 2(N)**	**spec 3(N)**	**Average(N)**	**strength(MPa)**	**St Dev**
2	2253	2299	2437	2330	1.46	0.0598
7	3408	3459	3574	3480	2.18	0.0531
14	3990	4205	4401	4199	2.62	0.1285
21	4409	4339	4264	4337	2.71	0.0453
28	5665	5525	5599	5596	3.50	0.0438

	w/c = 0.6 (7 days cured)					
Age (days)	**spec 1(N)**	**spec 2(N)**	**spec 3(N)**	**Average(N)**	**strength(MPa)**	**St Dev**
7	4687	4602	4597	4629	2.87	0.0316
10	4950	4699	4487	4712	2.80	0.1449
14	4405	4879	5536	4940	3.46	0.3550
21	5048	5385	5678	5370	3.55	0.1970
28	5936	5902	5976	5938	3.74	0.0232

Elastic modulus

	Sika LW (2 days cured)				
Age (days)	**spec 1(GPa)**	**spec 2(GPa)**	**spec 3(GPa)**	**Average(GPa)**	**St Dev**
2	3.5	4.8	4.0	4.1	0.7
7	8.6	9.6	10.3	9.5	0.9
14	10.7	11.7	11.5	11.3	0.5
21	17.1	19.2	19.5	18.6	1.3
28	19.8	20.9	23.8	21.5	2.1

	Sika LW (7 days cured)				
Age (days)	**spec 1 (GPa)**	**spec 2(GPa)**	**spec 3(GPa)**	**Average(GPa)**	**St Dev**
7	7.1	8.5	11.1	8.9	2.0
10	13.0	14.8	14.2	14.0	0.9
14	13.2	13.9	15.2	14.1	1.0
21	18.3	19.0	20.0	19.1	0.9
28	21.3	23.1	21.9	22.1	0.9

	Sika 615 (2 days cured)				
Age (days)	**spec 1(GPa)**	**spec 2(GPa)**	**spec 3(GPa)**	**Average(GPa)**	**St Dev**
2	12.4	14.3	15.4	14.1	1.5
7	16.9	15.6	17.6	16.7	1.0
14	20.5	22.5	22.7	21.9	1.2
21	22.5	22.1	23.5	22.7	0.7
28	28.7	29.8	30.3	29.6	0.8

	Sika 615 (7 days cured)				
Age (days)	**spec 1(GPa)**	**spec 2(GPa)**	**spec 3(GPa)**	**Average(GPa)**	**St Dev**
7	15.1	17.2	16.7	16.33	1.1
10	16.1	17.0	20.0	17.70	2.0
14	23.1	22.6	25.6	23.76	1.6
21	23.9	23.5	25.0	24.12	0.8
28	28.5	29.6	29.5	29.21	0.6

	Sika 612 (2 days cured)				
Age (days)	**spec 1(GPa)**	**spec 2(GPa)**	**spec 3(GPa)**	**Average(GPa)**	**St Dev**
2	1.5	2.1	1.5	1.7	0.3
7	3.4	4.3	4.0	3.9	0.5
14	4.9	3.8	4.5	4.4	0.6
21	6.5	6.6	8.8	7.3	1.3
28	10.3	12.4	10.6	11.1	1.1

	Sika 612 (7 days cured)				
Age (days)	**spec 1(GPa)**	**spec 2(GPa)**	**spec 3(GPa)**	**Average(GPa)**	**St Dev**
7	2.9	2.8	4.0	3.24	0.7
10	3.8	4.4	4.0	4.08	0.3
14	6.2	4.1	4.9	5.07	1.1
21	6.4	5.9	10.4	7.57	2.5
28	11.1	12.0	12.9	11.99	0.9

	w/c = 0.45 (2 days cured)				
Age (days)	**spec 1(GPa)**	**spec 2(GPa)**	**spec 3(GPa)**	**Average(GPa)**	**St Dev**
2	5.2	7.1	7.7	6.66	1.3
7	11.1	12.3	14.1	12.51	1.5
14	18.4	19.4	19.9	19.23	0.8
21	20.5	23.5	23.7	22.56	1.8
28	25.1	25.6	28.9	26.54	2.1

	w/c = 0.45 (7 days cured)				
Age (days)	**spec 1(GPa)**	**spec 2(GPa)**	**spec 3(GPa)**	**Average(GPa)**	**St Dev**
7	16.1	15.9	19.0	17.0	1.7
10	17.3	16.9	19.8	18.0	1.6
14	19.2	20.9	22.3	20.8	1.6
21	25.3	27.1	28.0	26.8	1.4
28	28.1	27.9	29.2	28.4	0.7

	w/c = 0.6 (2 days cured)				
Age (days)	**spec 1(GPa)**	**spec 2(GPa)**	**spec 3(GPa)**	**Average(GPa)**	**St Dev**
2	5.9	6.9	6.2	6.4	0.5
7	10.1	11.6	11.9	11.2	1.0
14	13.2	15.1	14.6	14.3	1.0
21	17.2	21.3	19.1	19.2	2.1
28	19.8	20.1	20.4	20.1	0.3

	w/c = 0.6 (7 days cured)				
Age (days)	**spec 1(GPa)**	**spec 2(GPa)**	**spec 3(GPa)**	**Average(GPa)**	**St Dev**
7	10.2	12.1	11.0	11.1	1.0
10	14.7	14.8	15.5	15.0	0.4
14	13.8	14.1	18.0	15.3	2.3
21	18.0	19.0	23.0	20.0	2.6
28	21.3	22.8	22.2	22.1	0.8

Compressive strength

	Sika LW						
Age (days)	**Spec 1(N)**	**spec 2(N)**	**spec 3(N)**	**spec 4(N)**	**Average(N)**	**strength(MPa)**	**St. Dev**
2	123000	104000	107500	119500	113500	11.35	0.92
7	285000	286000	320000	323000	303500	30.35	2.08
10	368000	374000	365000	377000	371000	37.10	0.55
14	431000	414000	418000	421000	421000	42.10	0.73
21	418000	407000	440000	393000	414500	41.45	1.98
28	428000	450000	458000	461000	449250	44.93	1.49

	Sika 615						
Age (days)	**Spec 1(N)**	**spec 2(N)**	**spec 3(N)**	**spec 4(N)**	**Average(N)**	**strength(MPa)**	**St. Dev**
2	303000	321000	306000	318000	312000	31.20	0.88
7	381000	407000	387000	375000	387500	38.75	1.39
10	387000	396000	393000	387000	390750	39.08	0.45
14	445000	428000	415000	407000	423750	42.38	1.66
21	452000	465000	446000	442000	451250	45.13	1.00
28	504000	482000	492000	454000	483000	48.30	2.13

	Sika 612						
Age (days)	**Spec 1(N)**	**spec 2(N)**	**spec 3(N)**	**spec 4(N)**	**Average(N)**	**strength(MPa)**	**St. Dev**
2	27000	29000	27600	28400	28000	2.80	0.09
7	63000	68000	97000	97000	81250	8.13	1.83
10	56000	59000	96000	118000	82250	8.23	3.00
14	83000	86000	127000	120000	104000	10.40	2.27
21	99000	111000	116000	94000	105000	10.50	1.02
28	110000	78000	120000	116000	106000	10.60	1.91

	w/c = 0.45						
Age (days)	**Spec 1(N)**	**spec 2(N)**	**spec 3(N)**	**spec 4(N)**	**Average(N)**	**strength(MPa)**	**St. Dev**
2	247000	231000	215000		231000	23.1000	1.60
7	395000	389000	380000	413000	394250	39.4250	1.39
10	423000	436000	446000	445000	437500	43.7500	1.07
14			435000	444000	439500	43.9500	0.64
21	455000	424000	489000	446000	453500	45.3500	2.70
28	478000	480000	491000	514000	490750	49.0750	1.65

	w/c = 0.6						
Age (days)	**Spec 1(N)**	**spec 2(N)**	**spec 3(N)**	**spec 4(N)**	**Average(N)**	**strength(MPa)**	**St. Dev**
2	146000	143000			144500	14.4500	0.21
7	286000	284000	316000	302000	297000	29.7000	1.50
10	291000	314000	293000	350000	312000	31.2000	2.74
14			335000	324000	329500	32.9500	0.78
21	315000	335000	319000	357000	331500	33.1500	1.91
28	348000	358000	369000	375000	362500	36.2500	1.20

Tensile relaxation

Sika LW (2 days cured)				
Age (days)	**spec 1(%)**	**spec 2(%)**	**Average(%)**	**St Dev**
2	42	46	44	2.83
7	33.2	34.8	34	1.13
28	16.9	18.1	17.5	0.85

Sika LW (7 days cured)				
Age (days)	**spec 1(%)**	**spec 2(%)**	**Average(%)**	**St Dev**
7	35.2	36.8	36	1.13
28	21.3	23.5	22.4	1.56

Sika 615 (2 days cured)				
Age (days)	**spec 1(%)**	**spec 2(%)**	**Average(%)**	**St Dev**
2	33.6	36.4	35	1.98
7	31.6	30.4	31	0.85
28	20.7	21.4	21.1	0.49

Sika 615 (7 days cured)				
Age (days)	**spec 1(%)**	**spec 2(%)**	**Average(%)**	**St Dev**
7	30.9	31.3	31.1	0.28
28	20	23.6	21.8	2.55

Sika 612 (2 days cured)				
Age (days)	**spec 1(%)**	**spec 2(%)**	**Average(%)**	**St Dev**
2	56	60	58	2.83
7	45.5	48.6	47	2.19
28	23	24.4	23.7	0.99

Sika 612 (7 days cured)				
Age (days)	**spec 1(%)**	**spec 2(%)**	**Average(%)**	**St Dev**
7	47	49	48	1.41
28	26.5	29.5	28	2.12

w/c = 0.45 (2 days cured)				
Age (days)	**spec 1(%)**	**spec 2(%)**	**Average(%)**	**St Dev**
2	39.6	41	40.3	0.99
7	31.8	32.6	32.2	0.57
28	21.6	21	21.3	0.42

w/c = 0.45 (7 days cured)				
Age (days)	**spec 1(%)**	**spec 2(%)**	**Average(%)**	**St Dev**
7	35.9	34.5	35.2	0.99
28	22.6	24	23.3	0.99

w/c = 0.6 (2 days cured)				
Age (days)	**spec 1(%)**	**spec 2(%)**	**Average(%)**	**St Dev**
2	45.6	46.8	46.2	0.85
7	35	37.6	36.3	1.84
28	24	24.4	24.2	0.28

w/c = 0.6 (7 days cured)				
Age (days)	**spec 1(%)**	**spec 2(%)**	**Average(%)**	**St Dev**
7	37.1	38.9	38	1.27
28	26.2	27.8	27	1.13